INVESTIGATION INTO THE ROLE OF SODIUM CHLORIDE DEPOSITED ON OXIDE AND METAL SUBSTRATES IN THE INITIATION OF HOT CORROSION

by

N. Birks

Sixth and Final Report
on Grant No. NAG 3-44

April 1980 - August 1983

Prepared for

NATIONAL AERONAUTICS AND SPACE ADMINISTRATION
Lewis Research Center
Cleveland, Ohio

Department of Metallurgical and Materials Engineering
University of Pittsburgh
Pittsburgh, PA 15261

TABLE OF CONTENTS

INVESTIGATION INTO THE ROLE OF SODIUM CHLORIDE DEPOSITED ON OXIDE AND METAL SUBSTRATES IN THE INITIATION OF HOT CORROSION

N. Birks

Metallurgical and Materials Engineering Department
University of Pittsburgh

Abstract

Sodium chloride is deposited on the surface of alumina substrates and exposed to air containing 1% SO_2 at temperatures between 500°C and 700°C. In all cases the sodium chloride was converted to sodium sulfate, the volatilization of sodium chloride from the original salt particles being responsible for the development of a uniform coating of sodium sulfate on the alumina substrate. At temperatures above 625°C, a liquid NaCl-Na_2SO_4 eutectic was formed on the substrate. The mechanisms for these reactions are given, one of the main roles of NaCl in low temperature hot corrosion lies in enabling a corrosive liquid to form.

When the alumina substrate is a scale growing on an alloy, the liquid salt that forms was found to attack the protective layer aggressively. It was found that this attack is initiated quite rapidly at 700°C by selective acidic attack of the alumina layer by the molten salt at unique sites situated primarily along the alumina grain boundaries. At the base of the pits formed, base metal oxides were growing which eventually caused the mechanical break-up of the alumina scale allowing the molten salt to gain access to and attack the metal surface.

When water vapor was added to the atmospheres, its reaction rate apparantly increased and the morphology of the product became more clearly crystalline representing stacks of hexagonal plates. The stacks of plates had void structures down their length. These features indicate a strongly volatile species to be involved in the reaction mechanism involving water vapor, but it was not identified.

THE ROLE OF SODIUM CHLORIDE, DEPOSITED ON OXIDE AND METAL SUBSTRATES IN THE INITIATION OF LOW TEMPERATURE HOT CORROSION

by

N. Birks

Department of Metallurgical and Materials Engineering
University of Pittsburgh

Introduction

Air and fuel contaminants such as sodium chloride and sulfur depositing on the turbine and stator blades in gas turbines can lead to accelerated attack known as hot corrosion. The mechanisms of hot corrosion above 900°C, based on liquid sodium sulfate deposition, are well understood [1,2] whereas accelerated attack in the 650–750°C range is not so well understood.

Low temperature hot corrosion occurs below the melting point of sodium sulfate, predominantly in marine environments. Ingested sodium chloride condenses on and coats compressor blades[3,4] and is shed when the engine is accelerated. Some of the pieces of sodium chloride are thought to be sufficiently large to survive passage through the combustion chamber to impinge on the turbine and stator stages.

The aim of this investigation is to understand the mechanisms by which deposited sodium chloride promotes low temperature hot corrosion attack. To this end a successful apparatus and experimental technique have been devised and experiments have been carried out over a wide range of conditions to study, initially, the conversion of sodium chloride to sodium sulfate on an alumina substrate and, secondly, the reaction leading to the initiation of hot corrosion of a preoxidized metal sample. The techniques, results and conclusions reached are described in this report.

Background

McCreath[3,4] has shown that a gas turbine compressor will efficiently remove salt particles from the air, a deposit that builds up, during cruising or idling is shed when the engine accelerates to full power producing a shower of sodium chloride particles. Such particles impact on the turbine blades and then react during operation. For this reason it is unlikely that sodium chloride deposits would be observed on stripdown.

Root and Stetson[5] used a burner rig to study the deposition of salt on specimen targets and found that a low-melting liquid of high chloride content was deposited on cycling the temperature through the 650-750°C zone resulting in high rates of attack. Thermal shock may also have been a contributing factor.

Kohl, Santoro, Stearns, Fryburg and Rosner[6] concluded that conversion of NaCl vapor to Na_2SO_4 solid requires about 2.2×10^{-3} sec. which is less than the residence time for gases in the combustion chamber. Any sodium chloride that deposits on the turbine or stator blades must therefore be particulate and originally large enough to survive passage through the combustion chamber.

Since the combustion gases contain sulfurous oxides and oxygen, it is necessary to inquire into the conversion of sodium chloride to sodium sulfate and its interaction with growing protective oxide scales.

Conde', Birks, Hocking and Vasantasree[7] injected brine with the exhaust of a burner rig and deposited the resulting condensed particles onto alumina disks. The fuel used contained 0.1% sulfur and the sodium chloride reacted readily in the temperature range 650-850°C producing a deposit structure of alternate NaCl and Na_2SO_4 lamellae typical of a solidified eutectic.

Fielder, Stearns, Kohl and Fryburg[8-10] studied the conversion of NaCl single crystals to Na_2SO_4, between 325-710°C, using an automatic thermobalance

They concluded that the reaction may proceed by two reactions depending on whether water vapor is present.

$$2NaCl_{(s)} + SO_{3(g)} + 1/2\ O_{2(g)} = Na_2SO_{4(s)} + Cl_{2(g)};\ \Delta G^{o} = -34900 + 21.30\ T\ cal\ (1$$

and $$2NaCl_{(s)} + SO_{3(g)} + H_2O_{(g)} = Na_2SO_{4(s)} + 2\ HCl_{(g)};\ \Delta G^{o} = -20900 + 5.15\ T\ cal\ (2)$$

In the anhydrous case an activation energy of only 5100 cal was obtained and the reaction product was a porous layer of sodium sulfate between 330-625°C, whereas a liquid product formed above 625°C.

The following stages were proposed for the mechanism of the reaction[8-10]:

1. A planar SO_4 species forms on the chloride surface.
2. This associates forming a trigonal bipyramid S_2O_7 species.
3. The trigonal bipyramid S_2O_7 rearranges to tetrahedral S_2O_7.
4. Electrons transfer to the S_2O_7, forming SO_4^{2-} stable ions and Cl_2 gas is released.

Step 3, rearrangement of S_2O_7, is considered to be the rate determining step, the surface reaction accounting for the low activation energy. The reaction rate was expressed as:

$$R = 4.5\ P_{SO_3}\ \exp.\ (-5100/RT)\ \ mg\ cm^{-2}\ sec.^{-1}$$

where P_{SO_3} is in atmospheres. The atmospheres used were equilibrated by catalysis using platinum[11].

Stearns, Kohl, Fryberg and Miller[12] showed that, at 900°C, Na_2SO_4 would absorb NaCl vapor from the atmosphere. However, due to the low concentrations of sodium chloride in the turbine engine atmospheres, the chances of absorbing substantial amounts of NaCl by this mechanism are low[12].

It appears therefore that the practical source of sodium chloride depositing downstream of the combustion chamber is the shedding of fairly large particles from the late stage compressor blades.

The work to be described is, therefore, concerned with the transformation of NaCl particles on an alumina substrate exposed to atmospheres containing sulfurous oxides. It is also concerned with the interaction of the deposits with the substrate and the mechanisms by which protective scales may be degraded in the presence of molten salts.

It is appropriate to consider the main mechanisms by which protective scales can be degraded by molten salts. The most important stage being the initiation of hot corrosion. If the initiation mechanism can be understood, it may be possible to take steps to lengthen the incubation period.

Hot corrosion studies carried out so far[1,2,5,8-20] indicate that initiation may be due to chemical attack or to physical damage of the protective scale.

Bornstein and DeCrescente[13,14] found that a thin layer of Na_2SO_4 placed on the surface of nickel alloys caused marked enhancement of the reaction rates in air at 1000°C. They concluded that the high rates of attack were due to the presence of oxygen ions, in the surface liquid layer, in sufficient concentration to flux any protective oxide that was in the process of forming. Thus the fused salt was allowed to contact the metal and rapid reaction ensued.

The subject of hot corrosion and an understanding of the relevant mechanisms was provided by Goebel and Pettit[1] and Goebel, Pettit and Goward[2] for the cases of nickel and nickel base alloys respectively. This was later extended into a unified treatment by Giggins and Pettit[21].

In the case of nickel, it is proposed that the sulfate melt contains oxygen ions by equilibration with the atmosphere

$$SO_4^{2-} = SO_3 + O^{2-} \qquad (3)$$

The respective activities of the sulfate ions and the oxide ions being determined by the salt composition and the SO_3 partial pressure of the atmosphere.

Figure 1 shows Goebel and Pettit's model for the Na_2SO_4 induced accelerated oxidation of nickel. Initially, the formation of the NiO on the metal surface removes some oxygen from the melt which consequently increases the sulfur potential.

$$SO_4^{2-} = S^{2-} + 2\ O_2 = S + 3/2\ O_2 + O^{2-} \quad (4)$$

The sulfur potential reaches a value at which nickel sulfide may form in the metal below the NiO layer. The removal of both oxygen and sulfur from the molten salt results in a net increase in the oxygen ion concentration reaching a level at which nickelate ions, soluble in the liquid salt, may form. This occurs at the scale-melt interface, the dissolved nickelate ions migrate out through the molten salt to the salt-gas interface where the high oxygen and sulfur partial pressures cause them to dissociate to form NiO particles.

<u>At metal-salt interface</u>

$$SO_4^{2-} = 3/2\ O_2 + 1/2\ S_2 + O^{2-} \quad (5)$$

$$3\ Ni + 3/2\ O_2 = 3\ NiO \quad (6)$$

$$3/2\ Ni + 1/2\ S_2 = 1/2\ Ni_3S_2 \quad (7)$$

$$2\ NiO + O^{2-} + 1/2\ O_2 = 2\ NiO_2^- \quad (8)$$

<u>At salt-gas interface</u>

$$O^{2-} + SO_3 = SO_4^{2-} \quad (9)$$

$$2\ NiO_2^- = 2\ NiO + O^{2-} + 1/2\ O_2 \quad (10)$$

Thus the Na_2SO_4 can, of its own accord, cause an initial reaction to occur, The continuation of the attack is ensured, however, only so long as the atmosphere can supply sulfurous gases to the melt surface. The practical result of this is the formation of a porous non-protective layer of NiO which leads to very high reaction rates.

These ideas also apply to the attack of alloys which rely for their protection on the formation of layers of slow growing Cr_2O_3 and Al_2O_3. Both of these oxides

may be fluxed by excess oxygen ions according to

$$Cr_2O_3 + O^{2-} = 2\ CrO_2^- \quad (11)$$

and $$Al_2O_3 + O^{2-} = 2AlO_2^- \quad (12)$$

These ions migrate through the salt layer to sites of higher oxygen potential close to the salt-gas interface where they precipitate out as the oxides Cr_2O_3 and Al_2O_3 releasing oxygen ions according to the reverse reactions.

Reactions such as 8, 11 and 12 represent the fluxing of solid oxides by oxygen ions in a melt to form a soluble product. This is called basic fluxing and occurs when an excess of oxygen ion is present.

When the conentration of oxygen ions is very low then the oxide may simply dissociate to form oxygen ions in the solution by reactions such as

$$Al_2O_3 = 2\ Al^{3+} + 3O^{2-} \quad (13)$$

This is called acid fluxing and it is fairly clear that for each oxide there exists a critical oxygen ion concentration which is defined by equilibria similar to the case below for aluminum,

$$AlO_2^- = Al^{3+} + 2O^{2-} \quad (14)$$

where $$[O^{2-}]^2 = \text{const.}\ \frac{[AlO_2^-]}{[Al^{3+}]} \quad (15)$$

Equation 15 defines the critical value of the O^{2-} concentration above which $Al_2O_{3(s)}$ will dissolve as AlO_2^- anions by basic fluxing and below which it will dissolve as Al^{3+} and O^{2-} ions by acid fluxing.

This concept has been expressed by Gupta and Rapp[16]. There is a specific critical oxygen ion concentration for each oxide. Thus it is possible, in a given melt with fixed P_{SO_3}, that one oxide will dissolve acidically and another will dissolve basically. This is a consequence of the widely different stabilities of the various complex anions that can be formed.

For instance the formation of very stable vanadate, molybdate and tungstate anions by basic fluxing may denude the molten salt of oxygen ions to the extent that other oxides such as Al_2O_3, Cr_2O_3 and NiO dissolve by simple ionization or acid fluxing.

This also has an important consequence as indicated by Deadmore and Lowell[17] in that the addition of impurities leading to the formation of stable anions such as vanadates, tungstates and molybdates not only increases the reaction rates but also allows liquids to form at lower temperatures due to the formation of deposits with melting points well below 700°C. A parallel case where mixing of anions leads to low melting point liquid deposits was reported by Root and Stetson[5] who found that mixtures of NaCl and Na_2SO_4 formed liquids that could be agressive down to 650°C.

The above lays down the conditions under which chemical attack of the scale may occur. The alternative mode of initial degradation of the scale is the physical rupture of the protective scale as proposed by several investigators[7,22-25]

Hancock and Hurst[22,26] monitored the condition of growing surface oxides by using a vibrational technique that is very sensitive to the integrity of the surface layers of the specimen. They showed that, whereas the alumina scale on B1900 was not strongly adherent and may allow the molten salts to gain access to the metal surface, it was not affected by the presence of NaCl in the atmosphere. On the other hand, protective scales based on Cr_2O_3 are very sensitive to the presence of NaCl and form volatile chromium chlorides and oxychlorides which can rupture the scale if they form at the metal-scale interface. In either case the loss of mechanical integrity of the scale allows the molten salts to gain access to the metal-scale interface resulting in accelerated corrosion.

The physical deteroriation of protective oxide scales is an important subject in concept but very difficult to investigate. Consequently there are more unsubstantiated hypotheses than hard facts concerning this subject.

Stearns[23] used high pressure sampling techniques to extract volatile species from preoxidized samples, heated in the presence of NaCl and H_2O, for identification in the mass spectrometer. Using IN-738 and 713C he isolated the following volatile species:

$$CrO_2(OH)_{(g)}, (NaCl)_x\ CrO_{3(g)}\ (x = 1, 2, 3),$$
$$(NaOH)_x CrO_{3(g)}\ (x = 1, 2, 3), (MoO_3)_{3(g)}, (MoO_3)_{4(g)},$$
$$(NaCl)_x(MoO_3)_{3(g)}(x = 1, 2), MoO_2(OH)_{2(g)}$$

Most of these species are relatively complex molecules, the simpler species CrO_2Cl_2, $CrCl_2$ and $CrCl_3$ were not idenfified.

Conde[7] proposed that NaCl was responsible for causing initial damage to Cr_2O_3 scales and, by formation of volatile chlorides, for transfering chromium through the scale. He did not justify the proposals thermodynamically.

Similarly Smeggil and Bornstein[24] proposed that the volatile species AlOCl or $AlCl_3$ help rupture alumina scales in the presence of NaCl and H_2O.

Other ideas proposed for the initial physical degradation of the scales included impact pressures, but salt particles up to 10μm were thought to be too small to cause damage[25]. Hossain and Saunders[20] suggested that the substitution of Cl^- on the oxide lattice would cause cation vacancies to form which may agglomerate and form voids at the alloy scale interface. This suggestion has not been substantiated and it is difficult to see how the agglomeration of vacancies of one charged species only can lead to the formation of voids, without the possibility of vacancies arising on the anion sub lattice, such a process would appear to be impossible.

In conclusion, the hot corrosion reaction mechanisms are well understood at high temperatures around 900°C, however, little attention has been paid to the low temperature range between 500-700°C and the mechanism in this temperature range is not clear. The initiation of the reaction may occur by chemical attack of the scale, mechanically by various mechanisms or by a combination of these processes.

In the program of investigation to be described, the work is split into two parts (a) the conversion of NaCl to Na_2SO_4 on an alumina substrate over the temperature range 500-700°C, (b) the reactions involved in the initiation of hot corrosion attack on an alumina scale growing on an alloy.

EXPERIMENTAL TECHNIQUES

The intention of this program was to inquire into the mechanisms by which NaCl transforms to Na_2SO_4 not to measure the kinetics of the reaction which was the subject of a parallel study by Fielder[8,9].

The initial work involved establishing sodium chloride particles on an alumina substrate at temperature, introducing an atmosphere of air and SO_2 with which the discrete salt particles can react and finally stopping the reaction by pulling the alumina tablet substrate into a cool zone of the furnace.

The apparatus used is shown in Figures 2-5. The sodium chloride single crystals, obtained from NASA-Lewis, were ground and sized in a moisture-free atmosphere in a perspex dry box containing P_2O_5 powder in several bowls. The crushed and graded NaCl particles were stored in sealed glass containers kept in the dry box. This is shown in Figure 2.

A second smaller dry box, over the furnace tube, is used to allow the NaCl particles to be added to their hopper without exposure to moisture in the transference. This can also be seen in Figure 2.

In Figure 3 is shown the diagramatic representation of the apparatus, a photograph of the actual assembly is given in Figure 4.

The dried salt powder is placed in a hopper above the reaction tube as shown in Figure 3. The hopper is connected via two greaseless taps to the reaction tube. Between the two taps is a space which is filled with salt powder by opening the upper tap. When this is full, the upper tap is rotated to exclude the hopper but to open to a supply of the gas to be used as the atmosphere. The bottom tap is opened and the metered salt powder is blown into the apparatus. Salt particles impinge on the specimen and are seen to be retained on the specimen surface. The two taps are now closed and the gas stream admitted to the furnace

through the preheater tube. The specimen and furnace were brought to temperature in the furnace before adding the salt but the air - SO_2 mixture is only added after the salt particles are introduced. The air-SO_2 mixture may be used to introduce the salt or a stream of nitrogen may be used for this purpose.

The gas exits at the top of the apparatus and is taken to a fume cupboard for disposal.

The specimen, which may be an alumina disc substrate or a preoxidized piece of metal, is supported on a contoured piece of alumina brick which sits on the top of a silica pedestal which is held and sealed into the furnace by two 'O' rings through which it may be withdrawn rapidly in order to bring the sample into the cold zone of the apparatus for rapid cooling.

The furnace is supported on a vertical track and counterbalanced so that it can be raised and lowered easily. The temperature is controlled to within $\pm$ 2°C and measured using either a chromel-alumel or a platinum/platinum 10% rhodium thermocouple inserted through the gas exit tube to the hot zone. Readings are supported by a similar couple inserted up the center of the hollow silica specimen support tube. Good agreement is obtained between the two thermocouples.

The gas stream of air and SO_2 is dried by passing over magnesium perchlorate and phosphoruspentoxide before entering the reaction tube. The gas composition could be adjusted by varying the flow rates of the component gases, air + SO_2 and air, using flow meters.

Alumina substrates were cut as disks about 2mm thick from an alumina rod 8mm in diameter. These disks were ground to a flat surface and finished with 600 grit SiC abrasive. They were then cleaned in acetone and stored in a dessicator for future use.

Metal samples of the alloy HOS 875 (Fe-20Cr-5Al-1Zr-0.5Si), supplied by

NASA-Lewis, were cut into coupons 12mm X 8mm X 1.5mm. These were also ground to 600 grit and cleaned with acetone.

These specimens were preoxidized at 1300°C for 12 hrs. to produce a layer of α-Al_2O_3 about 6μm thick. After preoxidation, the specimens were cooled to room temperature in the furnace, cleaned with acetone and stored in a dessicator.

To carry out an experiment, a specimen, alumina disk or HOS 875 preoxidized coupon, was placed on the silica support tube then placed in the reaction tube in the hot zone position and sealed.

The furnace was heated to the selected temperature and salt particles were introduced from the hopper as described. After introducing the salt, the desired gas flow was established through the furnace for the predetermined reaction time which could vary from one minute to several hours at temperatures between 500-700°C.

After the prescribed time the samples were withdrawn. The run being terminated by switching off the gas flow and the furnace. Alumina substrate specimens were cooled rapidly by pulling the silica support tube rapidly into the cool zone whereas, to avoid thermal stress cracking, the preoxidized HOS-875 specimens were cooled more slowly in the hot zone with the furnace as the power was switched off.

Certain specimens were coated with a saturated solution of NaCl or Na_2SO_4 in order to apply the salts initially to a specific surface area. In these cases the specimens were dried at 150°C.

After exposure the specimens were examined, optically and in the AMR-9000 SEM with energy dispersive x-ray analysis, to detect the presence and distribution of various elements on the specimen surface. Compounds present were identified by x-ray diffraction techniques.

Certain specimens were sectioned to examine the salt-scale-metal interfaces.

These specimens were mounted in epoxy resin and polished in kerosene, entirely excluding moisture from the procedure to avoid dissolving the salts, and cleaned with acetone.

Early examination using SEM-EDX were carried out using gold evaporated films for surface conduction. In spite of the proximity of the principal gold and sulfur lines, it was easy to define the presence of sulfur however, to avoid this conflict, carbon shadowing was used subsequently wherever feasible.

In order to study the effect of moisture when necessary, provision was made in the apparatus for the gas to be bubbled through a water bath so that water vapor is entrained. The water vapor pressure was measured satisfactorily by passing the gas stream through a chamber in which were sealed a thermometer and a humidity meter. It was found possible to add water vapor to a level of about 1%, according to a relative humidity reading of 40% at a temperature of 20°C, by bubbling the gas through an ice-water mixture at 0°C. By modifying the temperature of the entraining water bath, the water vapor content could be varied readily.

RESULTS

The very simple apparatus and techniques resulted in very few problems and the only difficulty has been controlling precisely the amount of NaCl that was retained on the specimen surface. However, there was always sufficient for the purpose and, if it was required to position the salt accurately, it could be done by applying the salt externally from a saturated solution and drying.

There has been little or no damage to the silica reaction tube due to salt attachment in the hot zone. The salt particles apparantly either adhere to the specimen or fall to the bottom of the reaction tube.

The salt particles, ground and sized to between 170 and 200 mesh, to produce

100μm particles, are angular as shown in Figure 6. This type of salt powder was used in all of the experiments except when the salt was applied as a saturated solution.

The program of investigation consisted of two parts. Firstly using alumina substrates to study the conversion of sodium chloride to sodium sulfate over the temperature range 500–700°C in several atmospheres. Secondly to use this information to interpret the role of NaCl in the initiation of low temperature hot corrosion especially over the temperature range 650–700°C.

I. CONVERSION OF NaCl TO Na_2SO_4 ON ALUMINA SUBSTRATES

The surface of the alumina disk freshly sectioned using a diamond cutter is shown in Figure 7.

Salt particles were dropped on to such disks which were then reacted in air + 0.2% SO_2 and air + 0.99% SO_2 atmospheres both anhydrous and containing 1% H_2O at temperatures of 500, 600, 650 and 700°C for various preselected times. The results of these experiments will now be presented below.

Anhydrous Conditions

500°C

The reaction apparantly proceeded very slowly at this temperature. A salt particle on the alumina substrate is shown after 120 minutes exposure in air + 0.2% SO_2 in Figure 8. The accompanying EDX trace shows strong chlorine and weak sulfur indications. Thus we may infer that the reaction has not proceeded very rapidly at this stage.

On the EDX trace there is an indication of the presence of aluminum on the upper surface of the partially converted salt particle. This gave rise to

speculation about the role of volatile aluminum compounds in the reactions. Later experiments however showed conclusively that these indications of aluminum, which appeared from time to time, were due to electrons, scattered from the angled salt particle face, striking the alumina substrate and giving rise to characteristic aluminum lines on EDX. This will be discussed later.

In Figure 9 is seen the surface of the NaCl particle exposed to air + 0.99% SO_2 for 240 minutes. In spite of the increased SO_2 concentration and longer time the sulfate layer does not appear to be very thick and there is a sign of only a very fine deposit of reaction product on the alumina substrate. After 480 minutes under these conditions, the deposit become very 'grainy' both on the original salt particle surface and also on the alumina substrate. This is shown in Figure 10 where accompanying EDX traces show that both particle surface and alumina surface have approximately the same composition and the same morphology.

600°C

After 10 minutes in air + 0.2% SO_2, the salt particle shows depressions on its surfaces and small spherical initial deposits of Na_2SO_4 appear on the surrounding alumina substrate as shown in Figure 11.

After 30 minutes, the reaction has proceeded much further and a porous layer of Na_2SO_4 has developed on the salt particle, apparantly initiating at many discrete sites and spreading to produce a porous product. This is shown in Figure 12.

When the exposure is increased to two hours, the layer is seen in Figure 13 to have grown to be quite thick but is still porous.

After four hours exposure, further growth has occured in the deposit both on the particle and on the substrate as shown in Figure 14.

No chlorine was detected by EDX analysis in any of these deposits on the Al_2O_3 substrate.

Increasing the sulfur dioxide content of the atmosphere to 0.99% increased the conversion rate as is evident from Figure 15 which shows the Na_2SO_4 formed on the salt particle after only 10 minutes. EDX response from the surrounding substrate indicates that Na_2SO_4 is starting to form there also.

After 30 minutes exposure to this SO_2 - air atmosphere, a thick Na_2SO_4 has grown that is porous as shown in Figure 16 and the deposit on the alumina substrate is shown in Figure 17. This deposit is shown by EDX to have no trace of chlorine.

Many of the particles at this stage are surrounded by a distinct zone, or 'halo', which is more pronounced in the specimens exposed at 650°C.

After 30 minutes at 600°C in air + 0.99% SO_2, the 'halo' has 2 zones. The outer zone deposit contains sodium and sulfur whereas the inner zone deposit contains sodium, sulfur and chlorine. It appears that the limit of the inner zone coincides with the original salt particle boundaries and that the inner zone is formed as the salt particle recedes due to sodium chloride evaporation. This feature is only seen at the higher temperature where NaCl evaporates strongly and is shown in Figure 19. After 60 minutes the evaporation process has proceeded so far that the original NaCl particle has largely evaporated and all that remains is a skeleton of Na_2SO_4 that formed on the NaCl and a small NaCl particle in the center as shown in Figure 18.

650°C

At this higher temperature, not only the reaction rate but also the evaporation of NaCl is expected to increase. Indeed, after 10 minutes, the salt particle is quite small and has well rounded features. The substrate is covered with a deposit of Na_2SO_4 and the 'halo' region immediately around the particle is also clear as shown in Figure 19. The discontinuous EDAX spectrum showing strong sulfur and sodium presence is from the outer region. The continuous spectrum is from the halo

zone and shows little sodium sulfur or chlorine. Similar results are shown in Figure 20 after 30 minutes and Figure 21 after 4 hrs.

These observations taken in sequence are significant. After 30 minutes the halo zone is again clearly seen. The particle is quite small and rounded in appearance, but the significant feature is that the area surrounding the particle not only has a deposit, but the deposit was liquid and had solidified on cooling to room temperature. EDX analysis shows the substrate to be covered with Na_2SO_4 only after 10 minutes. After 30 minutes the halo zone has a deposit of Na_2SO_4 only whereas elsewhere on the substrate, the dendritic deposit shows definite response to Na, S and Cl. This indicates that the liquid formed at temperature is the eutectic liquid in the Na_2SO_4 - NaCl system which at 650°C covers the composition range 55-70 mol. % Na_2SO_4 according to Figure 22.

After four hours exposure the deposit on the substrate is seen to contain no chlorine since, by this time, all of the NaCl has fully converted to Na_2SO_4 or has evaporated.

700°C

Very similar results were obtained at 700°C as at 650°C.

EFFECT OF WATER VAPOR

Several experiments were carried out to examine the effect of water vapor on the reaction morphology. These are described below.

500°C

The sodium chloride particles were exposed to air + 0.2%SO_2 + 1.0% H_2O.

After short times of 10 minutes there is evidence that sulfate formation is starting, the growth after 30, 60 and 240 minutes providing more complete coverage of the surface of the NaCl crystal. Whereas, without water vapor, the individually nucleated sulfate sites grew independently and impinged on each other, in the

presence of water vapor these individual growths appear to be well sintered together, almost as well as if they had been molten. This is shown in Figure 23 where spangles on the surface are also visible. The water vapor has also introduced the artefact of silica whiskers which were formed on the substrate surface presumably by reaction involving the silica tube. It appears that the presence of water vapor in the system may introduce more vapor species into the reaction sequences.

Experiments were repeated at 0.1 and 0.5% SO_2 contents but the reaction was not changed substantially. The initial nucleation of Na_2SO_4 on the NaCl surface, at discrete sites is shown in Figure 24. . After 240 minutes, the sodium chloride particle with its growth of Na_2SO_4 has well defined contours, emphasising the much smaller role played by NaCl evaporation at 500°C. After 4 hrs. in 0.5% SO_2 + 0.5% H_2O well defined hexagonal plates appear to be developing on the side of the particle. As shown in Figure 25, these plates have pores or holes in their centers and this feature may give evidence of the role of a vapor species in their formation and growth. In the 0.5% SO_2 + 1% H_2O atmosphere such clusters appear to have grown more rapidly than the rest of the deposit.

600°C

In air 0.1% SO_2, 1% H_2O at 600°C, Figures 26 and 27 show that after 30 minutes the original salt particle is covered in a growing layer of sulfate. Sulfate deposits are also evident around the particle on the alumina substrate where, after 60 minutes and beyond a heavy compact deposit of Na_2SO_4 is seen.

As shown in Figure 28 , after 30 minutes in air 0.1% SO_2+1% H_2O,the sulfate clusters are well packed on the particle surface and grow predominantly as hexagonal columns which have a system of pores down the center. This is clear

from Figure 28, which also shows the deposit, of Na_2SO_4 on the substrate to be growing quite uniformly and evenly. The pores within the columns have sides that have crystallographic faces and EDX indicates the presence of Na and S only, as shown in Figure 28. This type of growth and morphology is not seen in the absence of water vapor. Both the pores and the crystallographic features give evidence of the important role of vapor species in the presence of water.

700°C

In air, 0.2% SO_2 1% H_2O after 10 minutes, the particles have rounded edges and the surface is covered in a fairly dense layer that appears to have been liquid as seen in Figure 29. Even after so short a time as 10 minutes, substantial evaporation has occured and the size of the particle has been reduced considerably. Both chlorine and sulfur are present in the fairly thick layer that surrounds the original particle site. This layer also has been liquid at temperature.

After 30 and 60 minutes, the reaction is virtually complete and Figure 30 shows the site of an original salt particle fully converted. The reaction has exhausted the original sodium chloride particle and the substrate cover, which was originally a NaCl-Na_2SO_4 eutectic, now shows many secondary growth nodules of Na_2SO_4. These occur as the NaCl in the liquid converts to solid Na_2SO_4, as the NaCl vapor supply is cut off when the original particles are exhausted.

Discussion

In some of the experiments where particles, after exposure, had been examined by EDX, indications of the presence of aluminum in the reaction product were found. This had implied that volatile aluminum compounds may have formed during the reaction. This was checked by two experiments.

First a disk of Al_2O_3 was coated with NaCl from a saturated aqueous solution,

dried and placed on the support pedestal as indicated in Figure 31. A nickel substrate was placed 6" below this in the cold zone of the furnace. The disc coated with NaCl was heated in air + 0.99% SO_2 for one hour at 600°C and, using another specimen, for one hour at 700°C. The nickel substrates in both cases were examined using EDX in the SEM but only sodium and sulfur were found to be present. No trace of aluminum was found. Aluminum was not detected either in the solutions obtained by leaching other exposed specimens.

To check the possibility that the aluminum peaks arise from stray electron beam reflections, a specimen was placed in the SEM and examined at various tilt angles to the incident beam. Figure 32 shows the arrangement. When the specimen was normal to the beam and the electron beam was incident on the salt particle no aluminum peak was observed. However, when the specimen was tilted, some of the electron beam incident on the particle was reflected to hit the alumina substrate and give rise to alumina peaks in the EDX spectrum. This is shown in Figure 32 and it appears that the aluminum peaks sometimes observed from the salt or deposit surfaces are artefacts caused by the above mechanism. In the light of this explanation it is now possible to discuss the conversion of sodium chloride to sodium sulfate on alumina substrates.

Sodium chloride may react with O_2, SO_2 and SO_3 in the gas stream to form sodium sulfate as a surface layer on the original salt crystal. Alternatively sodium chloride may evaporate and form sodium sulfate on the alumina substrate by interacting with the sulfurous gas species there. A further possibility is that NaCl gas may react with O_2, SO_2 and SO_3 in the gas phase and form Na_2SO_4 which will then deposit on the alumina substrate. This latter possibility is ruled out by the appearance of the alumina substrate at short reaction times which shows discrete nucleation sites where Na_2SO_4 formation has started. It is also

unlikely that stable nuclei of the solid Na_2SO_4 would be able to form in the gas phase, heterogeneous nucleation on the alumina surface being more likely.

The amount of deposit that occurs on the alumina substrate depends upon the vapor pressure of sodium chloride, since this increases with temperature it is expected, and observed, that at higher temperatures a greater fraction of the sodium sulfate is formed from the gas phase on the alumina substrate and a smaller fraction actually forms on the original salt crystal surface.

Data on sodium chloride vapor pressures are available.[27] According to the $NaCl-Na_2SO_4$ phase diagram[28], in Figure 22, a eutectic liquid containing about 63 mol% Na_2SO_4 is formed at 625°C. Flood, Forland and Nesland[29] have determined that the $NaCl-Na_2SO_4$ liquid solutions are practically ideal, however in eutectic liquids, especially close to the eutectic temperature, some deviation is to be expected. In the absence of data in this region however, ideal solution behavior will be assumed in order to calculate the approximate sodium chloride vapor pressures that are in equilibrium with the liquids. Details of the calculations are given in Appendix IA and presented in Table I from which it can be seen that the values of P_{NaCl} increase substantially with increasing temperature indicating that the role of evaporation of sodium chloride in the conversion reaction becomes more predominant at higher temperatures.

Table I also contains values of the equilibrium SO_3 partial pressures for each atmosphere and temperature calculated according to the equation.

$$SO_2 + 1/2\ O_2 = SO_3;\quad \Delta G^\circ = -22600 + 21.36\ T\ \text{cal}. \tag{16}$$

using the conditions for air containing, initially, 1% SO_2 and 0.2% SO_2 respectively

$$P_{SO_2} + P_{SO_3} = 0.01 \tag{17}$$

and

$$P_{SO_2} + P_{SO_3} = 0.002 \tag{18}$$

Fielder, Stearns and Kohl[8,9] followed the conversion of sodium chloride single crystals in air containing SO_2, over the temperature range 400-550°C, where evaporation of NaCl was not predominant and could even be neglected up to 500°C. They found that the reaction proceeded at a constant rate which could be represented by

$$k = 0.6\ P_{SO_3}\ \exp\ (-22000/RT)\ \text{mg cm}^{-2}\ \text{sec.}^{-1} \qquad (19)$$

where P_{SO_3} is in atmospheres and R is in J mol^{-1} deg.^{-1}

These rates are also given in Table I for each temperature together with the times required for a particle 100μm thick to be converted completely. The estimation of these rates and reaction times is given in Appendix IB. It can be seen that the time for conversion to Na_2SO_4 by reaction remains fairly constant at 160-200 minutes whereas the evaporation time is reduced from 18000 minutes at 500°C to about 13 minutes at 700°C.

This is broadly in confirmation of the results obtained in the present investigation when, at 500°C, some sodium chloride remained after 240 minutes whereas the reaction was substantially complete after 30 minutes at 700°C. This confirms that the gas atmospheres had achieved equilibrium or very close to it, since Fielder et al[8,9] found that unequilibrated gas mixtures reacted at rates slower by three orders of magnitude than rates observed with equilibrated mixtures. Initial experiments were catalysed using platinum but in the majority of experiments catalysis occured on the base metal thermocouple wire. The survival of NaCl in the present experiments, carried out at 700°C, for times greater than several minutes indicates that the Na_2SO_4 coating formed on the NaCl particle serves to restrict the evaporation of NaCl from the salt particle surface. It is not clear where the primary reaction site is, however, there will be transport of NaCl, SO_3, SO_2 and O_2 gas species in opposite directions through the Na_2SO_4 layer.

Thus, reaction to produce Na_2SO_4 may occur at three positions, the NaCl surface, within the porous Na_2SO_4 deposit and at the Na_2SO_4 – gas interface. At low temperatures, a compact Na_2SO_4 scale should be expected to form which will restrict NaCl evaporation which will be small in any case. This will result in long reaction times as the transport of gas species through a more compact layer is slow. In this case the reaction site is likely to be the NaCl surface as SO_3 and O_2 arrive there. At higher temperatures, as the NaCl pressure increases, the scale formed is more porous and the NaCl flux increases such that the reaction site moves to the outer surface of the Na_2SO_4. In all cases some NaCl evaporates to form Na_2SO_4 on the surrounding substrate. This process becomes more important at the higher temperatures.

A further very important factor in the reaction is that liquids may form as mentioned previously. The formation of liquids occurs both on the salt particle and on the surrounding alumina substrate. For instance, during experiments carried out at 650 and 700°C a zone of liquid has apparantly been formed around the original salt particles. This is particularly wide spread at 700°C.

The liquid is thought to form by the dissolution of NaCl from the vapor phase to form a eutectic liquid with the Na_2SO_4 deposit that has formed. This occurs very rapidly since, where the liquid forms, it is present after very short times into the reaction and probably forms immediately the first Na_2SO_4 formation occurs. Since the source of the sodium chloride vapor is the original salt particle, the vapor pressure of NaCl will be greatest over the particle and will then decrease at sites further away from the particle. There will, therefore, exist a sodium chloride vapor pressure gradient around any salt particle. The liquid will form at sites on the alumina substrate where the sodium chloride vapor pressure corresponds to those over a eutectic liquid of the appropriate composition. For instance at 650°C, the eutectic composition ranges from 0.32 to 0.47 mol fraction NaCl and from 0.25 to 0.58 mol fraction NaCl at 700°C. Correspondingly it is

expected that the liquid phase will be more widespread at the higher temperatures.

The formation of sodium sulfate on the alumina substrate will proceed so long as the original sodium chloride particle is capable of maintaining a partial pressure of NaCl in the gas phase. Thus, at 500°C, where the partial pressure of NaCl is low only sparse Na_2SO_4 formation on the alumina is expected. Of course the reaction will continue for longer times than at higher temperatures and the salt particle is not exhausted even after several hours. Under these conditions, below the NaCl-Na_2SO_4 eutectic temperature, liquid phases cannot form and, correspondingly, formation of Na_2SO_4 only, with no deposition of NaCl, can occur on the substrate. The only opportunity for NaCl deposition to occur would be on areas whose temperatures are lower than that of the original particle.

Very similar observations can be made for the reactions carried out at 600°C. The only difference being that, due to the higher NaCl partial pressure, more copious formation of Na_2SO_4 occurs on the alumina substrate. Since 600°C is below the NaCl-Na_2SO_4 eutectic temperature there is no trace of NaCl in the deposits formed on the alumina.

The mechanism by which NaCl converts to Na_2SO_4 at temperatures below 625°C is given in Figure 33. This illustrates clearly the formation of the sulfate both on the substrate and on the original particle.

At temperatures above 625°C at which the NaCl-Na_2SO_4 eutectic may form, the reaction proceeds in a very similar manner and the mechanism is illustrated in Figure 34.

The initial sodium sulfate formation occurs on the salt particle from which NaCl vapor evaporates rapidly at these temperatures. The NaCl vapor reacts with O_2, SO_2 and SO_3 on the surface of the alumina substrate to form the deposit of Na_2SO_4. Simultaneously, at sites close to the original NaCl particle, NaCl from the vapor forms a eutectic liquid with the Na_2SO_4. This can only occur where the

NaCl partial pressure is sufficiently high to support the presence of the appropriate mol fraction of NaCl in the liquid. At sites further from the original particle only solid sodium sulfate forms. The liquid can only remain so long as the appropriate NaCl vapor pressure is maintained above it. Therefore the later stages of tl reaction involve the exhaustion of the original salt particle by the joint processes of NaCl evaporation and conversion in situ to Na_2SO_4, when this occurs the NaCl in the liquid cannot be supplied continuously and it also converts to Na_2SO_4. Thus, once the NaCl supply has been exhausted, the deposit becomes solid Na_2SO_4. Conversely the deposition of fresh sodium chloride on surfaces covered with solid sodium sulfate will give rise to the formation of the liquid phase above 625°C. The liquid will have only a transient existence, unless the supply of NaCl can be maintained.

Thus, it is feasible that attack typical of that in the presence of liquid Na_2SO_4 may occur at temperatures below the melting point of sodium sulfate and, on examination, only solid sodium sulfate be detected.

The halo areas that have been observed are thought mainly to represent the larger size of the originally applied NaCl particles before they underwent shrinkage by evaporation

The effects of water vapor were seen to be twofold. First the morphology of the sodium sulfate produced a change to definite, regular, large crystalline growths with pores down the center that had well developed crystal faces. Secondly the reaction rate appeared to be increased. This was more evident at the higher temperature. Both of these observations can be explained by assuming that a new vapor species is formed in the presence of water vapor. Such a species is unlikely to involv simply the addition of oxygen to give oxychloride molecules involving sodium since these could form in the absence of water in the oxidizing atmospheres used. Stearns[23] has identified complex molecules involving (NaOH) groups in volatile.

species, similarly the possibility of forming NaCl $(H_2O)_x$ or $(NaCl)_x(NaOH)_y$ types exists. There is also the possibility that enhanced surface diffusion may explain the more definite crystalline form of the Na_2SO_4 produced as well as the apparent faster reaction rates in the presence of H_2O.

The faster reaction, better defined crystallinity of the sulfate product and its mode of growth all indicate that a vapor species is being produced and evaporating more rapidly than the NaCl.

The rapid evaporation confines the reaction with the atmosphere to the outer surfaces of the sulfate crystals that are forming, thus promoting the well defined crystallinity that is observed.

The development of a new vapor species, of greater volatility than NaCl, also explains the apparently faster reaction rates since, as shown later and given in Table I, the chemical reaction proceeds at about the same rate over the 500–700°C temperature range whereas the increase in reaction rate observed at higher temperatures arises from the increased volatility of NaCl. Thus an increase in reaction rate at constant temperature can be achieved by the formation of a highly volatile species.

It is expected that the vapor species is produced by reaction between H_2O and NaCl either at the NaCl surface or within the gas space in the porous Na_2SO_4 reaction product. The vapor flux produced apparantly excludes SO_2 and O_2 from penetrating the porous reaction product to any marked extent and confines the reaction forming Na_2SO_4 largely to the outer surfaces of the crystalline deposit.

The vapor species has not been identified and further work using mass spectrometry will be needed to identify it.

II. REACTIONS BETWEEN NaCl DEPOSITED ON A GROWING ALUMINA SUBSTRATE IN AN OXIDIZING ATMOSPHERE CONTAINING SULFUR DIOXIDE.

RESULTS

In these experiments the alloy HOS 875 (Fe-20Cr-5Al-1Zr-0.5Si) was used, supplied by NASA-Lewis. The α-Al_2O_3 scales formed on this alloy have been well characterized by Smialek and found to be mechanically stable and capable of surviving the heating and cooling stresses associated with preoxidation treatment.

Coupons measuring 10 X 5mm were preoxidized for 12 hours at 1300°C which produced an adherent α-Al_2O_3 film about 6μm thick. The typical surface and cross section after preoxidation are shown in Figure 35 in which the smooth metal-scale interface and the complete absence of iron and chromium in the alumina scale is shown. Specimens cooled slowly in the furnace formed a compact adherant scale free from cracks and spallation.

The preoxidized specimens were mounted on the pedestal and inserted into the hot zone of the reaction furnace. Particles of NaCl were placed on the specimen which was then exposed to the atmosphere of air containing sulfur dioxide. These experiments were carried out at 600, 650 and 700°C for 10, 20, 30 and 60 minutes.

In general, the morphological changes of the salt particles were identical to those observed on an alumina substrate and reported previously, however, the deposits formed on the substrate surface were different. The results of this part of the investigation, carried out in an atmosphere of air + 1% SO_2, are presented below.

600°C

In the early stages of reaction under these conditions the salt particles become covered with sodium sulfate growing from many nucleation centers on the salt particle and sodium sulfate also forms on the surrounding substrate surface.

After 60 minutes much of the original salt has evaporated or reacted leaving a surface coated with sodium sulfate.

650°C

The reaction begins by early coverage of the salt and substrate by sodium sulfate reaction product. After 20 minutes the original alumina scale appears to have been lost from some areas, perhaps by spallation. The surface exposed in these areas shows strong EDS response for Fe, Cr and Al only and is therefore presumably the metal surface underlying the original scale. It is not clear whether this separation occured at temperature or during cooling from the reaction temperature. The general deposit on the substrate surface did not appear to have been liquid in spite of the fact that, under identical conditions, using an alumina substrate, the eutectic $NaCl-Na_2SO_4$ liquid was found to form. EDS results showed very clear evidence of sodium and sulfur in the deposit but not a trace of chlorine.

700°C

As at the lower temperatures, a general Na_2SO_4 reaction product deposit is formed, there is also some clear evidence of freshly spalled and severely disrupted areas as seen in Figure 36 which shows the surface after 20 minutes reaction time. These areas have very strong Fe and Cr EDS peaks as if these elements have managed to diffuse out to the scale-gas interface to a greater extent than in other areas which appear to be rich in aluminum. The general scale areas, showing Al, Na and S EDS peaks have a glazed appearance of having been liquid with typical rounded features although no eutectic structure can be seen.

Very similar features are observed after an exposure of 60 minutes at 700°C. In the cases of both solid alumina and a growing alumina scale as substrates, the early formation of sodium sulfate on the salt particle is identical in morphology,

however no liquid formation is apparent on the growing alumina scale after 20 minutes whereas on the pure alumina substrate there is ample evidence of the existence of $NaCl-Na_2SO_4$ eutectic liquid.

In order to obtain further information about the reactions occuring on pre-oxidized samples, those samples exposed at 700°C were mounted, sectioned and polished under kerosene to avoid dissolution of water soluble products.

The sample exposed at 700°C to air + 1% SO_2 for 30 minutes shows, from Figure 37, a compact layer of alumina next to the metal with an overlying layer of sodium sulfate which is, in places, rich in iron and chromium being brown in color at these places.

Figure 37 is a section through a site where a salt particle impacted and then converted to sodium sulfate. An area where Na_2SO_4 deposited by reaction of NaCl, SO_2, SO_3 and O_2 gases on the alumina surface was also evident to the right of this particle. There is no chlorine response from this section.

The alumina layer appears to be compact, continuous and uncontaminated, on the other hand, strong EDX responses for iron and chromium do not appear above the alumina layer in surrounding areas where the sodium sulfate covering the alumina formed by vapor reaction as described previously It is most likely that the iron and chromium gained access to the scale-gas interface from an adjacent site where the alumina scale was disrupted physically.

Such a possibility is verifiedby the appearance of a section of a specimen similarly exposed for 60 minutes. In this case the section, shown in Figure 38, has cut through a severely disrupted alumina layer. The alumina layer is still seen to be quite pure and compact but also physically damaged, being broken in several places and displaced from the metal surface by the formation of compounds rich in iron and chromium at the metal-scale interface. From the distribution of elements shown in Figure 38 it appears that the alumina layer is surmounted by the sodium

sulfate layer which contains a substantial amount of iron. Below the alumina layer exist chromium compounds, mainly a thin layer of sulfide with iron and chromium oxide above it. Chlorine is again absent from this specimen, however, after 30 minutes at 700°C, chlorine has usually left the system as volatilized NaCl or Cl_2 from the conversion reaction. The absence of chlorine in these sections indicates that other, non volatile, chlorides had not formed. The predominant features are the outward migration of iron and chromium, the inward migration of sulfur and the rupture of the protective alumina scale.

The reaction sequence appears to consist of deposition of sodium sulfate, formation of the chloride-sulfate eutectic, penetration of the alumina scale leading to inward sulfur migration and outward iron migration. From the appearance of the alumina scale fragments in Figure 38, it is most likely that the elimination of protective behavior is due to physical disruption of this scale. The mechanism by which such disruption occurs apparently involves the formation of iron and chromium compounds, involving sulfur, at the metal-scale interface which can only occur if sulfur has access to the metal-scale interface. Therefore, the initial vital step in the mechanism, leading to distruction of the protection afforded by the alumina scale, is the penetration of this scale by sulfur bearing species. This may occur by physical mechanisms involving cracks or by chemical mechanisms involving dissolution of the alumina.

Since preliminary experiments had shown preoxidized slow cooled scales to be free from cracks, attention was turned to the attack of the alumina scale by the liquid $NaCl-Na_2SO_4$ eutectic.

In order to examine simply the attack of the liquid on alumina, alumina disk substrates were used once more. This time the salt was applied to one end only as a saturated aqueous solution to control the distribution of the salt on the

alumina surface. Two such specimens were coated, dried, and exposed to air + 1% SO_2 for 60 minutes at 653 and 700°C. After exposure, the specimen surface showed three zones of quite different morphology as illustrated for the 653°C specimen in Figure 39. The presence of three zones can be understood from the conclusions of Section I concerning the mechanism of conversion of NaCl to Na_2SO_4 in these atmospheres, as follows.

The initial reactions are for the NaCl to evaporate and for Na_2SO_4 to form both on the salt deposit and on the surrounding substrate. Where the NaCl vapor pressure is high enough, eutectic liquid solutions of NaCl-Na_2SO_4 may also form. Thus it is expected that close to the salt deposit a liquid will form, further away only solid sodium sulfate will form. However the liquid deposit is only stable so long as sufficient NaCl is supplied from the original deposit. When this supply falls off, at longer times, the NaCl in the eutectic that converts to Na_2SO_4 can no longer be replaced by NaCl from the atmosphere and the liquid begins to undergo constitutional solidification. This forms a porous zone of Na_2SO_4.

Thus the three zones on the above specimen, shown in Figure 39 are the outer zone which is the original, solid, Na_2SO_4 deposit, the intermediate zone which is the porous Na_2SO_4 formed by constitutional solidification at temperature, and the inner zone which is the zone that was always liquid and shows a solidified eutectic structure.

The same zones, formed on the similar specimen exposed at 700°C, are shown in Figure 40. In this case, the intermediate zone is composed of a compact solid of Na-Cl-S-O eutectic structure in a matrix of Na_2SO_4. The whole had been molten at temperature and, on cooling, primary sodium sulfate and residual eutectic solidification have produced the structure shown in Figure 40. In this Figure it is shown how the observed structures fit the Na-Cl-S-O phase diagram with the chlorine content decreasing from the neighborhood of the original salt deposit through the inner

and intermediate zones to the outer zone which is composed entirely of sodium sulfate.

Both specimens were boiled in slightly acidified, distilled, water in order to dissolve out any soluble salts. Figure 41 shows the surface of the alumina that had been in contact with both liquid and solid (outer zone) deposits at 650°C. From Figure 41, it can be seen that the alumina that had been covered by eutectic liquid at temperature has been severely attacked or etched by the liquid salt. In contrast, little or no attack is seen on the alumina that had been covered by the outer solid Na_2SO_4 zone at temperature.

A similar procedure was followed using preoxidized specimens of HOS 875 in place of the alumina disks. After 60 minutes exposure to air + 1% SO_2 at 650°C the surface showed that a severe attack, shown in Figure 42, had occured similar to that shown in Figure 36 after 20 minutes at 700°C. The scale of this specimen was leached in slightly acidified water which was found to contain traces of sodium chlorine and sulfur, whereas pieces of solid scale that separated and settled during leaching were found to be Al_2O_3 and Fe_2O_3.

Clearly the protective nature of the preformed alumina scale is lost early in the process exposing the more rapidly reacting elements, iron and chromium, to attack. In order to determine whether a liquid NaCl-Na_2SO_4 solution is necessary to initiate such attack, it was decided to examine the effect of various conditions, designed to avoid the formation of liquid phases, on the integrity of the alumina scales formed on HOS 875. To this end two samples of preoxidized HOS 875 were coated with NaCl only and exposed to air for two hours at 650°C and 700°C, two samples were coated with Na_2SO_4 and exposed to air + 1% SO_2 for two hours at 650 and 700°C, a final sample was coated with NaCl and exposed to air + 1% SO_2 at 600°C for two hours.

None of these conditions would lead to the formation of liquid phases and

none of the experiments showed any attack on, or disruption of, the preformed alumina scales as is evident from Figure 43. In all cases the alumina scale appears to be intact and still very protective, furthermore the metal-scale interface is quite free from attack. In repeat experiments,the specimens were leached in boiling acidified water and the resulting alumina surfaces examined. In all cases the alumina retained features characteristic of the original scale surface and showed no signs of chemical attack. These surfaces are shown also in Figure 43. It therefore appears to be necessary for a liquid salt to be present for the initiation of rapid attack of this alloy to proceed.

This still does not explain how the initiation of such attack is achieved. The possibilities are that the liquid dissolves the alumina and exposes the metal to attack, alternatively the liquid may penetrate down existing cracks in the alumina scale to reach the metal and spread along the metal-scale interface forming solid oxide and sulfide phases resulting in expansion and bursting of the alumina layer.

III. INITIATION OF ACCELERATED ATTACK

The aim of this section is to shed light on the mechanisms by which accelerated attack of alumina scales is initiated by $NaCl-Na_2SO_4$ liquid deposits.

The first step taken was to use the technique of 'interrupted' testing to provide a sequence of specimens illustrating the development of morphological features of the attack with time. This technique only produces one result per specimen since the examination in section is destructive, however, it generally yields very valuable information.

Preoxidized specimens of HOS 875 were coated with a saturated aqueous solution of sodium chloride, dried and exposed to the atmosphere containing air + 1% SO_2 at 700°C for 5, 10, 15, 20, 25 and 30 minutes. After exposure, the specimens were mounted, sectioned and examined in the SEM with EDS analysis. The

results are presented below and shown in Figure 44.

5 Minutes Exposure

The alumina layer was intact and apparently unchanged. The sodium chloride coating already contained regions that are sulfur-rich where transformation to Na_2SO_4 had begun. Presumably liquid formation began in these areas. The distribution of sulfur-rich areas throughout the original sodium chloride deposit is an indication of the porous nature of this layer which is, clearly, very easily penetrated by gases. At this stage, there does not appear to have been any accumulation of sulfur at the base of the alumina layer at the metal-scale interface.

10 Minutes Exposure

The alumina layer still appeared to be intact. The sodium chloride layer contained more sulfur with a very strong concentration at the metal-scale interface coincident with a strong presence of chromium and iron. The chromium pattern in particular is a perfect match with that of sulfur and it appears that, in this specimen, a layer of chromium sulfide has formed surmounted by a layer of iron oxide just below the alumina preoxidized scale. The alumina scale itself is not ruptured but is tilted and it is more than likely that this section is taken to one side of a site at which disruption of the alumina scale occured.

15 Minutes Exposure

By this stage of the reaction even random sectioning of the sample produces evidence that the alumina layer has become bent and broken as seen in Figure 44. Some areas may also be found where the alumina has remained in firm contact with, and adhered to, the surface.

The zone between the broken alumina layer and the metal shows a strong iron presence, some Cr and a little sulfur. The salt layer shows high concentrations of sulfur and chlorine and has been molten. Some iron is distributed both above

and below the broken alumina layer, probably as iron oxides. There is also evidence, from EDS responses, that some sodium, chlorine and sulfur is present inside the broken alumina layer between it and the metal surface. These EDS responses coincide and indicate the presence of liquid $NaCl-Na_2SO_4$ eutectic in this zone with which some aluminum is evidently associated at the metal surface.

20 Minutes Exposure

The observations are essentially similar to those described above after 15 minutes exposure, the difference is one of degree only in that the presence of sodium, chlorine and sulfur, above and below the broken alumina scale, is more definite and is also associated with iron in these areas, the iron EDX image does not correspond as precisely to the sulfur as the sodium image does and the iron is probably present partially as oxide. There appear to be responses also to chromium, iron and sulfur on the metal surface, a weak response to aluminum is also seen generally in the area covered by molten salt above and below the broken alumina layer.

25 Minutes and 30 Minutes Exposure

Chromium remains concentrated on the metal surface and also just below the alumina layer, whereas iron is more generally distributed on both sides of the broken alumina layer. Sulfur shows a concentration on the metal surface that coincides with the iron and chromium there, also on both sides of the broken alumina layer coinciding with the presence, in these places, of sodium and chlorine.

In addition, after 30 minutes there is clear evidence of some layering of the aluminum, chromium and sulfur, immediately above the metal surface; these EDX images are not coincident with any other images and indicate the formation of of chromium sulfide and alumina at this place. Immediately above this is an iron-rich zone of, probably, iron oxides which is surmounted by another layer rich in aluminum, chromium, sulfur, sodium and chlorine. Immediately

above this is the broken alumina scale above which is the melt of $NaCl-Na_2SO_4$ with some NaCl particles that have not completely reached yet, although clearly less NaCl remains than at shorter times.

Discussion

The most important conclusion drawn from the above observations is that steps in the initiation of hot corrosion begin as soon as a liquid $NaCl-Na_2SO_4$ can form in contact with the alumina layer. The alumina layer remains whole and undistorted while a layer of chromium and aluminum sulfides and oxides forms below it; between this layer and the alumina layer, formation of iron oxides apparantly occurs. The formation of these compounds between the alumina scale and the metal surface causes expansion, lifting and breaking the alumina scale as shown in subsequent micrographs. From this point the liquid salt melt gains ready access to the metal surface and proceeds to lead to the formation of sulfides of aluminum and chromium and oxides of iron and aluminum. The question that arises, consequently, is how the sulfur, and oxygen, penetrate the alumina scale initially.

In order to answer this question, two experiments were carried out in which specimens of HOS 875 were coated with NaCl and exposed to the air + 1% SO_2 atmosphere for 5 minutes and 10 minutes respectively at 700°C. They were then leached in dilute, 0.1N, hydrochloric acid to remove all soluble salts. The washed surface of the scale was then examined under the scanning electron microscope. The surface observed after 5 minutes is shown in Figure 45 and it is clear that the alumina scale has been heavily etched, or attacked, the grain corners became rounded and pinholes are revealed especially at the grain boundaries. Some of these features are merely depressions while others are holes in the alumina at the base of some of which small nodules are growing. These nodules, which are more clearly shown in Figure 46, after 10 minutes, are

rich in iron and chromium, the grain boundaries are also attacked. The alumina grains of the scale on each side of the boundary appear to be starting to bulge away from the metal surface as a result of the iron, chromium and aluminum compounds growing under the boundary. This represents the first stages in the initiation of cracking. It is apparent from Figures 45 and 46 that pinholing of the alumina and attack at the grain boundaries by the molten salt has lead to the ingress of the molten salt to attack the metal below at the metal-scale interface, however alternative possibilities must also be considered.

The first possible alternative is that thermal cracking may be responsible for the initial damage to the alumina layer. All of the above experiments were carried out under slow heating and cooling of the specimens to avoid inducing thermal cracking. However, two further experiments were carried out in which preoxidized metal substrates without NaCl coatings were heated, under identical conditions to the previous specimens, in air without SO_2 at 650°C and 700°C for one hour. These specimens were cooled to room temperature with the furnace. Figure 47 shows that no obvious change in appearance of the surface scale occured during this treatment, in particular no evidence of crack formation was found. It is therefore unlikely that the initial damage to the alumina is caused by thermal cracking.

A further possible mechanism to explain the initial lifting of the alumina scale is by the formation of volatile chlorides at the scale-metal interface, once the initial penetration of the alumina scale has been achieved which previous experiments, illustrated in Figure 43, have confirmed requires the presence of the $NaCl-Na_2SO_4$ liquid.

A further possibility would be that sulfurous gases penetrate the alumina layer from the atmosphere and lead to formation of sulfides and oxides at the metal-scale interface. Evidence of this occurring in nickel and cobalt systems has already been documented (30,31) therefore it was prudent to check the

possibility in this case. Penetration of the alumina scale was not observed in the cases referred to in Figure 43 which involved various salt deposits exposed to air + 1% SO_2 at temperatures which avoided liquid formation. In order to confirm this at 700°C, a preoxidized HOS 875 specimen, uncoated, was exposed at 700°C to air + 1% SO_2 for one hour. After this treatment, the surface and cross section were examined by SEM and EDS techniques. It was found, as shown in Figure 48, that the scale surface was unaltered by this treatment and that there is no evidence of sulfur having been transported across the alumina layer.

Since all of these tests involved exposures of one hour and failed to provoke either damage to the alumina layer or its penetration by sulfur, and since sulfides begin to form after 5-10 minutes at the alumina-metal interface when a molten $NaCl-Na_2SO_4$ salt is formed on the surface, it must be concluded that a molten salt is neccessary for the initiation of the breakdown of the alumina scale which occurs by chemical attack to form pinholes as shown in Figures 45 and 46.

The mechanisms by which alumina dissolves in the salt is almost certainly by acid dissolution as shown in Appendix II.

An alternate mechanism by which the scale could be attacked is by the formation of volatile $AlCl_3$. According to the reaction

$$Al_2O_{3(s)} + 6\ NaCl_{(e)} = 2\ AlCl_{3(g)} + 3\ Na_2O_{(e)} \qquad (20)$$

This is considered also in Appendix II and rejected as being most unlikely.

Once the pinholes form and the liquid salt gains access to the metal surface the conditions are somewhat different since the presence of the metal will cause metal sulfides and oxides to form thus imposing low sulfur and oxygen partial pressures on the system. In this case the formation of volatile chlorides by direct reaction between the salt and metal should be considered according to reactions such as

$$4M + 2\ NaCl + Na_2SO_4 = MCl_{2(g)} + MS + 2\ MO + 2\ Na_2O \qquad (21)$$

This possibility is considered also in Appendix II, taking the case most likely to produce the volatile chlorides which involves the formation of Cr_2O_3 and Cr_2S_3. As shown in Appendix II these reactions result in low partial pressures of the chlorides.

After the pinholes have been made, the next step is that the original alumina scale lifts from the metal and cracks. At this point the liquid salt gains easy access to the scale-metal interface in general and very rapid reaction ensues.

From the calculations made in Appendix II, it is almost certain that the vapor pressures of the volatile chlorides are not high enough to cause the alumina scale to lift. Thus it can be confirmed that the original alumina scale is lifted and caused to break by the formation of sulfides and oxides of iron and chromium at the scale-metal interface by direct reaction between the metal and the molten salt penetrating from the pinholes.

As a result of the observations made during this program, the following conclusions may be drawn.

Conclusions

1. The conversion of sodium chloride to sodium sulfate proceeds by two parallel mechanisms. Reaction on the surface of the NaCl with SO_2 and O_2 leads to the formation of a porous layer of Na_2SO_4, simultaneously the evaporation of NaCl from the NaCl surface into the gas stream leads to the formation of Na_2SO_4 as a deposit on the substrate surrounding the particles.
2. The relative importance of the two mechanisms changes with temperature, in situ conversion being more important below 550°C whereas evaporation is overwhelmingly more important above 600°C.

3. Above 625°C, the eutectic temperature in the $NaCl-Na_2SO_4$ system, the sodium sulfate formed takes up some sodium chloride to produce an aggressive liquid in the atmospheres used.
4. In the atmospheres used, the liquid salt formed above 625°C attacks the alumina substrate by acidic dissolution.
5. When the substrate is a growing layer, the attack by liquid $NaCl-Na_2SO_4$ is not uniform but is more pronounced at selected sites such as grain boundaries and unidentified sites on the grain surface. The alumina layer is rapidly penetrated by the liquid salt at these sites to make contact with the metal.
6. When the salt contacts the metal, oxidation and sulfidation of the metal results in the formation of iron and chromium oxides and sulfides in the case of HOS 875.
7. It is thought that some of the oxide formed will dissolve in the salt and eventually diffuse out to be precipitated on the outside where the oxygen potential is higher.
8. The growth of oxide and, mainly, sulfide at the scale-metal interface leads to the massive lifting of the alumina scale with consequent disruption and loss of protection. From this point very greatly accelerated attack ensues as the molten salt solution gains ready access to the metal surface.
9. It is thought to be unlikely that the formation of volatile chlorides is responsible for the lifting and fracture of the alumina scale.
10. It has not been possible to establish whether the role of NaCl is simply to provide a low temperature liquid phase or whether it plays a specific role in the aggressive attack of this liquid on the alumina.

APPENDIX I

A. Calculation of NaCl Vapor Pressures and Evaporation Rates

The vapor pressures of NaCl in equilibrium with solid and liquid NaCl respectively are given by[27]

$$(\text{Solid}) \log P_{NaCl} = -12440/T - 0.9 \log T - 0.46 \times 10^{-3} T + 14.31 \quad \text{(AI.1)}$$

$$(\text{Liquid}) \log P_{NaCl} = -11530/T - 3.48 \log T + 20.77 \quad \text{(AI.2)}$$

where the pressures are in mm of mercury.

Values of the partial pressure of sodium chloride at temperatures between 500-700°C are given in Table I. At 650°C the liquid phase that exists may contain a range of sodium chloride contents as indicated. The relevant sodium chloride partial pressures are also given using the assumption of ideal solution

$$P_{NaCl} = X_{NaCl} P^{\circ}_{NaCl} \quad \text{(AI.3)}$$

where X_{NaCl} is the mole fraction of NaCl in the liquid and P°_{NaCl} is the partial pressure of NaCl that would be in equilibrium over pure liquid NaCl at that temperature.

The rate of evaporation of NaCl from the salt surface will depend on its vapor pressure and the flow of the furnace atmosphere gases over the specimen surface. In general the evaporation flux may be expressed as

$$\mathcal{J}_{NaCl} = k (P_{NaCl} - P^{at}_{NaCl}) \quad \text{(AI.4)}$$

where P_{NaCl} and P^{at}_{NaCl} are the partial pressures in equilibrium with the NaCl and in the general atmosphere respectively. The transfer coefficient k can usually be expressed as D/δ where D is a diffusion coefficient and δ is a boundary layer thickness. Values of D for sodium chloride vapor are not available however values could be calculated from ideal gas kinetics and found to be in the range of 1-2 $cm^2\ sec^{-1}$ over the temperature range 500-700°C. Values of δ will vary over the surface. However it is expected that both δ and D will increase with temperature and to a first approximation k will be assumed to be constant over the narrow temperature range 500-700°C.

In the present case the partial pressure of sodium chloride in the furnace atmosphere, P^{at}_{NaCl}, is negligible, thus it can be assumed that the of NaCl is given by

$$J_{NaCl} = k\, P_{NaCl} \tag{AI.5}$$

where k is approximately independent of temperature between 500-700°C.

The maximum possible rate of evaporation of NaCl may be calculated using the Hertz-Langmuir equation

$$J_{NaCl} = \alpha \frac{P_{NaCl}\ 1.06 \times 10^{6}}{(2\Pi M_{NaCl}\ RT)^{1/2}} \tag{AI.6}$$

where J_{NaCl} is the flux of NaCl in mol cm^{-2} sec^{-1}

P_{NaCl} is the pressure in atmospheres

M_{NaCl} is the molecular weight of NaCl in gm mol^{-1}

R is the gas constant in ergs mol^{-1} deg^{-1}.

α is a constant less than or equal to unity.

Values obtained from this equation are the maximum possible and may not be achieved even when evaporating into a vacuum. In practice, evaporation rates substantially below those predicted from this equation are expected to be observed.

Since evaporation is known to be strongest at 700°C in the present study where the vapor pressure is about 10^{-5} atm. a value of k may be found and applied to other temperatures, thus it is seen that

$$\frac{(J\,NaCl)_{T1}}{(J\,NaCl)_{T2}} = \frac{(P\,NaCl)_{T1}}{(P\,NaCl)_{T2}} \tag{AI.7}$$

It is therefore possible to estimate the time that would be required to remove a 100μm thick NaCl particle if it is noted that such a particle survives for 60 minutes at 650°C. Particle survival times, in the absence of reaction may be calculated as

$$\frac{(t_{50})_{T2}}{(t_{50})_{T1}} = \frac{(P_{NaCl})_{T1}}{(P_{NaCl})_{T2}} \qquad \text{(AI.8)}$$

values calculated for evaporation times at the various temperatures used are given in Table I.

It can be seen that the evaporation rate is very slow at 500°C taking an estimated 18,000 minutes to remove the 100μm particle compared with 1016 minutes for the complete conversion by reaction following Fielder. On the otherhand the 100μm diameter particle will be removed in 13 minutes at 700°C. This is largely in accordance with observations made in this study which showed that general deposition over the alumina surface increases markedly with temperature.

B. Calculation of Rate of Conversion of NaCl to Na_2SO_4

According to Fielder et al (8,9). The rate of conversion of NaCl single crystals in air containing SO_2 over the temperature range 400-550°C is represented by

$$k = 0.6\ P_{SO_3} \exp(-22000/RT)\ \text{mg cm}^{-2}\ \text{sec.}^{-1} \qquad \text{(AI.9)}$$

where P_{SO_3} is in atmospheres and R is in J mol.^{-1} deg.^{-1}. Over this temperature range evaporation of sodium chloride is extremely slow, as shown in Table I, and may be neglected. The reaction by which conversion of NaCl to Na_2SO_4 occurs is

$$2\ NaCl + SO_2 + O_2 = Na_2SO_4 + Cl_2 \qquad \text{(AI.10)}$$

Thus, for every mole of NaCl converted, the weight gained is

$$m = 1/2\ (M_{SO_2} + M_{O_2} - M_{Cl_2}) \qquad \text{(AI.11)}$$

where M_x is the molecular weight of species X. Thus weight is gained at the rate of 1.25×10^4 mg. per mol of NaCl converted, and the above reaction rate may be expressed as

$$R = 4.8 \times 10^{-5}\ P_{SO_2} \exp(-22000/RT)\ \text{mol cm}^{-2}\ \text{sec. 1)} \qquad \text{(AI.12)}$$

Values of the calculated rates are given in Table I for both air + 1% SO_2 and air + 0.2% SO_2 atmospheres.

Since the reaction rate is constant for a given atmosphere and temperature, being controlled by a surface process, it is possible to estimate the time required to to completely react a 100μm thick NaCl crystal. This is the time to convert a 50μm thickness of NaCl which is estimated as

$$t = \frac{50 \times 10^{-4}}{R. \bar{V}_{NaCl}} \text{ seconds}$$

where R is the appropriate reaction rate in mol cm^{-2} $sec.^{-1}$ and $\bar{V}_{NaCl}$ is the molar volume of NaCl (27 cm^3 mol^{-1}). Similar estimates for the removal of NaCl by evaporation can be carried out using the appropriate evaporation rate in place of R.

Values for the estimated times to convert or remove 50μm of NaCl by reaction or evaporation respectively are given in Table I.

TABLE I

RATES OF REACTION AND EVAPORATION DURING CONVERSION OF NaCl to Na_2SO_4

TEMP. °C	500	550	600	650	700
$P_{NaCl(s)}$ atm	2.4×10^{-8}	2.0×10^{-7}	1.3×10^{-6}	7.2×10^{-6}	3.3×10^{-5}
$P_{NaCl(\ell)}$ atm	8.3×10^{-8}	5.0×10^{-7}	2.8×10^{-6}	1.2×10^{-5}	4.4×10^{-5}
$X_{NaCl(\ell.sol)}$				0.32 - 0.47	0.25 - 0.58
$P_{NaCl\ (\ell.sol)}$				$(3.8\text{-}5.6) \times 10^{-6}$	$(1.1\text{-}2.5) \times 10^{-5}$
P_{SO_3} atm(air + 0.99% SO_2)	0.010	0.009	0.008	0.007	0.005
P_{SO_3} atm (air+0.2% SO_2)	0.0019	0.0018	0.0016	0.0014	0.0011
Reaction Rates from Fielder (mol cm^{-2} sec^{-1})					
K(air + 0.99% SO_2)	1.60×10^{-8}	1.71×10^{-8}	1.84×10^{-8}	1.89×10^{-8}	1.55×10^{-8}
time for 50µm min.	193	181	168	163	199
K(air + 0.2% SO_2)	3.04×10^{-9}	3.42×10^{-9}	3.68×10^{-9}	3.78×10^{-9}	3.41×10^{-9}
time to remove 50µm min.	1016	903	839	817	905
time, min., to remove 50µm. by evaporation only	18000	2160	332	60	13

APPENDIX II

A. Mechanism of Dissolution of Alumina in $NaCl-Na_2SO_4$ Melts.

According to Stroud and Rapp[32] alumina shows its minimum solubility in Na_2SO_4 melts at a sodium oxide activity of 10^{-9}. Thus alumina is expected to dissolve by basic dissolution, forming aluminate ions, at sodium oxide activities greater than 10^{-9} according to a basic fluxing mechanism.

$$Al_2O_{3(s)} + Na_2O_{(\ell)} = 2\ NaAlO_{2(\ell)} \qquad \text{(AII.1)}$$

or

$$Al_2O_3 + O^{2-} = 2\ AlO_2^- \qquad \text{(AII.2)}$$

At sodium oxide activities less than 10^{-9} alumina is expected to dissolve according to an acid fluxing mechanism

$$Al_2O_3 = 2\ Al^{3+} + 3O^{2-} \qquad \text{(AII.3)}$$

The data of Stroud and Rapp has recently been revised quite drastically by Pullockaran and Rapp[33] such that the minimum solubility of alumina in liquid sodium sulfate is now thought to occur at sodium oxide activities of 10^{-15}. Furthermore these data refer to a temperature of 927°C and do not extend to the lower temperatures that can only be reached in the liquid state by multicomponent systems.

However the activity of sodium oxide may be calculated in the case of the $NaCl-Na_2SO_4$ liquids obtained in this investigation at 700°C as follows.

$$Na_2SO_4 = Na_2O + SO_3;\ \Delta G^\circ = 101600\ \text{cal.} \qquad \text{(AII.4)}$$

the equilibrium constant for which is

$$K = 1.5 \times 10^{-23}$$

Putting the mol fraction of sodium sulfate, $X_{Na_2SO_4}$, equal to 0.75 and 0.42 to represent the range of liquid composition possible at 973K and putting $P_{SO_3} = 5 \times 10^{-3}$ atm and 1.1×10^{-3} atm for the atmospheres used (from Table I) it can be seen that the

sodium oxide activities in the liquids formed in the present work are expected to lie between 1.02×10^{-20} and 1.26×10^{-21}. Under all of the conditions used at 700°C, the low sodium oxide activity should ensure that dissolution of alumina occurs by the acid mechanism.

The presence of NaCl is expected to have the effect simply of ensuring that a liquid phase is formed and that the Na_2SO_4 exists in the liquid at an activity somewhat less than unity. The possibility that it may affect the sodium oxide activity should be examined however. The sodium chloride in converting to Na_2SO_4. consumes SO_2 and O_2

$$2NaCl + SO_3 + 1/2\ O_2 = Na_2SO_4 + Cl_2 \qquad \text{(AII.5)}$$

This reaction will control the partial pressure or chemical potentials of SO_2 O_2 and Cl_2 so long as both NaCl and Na_2SO_4 are present in the melt.

Thus the activity of Na_2O which is set up according to

$$Na_2SO_4 = Na_2O + SO_3 \qquad \text{(AII.6)}$$

will be influenced by the presence of NaCl and the appropriate reaction to consider would be the sum of the two above reactions

$$2\ NaCl + 1/2\ O_2 = Na_2O + Cl_2 \quad ; \quad \Delta G^\circ_{973} = 87425 \text{ cal.} \qquad \text{(AII.7)}$$

If it is assumed that equilibrium is reached in this reaction (which is by no means certain) then we have

$$a_{Na_2O} = a^2_{NaCl} \frac{P_{O_2}^{1/2}}{P_{Cl_2}} \times 2.3 \times 10^{-20} \qquad \text{(AII.8)}$$

Unfortunately, values of P_{O_2} and P_{Cl_2} are not available, they are also difficult to estimate since the reaction will almost certainly, in practice, involve dissolved oxygen and chlorine. If the reaction proceeds quickly then the chlorine concentration is likely to be increased to saturation with P_{Cl_2} = 1 atm whereas the oxygen will be consumed and its content reduced. The instantaneous oxygen content cannot be estimated since the dissolution kinetics for oxygen in the salt are unknown.

However it appears sensible to assume P_{Cl_2} = 1 atm in the salt melt (not

in the atmosphere) in which case

$$a_{Na_2O} = a^2_{NaCl} \cdot P^{1/2}_{O_2} \quad 2.3 \times 10^{-20} \qquad \text{(AII.9)}$$

The value of a_{NaCl} is of the order of 0.5 in these melts whence

$$a_{Na_2O} = P^{1/2}_{O_2} \times 5.8 \times 10^{-21} \qquad \text{(AII.10)}$$

It is therefore not likely that the presence of NaCl in the melt can markedly affect the Na_2O activity and alumina is expected to be attacked by acid dissolution. The formation of intermediate phases in the Al-Na-O-Cl-S system that may increase the rate of attack is possible but at the present time purely speculative.

When the liquid salt penetrates the alumina scale at the pin hole sites it enters a region where the oxygen potential is very low, being controlled by the presence of the alloy. Thus, at the scale-metal interface, the sulfur trioxide partial pressure will be much lower than in equilibrium with the atmosphere and, correspondingly, the oxygen ion activity, or Na_2O activity, will rise. The presence of a low oxygen activity, due to the formation of alloy metal oxides, will also increase the sulfur activity to levels at which metal sulfides can form which accounts for the observed iron and chromium oxides and sulfides indicated in Figure 44. For instance in Figure 44, after 5 minutes exposure, a layer is seen below the alumina layer that has a high Cr content but low Fe and S contents and is, therefore, probably a layer of Cr_2O_3. Such Cr_2O_3 formation would greatly reduce the oxygen activity of the liquid salt and thus cause the sulfur activity to increase and lead to the formation of iron and chromium sulfides. This is infact seen after 10 minutes, in Figure 44, where a high sulfur content layer is seen also with relatively high chromium and low iron content. This is exactly as would be predicted from thermodynamic considerations of the relative stabilities of chromium and iron sulfides. Since Cr will be depleted by forming oxide and sulfide and since diffusion from the bulk of the alloy is slow at these temperatures, iron is gradually enriched in the alloy and eventually iron oxide and sulfide formation would predominate.

The formation and growth of the iron and chromium oxides and sulfides would cause a net volume increase and hence tend to detach the protective alumina scale from the metal surface. This is also seen to occur progressively in Figure 44 in which, at times up to 60 min, the original alumina scale is still very sharply defined and has not dissolved in the molten salt.

The above argument confirms that corrosion of the alumina layer by the molten salt at selected sites, leading to pit formation, is one of the major steps in the initiation of the molten salt attack on the alloy.

B. Possibilities for Volatile Chloride Formation

One final possibility that may lead to rupture of the alumina scale following pitting of the scale is the formation of volatile chlorides of iron, chromium and aluminum. This will now be examined.

The NaCl may react either with the oxides present or with the metal phase. The reactions with the oxides are represented by

$$Al_2O_{3(s)} + 6\ NaCl_{(\ell)} = 2\ AlCl_{3(g)} + 3\ Na_2O_{(\ell)};\ \Delta G^\circ_{473} = 322400\ cal \qquad (AII.11)$$

$$\text{Thus } P_{AlCl_3} = a_{Na_2O}^{-3/2} \times 10^{-38} \qquad (AII.12)$$

where X_{NaCl} is taken to be 0.25 in the liquid $NaCl\text{-}Na_2SO_4$. Thus if $a_{Na_2O} = 10^{-21}$, as calculated for the liquid in equilibrium with the atmosphere, the value of P_{AlCl_3} is 3×10^{-7} atm. However, at the metal scale interface the value of a_{Na_2O} is likely to be substantially higher than 10^{-21} and so P_{AlCl_3} is expected to be correspondingly lower than 3×10^{-7} atm. Thus formation of $AlCl_3$ gas by this mechanism is not expected to reach significant pressures.

Calculation of the vapor pressures expected to obtain at the metal-scale interface is difficult. The reaction involved will be similar to

$$4M + 2\ NaCl + Na_2SO_4 = MCl_2 + MS + 2MO + 2Na_2O \qquad (AII.13)$$

The oxygen and sulfur partial pressures are reduced by reaction with the alloy to form sulfide and oxide. However the activity of the metal species involved is not known, even the species that form sulfide and oxide are not certain.

However since both chromium sulfide and oxide have been observed in the cross sections and since chromium chloride is one of the more volatile chlorides, it is instructive to examine the equilibrium situation of the following reaction which may occur at the metal-scale interface.

$$10/3\ Cr + 2\ NaCl + Na_2SO_4 = CrCl_2 + CrS + 2/3\ Cr_2O_3 + 2\ Na_2O \qquad \text{(AII.14)}$$

$$\Delta G^{o} = 33625 \text{ cal.}$$

The equilibrium situation is given by

$$\frac{P_{CrCl_2} \cdot a_{CrS}\ a^{2/3}_{Cr_2O_3} \cdot a^{2}_{Na_2O}}{a^{10/3}_{Cr} \cdot a^{2}_{NaCl} \cdot a_{Na_2SO_4}} = \exp.\ \frac{-33625}{RT} \qquad \text{(AII.15)}$$

Putting $a_{NaCl} = 0.25$, $a_{Na_2SO_4} = 0.75$, $a_{Cr_S} = 1$

we obtain

$$\frac{P_{CrCl_2} \cdot a^{2}_{Na_2O}}{a^{10/3}_{Cr} \cdot 0.047} = 10^{-7.55} \qquad \text{(AII.16)}$$

The activity of chromium at the alloy scale interface is not known but may be set at $a_{Cr} = 0.2$ from the alloy composition.

since the concentration in the bulk alloy is 20%.

Thus

$$P_{CrCl_2} = \frac{6.2 \times 10^{-12}}{a^{2}_{Na_2O}} \qquad \text{(AII.17)}$$

The value of a_{Na_2O} in the liquid formed at the metal-scale interface is difficult to assess, however, the strong tendency of the metals to form oxides and sulfides will force the reaction below to the right

$$Na_2SO_4 = Na_2O + SO_3 \qquad \text{(AII.18)}$$

and thus the activity of Na_2O is expected to be high rather than low.

In this case the pressure of $CrCl_2$ is expected to reach values between 10^{-4}

and 10^{-12} atm at the metal-scale interface.

It therefore appears reasonable to conclude that the formation of volatiles at the metal-scale interface is unlikely to reach pressures high enough to cause the alumina scale to lift and fracture.

REFERENCES

1. J. A. Goebel, F. S. Pettit, "Na_2SO_4-Induced Accelerated Oxidation (Hot Corrosion) of Nickel," Metallurgical Transactions, (July, 1970), pp. 1943.

2. J. A. Goebel, F. S. Pettit and G. W. Goward, "Mechanisms for the Hot Corrosion of Nickel-Base Alloy," Metallurgical Transactions, Vol. 4, (January, 1973), pp. 261.

3. The 3rd Conference on Gas Turbine Materials in a Marine Environment, Bath, England, September, 1976, "The Fate of Sea Salt in a Marine Gas Turbine, by C. G. McCreath" pp. 1-19.

4. Proceedings of 4th Conference on Gas Turbine Materials in a Marine Environment, June, 1979, "The Fate of Sea Salt in a Marine Gas Turbine, by C. G. McCreath " pp. 339-356.

5. The 3rd Conference on Gas Turbine Materials in a Marine Environment, Bath, England, September, 1976, "Salt Particle Size Effects on Deposit Composition and Hot Corrosion, by C. G. Root, A. R. Stetson".

6. F. J. Kohl, G. J. Santoro, C. A. Fryburg, and D. E. Rosner, "Theoretical and Experimental Studies of the Deposition of Na_2SO_4 from Seeded Combustion Gases," Journal of Electrochemical Society, Vol. 126, No. 6 (June, 1979), pp. 1054-1061.

7. Proceedings of the 4th Conference on Gas Turbine Materials in a Marine Environment, June, 1979, "Aspects of the Aetiology and Mechanisms of Hot Corrosion, by J. F. G. Conde, N. Birks, M. G. Hocking, V. Vasantasree" pp. 385-402.

8. NACE International Conference on High Temperature Corrosion, San Diego, CA., March, 1981, "Formation of $Na_2SO_{4(c)}$ from $NaCl_{(c)}$, and $O_{2(g)}$, by W. L. Fielder, C. A. Stearns, F. J. Kohl, G. C. Fryburg.

9. W. L. Fielder, C. A. Stearns and F. J. Kohl; Reactions of NaCl with gaseous SO_3, SO_2 and O_2. NASA TM 83423, 1983.

10. C. A. Stearns, F. J. Kohl, G. C. Fryburg, The Chemistry of Sodium Chloride Involvment in Processes Related to Hot Corrosion, NASA TM-79251 (Cleveland, Ohio: NASA-Lewis Research Center, 1979).

11. Proceedings of 4th Conference on Gas Turbine Materials in a Marine Environment, June, 1979, "The Influence of Surface on the Conversion of Sodium Chloride to Sodium Sulfate in a Gas Turbine Environment, by E. R. Duffy, A. R. Stetson" pp. 543-563.

12. C. A. Stearns, F. J. Kohl, G. C. Fryburg, R. A. Miller, Interaction of $NaCl_{(g)}$ and $HCl_{(g)}$, with Condensed Na_2SO_4, NASA TM-73796 (Cleveland, Ohio: NASA-Lewis Research Center, 1977).

13. N. S. Bornstein and M. A. DeCrescente, "The Relationship Between Compounds of Sodium and Sulfur and Sulfidation," Trans. Met. Soc. AIME, Vol. 245, (September, 1969), pp. 1947.

14. N. S. Bornstein, M. A. DeCrescente, "The Role of Sodium in the Accelerated Oxidation Phenomenon Termed Sulfidation," Metallurgical Transactions SO_2, (October, 1971), pp. 2875.

15. N. S. Bornstein, M. A. DeCrescente, and H. A. Roth, "The Relationship Between Relative Oxide Ion Content of Na_2SO_4, the Presence of Liquid Metal Oxide and Sulfidation Attack," Metallurgical Transactions, Vol. 4, (August, 1973), pp. 1799.

16. D. K. Gupta and R. A. Rapp, "The Solubilities of NiO, Co_3O_4, and Ternary Oxides in Fused Na_2SO_4 at 1200°K," Journal of Electrochemical Society, Vol. 127, (1980), pp. 2194.

17. D. L. Deadmore, and C. E. Lowell, Effects of Impurities in Coal-Derived Liquids on Accelerated Hot Corrosion of Superalloys, NASA TM-81384 (Cleveland, Ohio: NASA-Lewis Research Center, March, 1980).

18. N. Birks, and G. H. Meier, Introduction to High Temperature Oxidation of Metals (1st Ed.; London, England: Edward Arnold Ltd., 1983).

19. G. C. Fryburg, F. J. Kohl, C. A. Stearns, and W. L. Fielder, "Chemical Reaction Involved in the Initiation of Hot Corrosion of B-1900 and NASA-TRW VIA," Journal of Electrochemical Society, Vol. 129, (March, 1982), pp. 571.

20. M. K. Hossain and S. R. J. Sanders,"A Microstructural Study of the Influence of NaCl Vapor on Oxidation of a Ni-Cr-Al Alloy at 850°C," Oxidation of Metals, Vol. 12, No. 1 (1978), pp. 3.

21. C. S. Giggins and F. S. Pettit "Hot Corrosion Degradation of Metals and Alloys - A Unified Theory" Final Report AFOSR Contract No. F44620-76-C-0123 Pratt and Whitney Aircraft, June 1979.

22. J. B. Johnson, J. R. Nicholls, R. C. Hurst and P. Hancock, "The Mechanical Properties of Surface Oxides on Nickel-Base Superalloys," Corrosion Science, Vol. 18, (1978), pp. 527.

23. G. C. Fryburg, R. A. Miller, F. J. Kohl, C. A. Stearns, "Volatile Products in the Corrosion of Cr, Mo, Ti, and Four Superalloys Exposed to O_2 Containing H_2O and Gaseous NaCl," Journal of Electrochemical Society, Vol. 124, (November, 1977), pp. 1738.

24. J. G. Smeggil, N. S. Bornstein, "Study of the Effects of Gaseous Environments on Sulfidation Attack of Superalloys," Journal of Electrochemical Society, Vol. 125, (August, 1978), pp. 1283.

25. V. E. Henkes, T. E. Strangman, J. B. Wagner, Jr., Effect of Impacted Salt Particles on Hot Corrosion of Coated Superalloys, Final Technical Report for Contract No. N00173-79-C-0475 (Phoenix, Arizona: Garrett Turbine Engine Company, March, 1981).

26. P. Hancock and R. C. Hurst; "Mechanical Properties and Breakdown of Surface Oxide films at Elevated Temperatures" in Advances in Corrosion Science and Technology, ed. R. W. Staehle and M. G. Fontana, Plenum Press, New York, 1974.

27. D. R. Stull, and H. Prophet, JANAF Thermochemical Tables (2nd Ed.; Washington, D.C.: U. S. Department of Commerce National Bureau of Standard, 1971).

28. Ernest M. Levin, Carl R. Rubbins and Howard F. McMurdie, Phase Diagrams for Ceramists (1st Ed., 1969 Supplement, 1975 Supplement; Columbus, Ohio: The American Ceramic Society Inc., 1964, 1969, 1975).

29. H. Flood, T. Forland and A. Nesland, Acta Chem. Scand., Vol. 5, (1951), pp. 1193.

30. M. C. Pope and N. Birks; Oxidation of Metals, 12, 173 (1978).

31. P. Singh and N. Birks; Oxidation of Metals, 19, 37 (1983).

32. Proceedings of the Symposium on High Temperature Metal Halide Chemistry, October, 1977, "The Solubilities of Cr_2O_3 and α-Al_2O_3 in Fused Na_2SO_4 at 1200°K, by W. P. Stroud and R. A. Rapp, pp. 574-594.

33. R. A. Rapp private communication quoted by K. H. Stern in Naval Research Laboratory, Report Memo 4772, March 1982.

STATEMENT

During the period of this contact the following students have been supported:

A. Ashary: Left the project after one year to pursue research into the mechanical stability of growing oxide scales in the same Department.

C. S. Wu: Gained his M.S. as a result of his work carried out between 1981-83 on this project. He has returned to China Steel, Taiwan.

PUBLICATIONS

The substance of this final report is being prepared in the form of a publication and a presentation to the Electrochemical Society, probably in New Orleans, Oct. 1984.

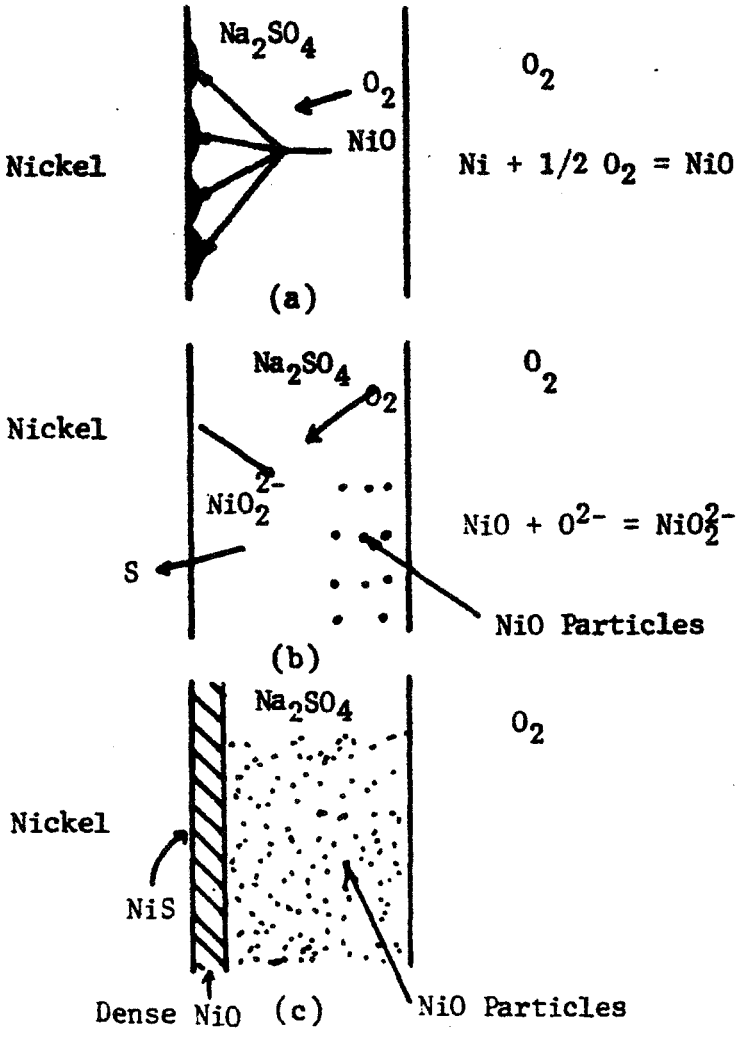

Figure 1: Model for the Na_2SO_4-induced accelerated oxidation of nickel.(following J. A. Goebel, F. S. Pettit)

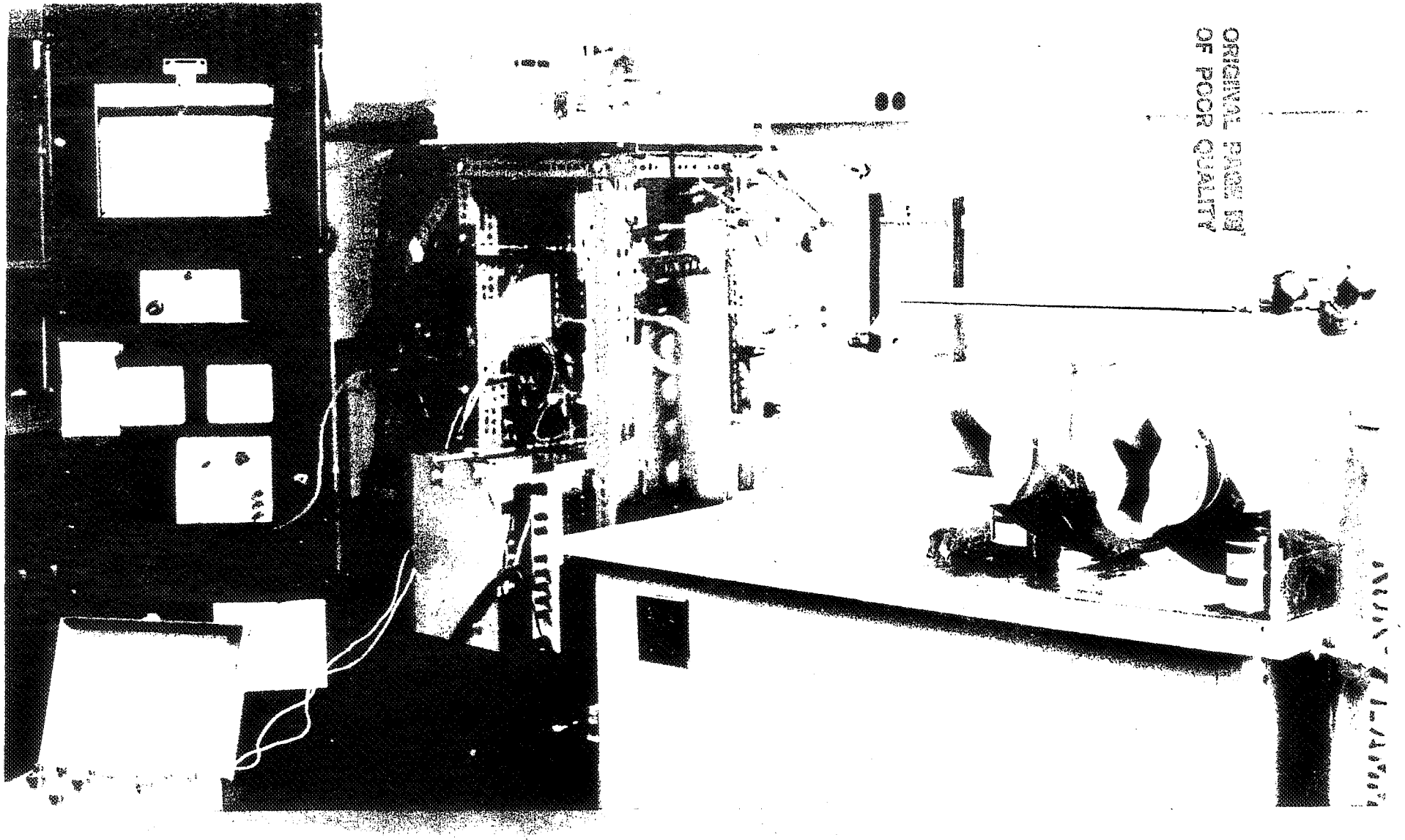

FIGURE 2 Arrangement of the apparatus for investigating the conversion of NaCl to Na_2SO_4.

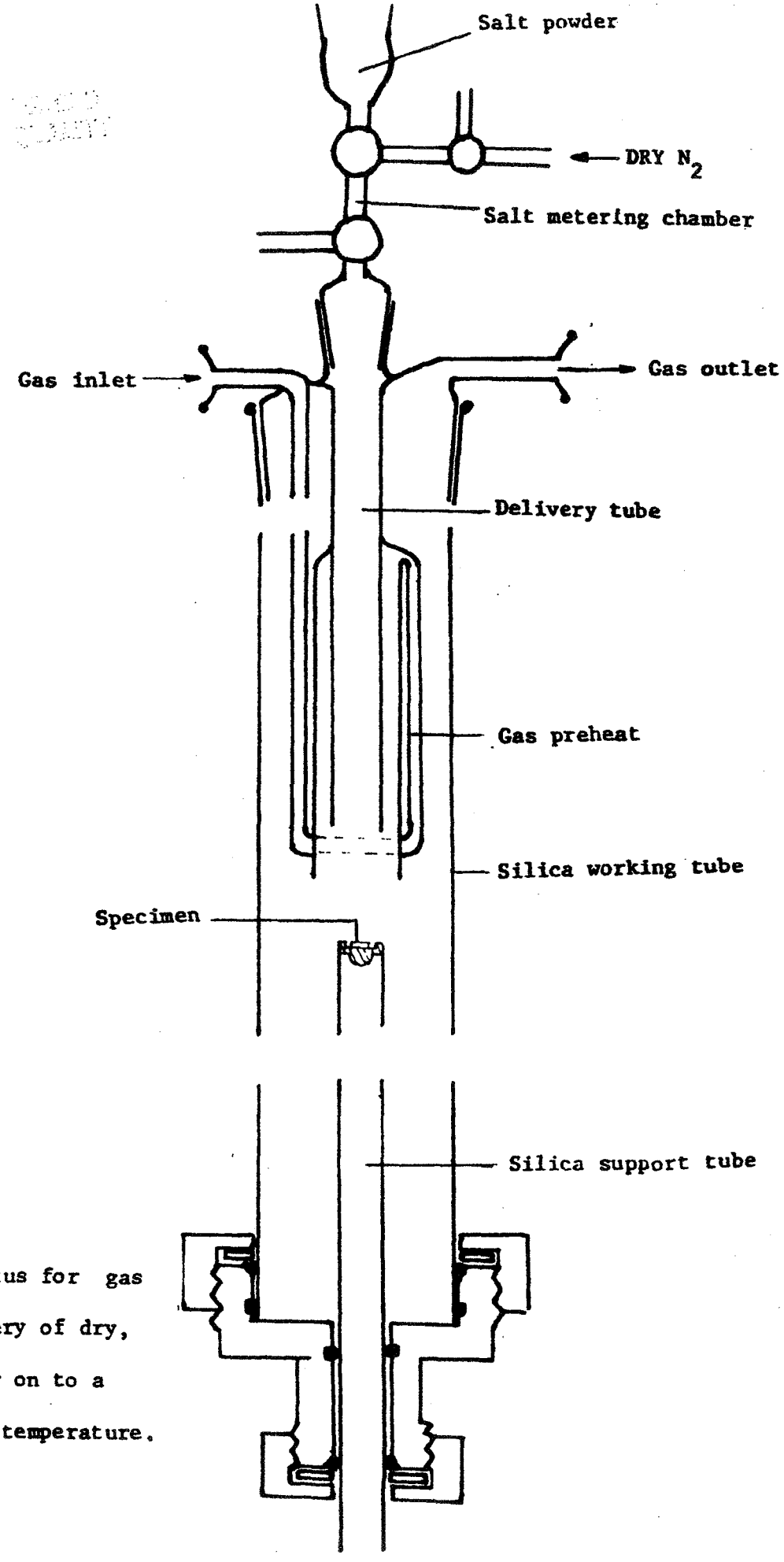

FIGURE 3

Diagram of apparatus for gas preheat and delivery of dry, sized, NaCl powder on to a substrate held at temperature.

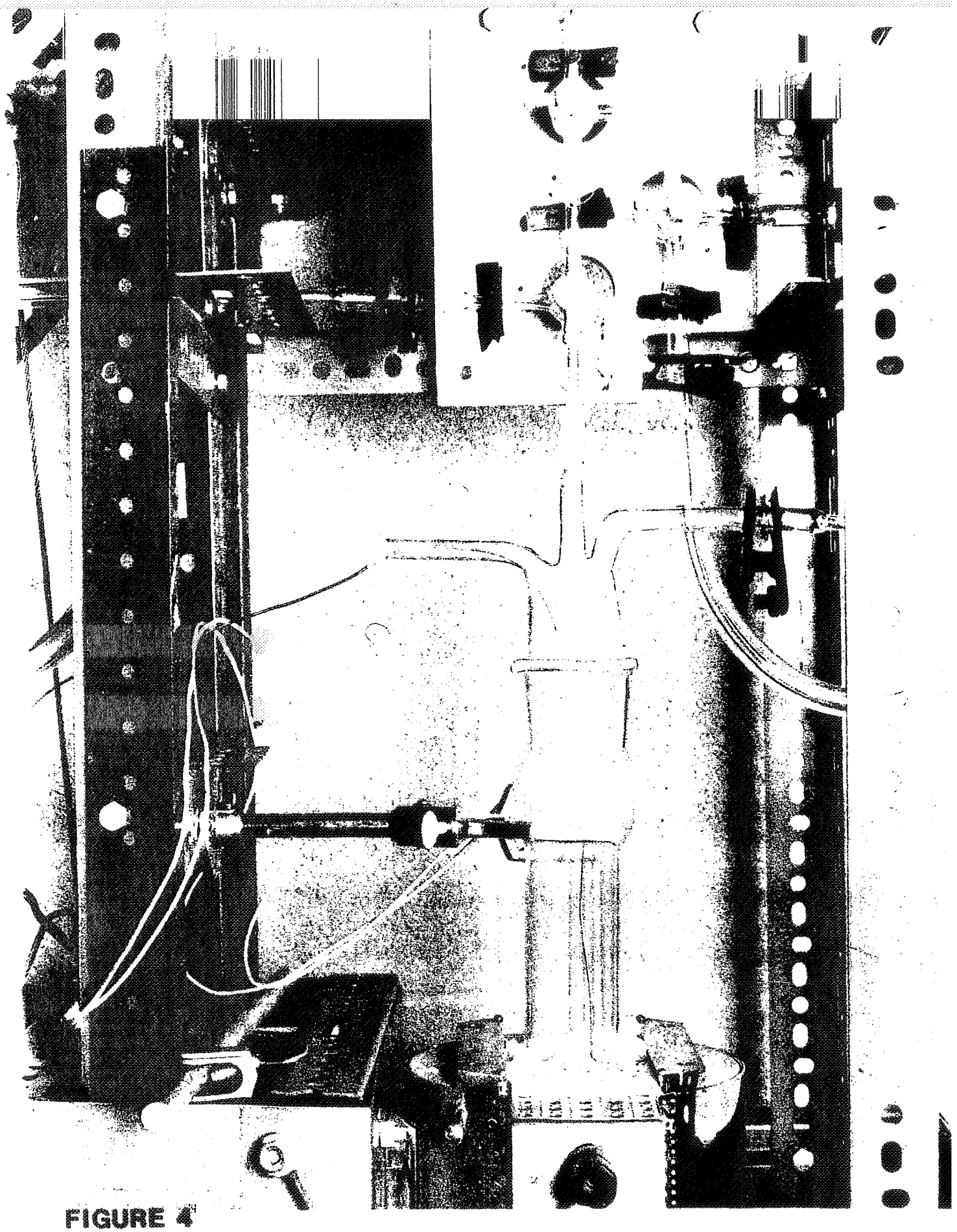

FIGURE 4
Assembly of reaction chamber, furnance, and gas inlet tube.

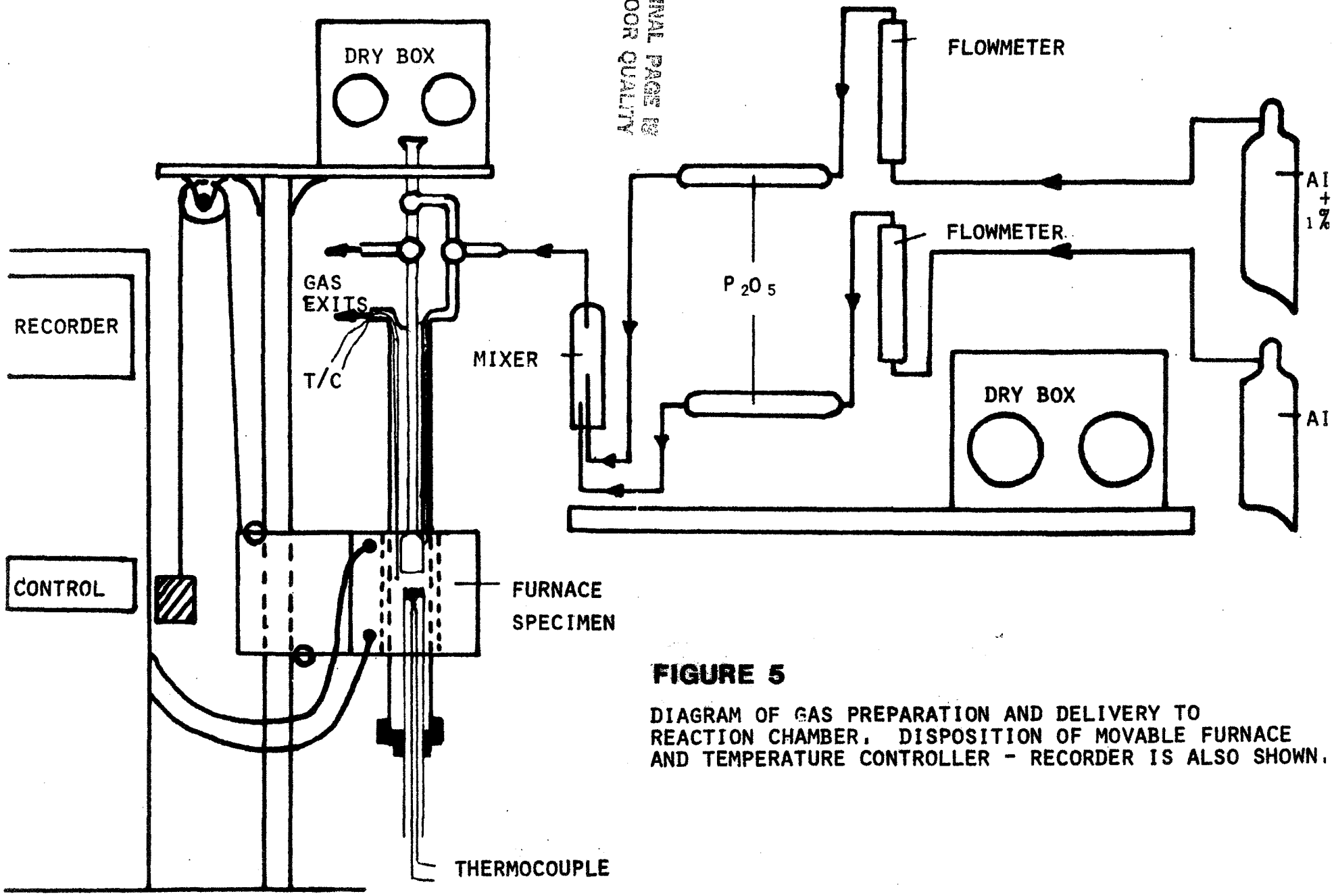

FIGURE 5

DIAGRAM OF GAS PREPARATION AND DELIVERY TO REACTION CHAMBER. DISPOSITION OF MOVABLE FURNACE AND TEMPERATURE CONTROLLER - RECORDER IS ALSO SHOWN.

FIGURE 6 Original NaCl particle

FIGURE 7 Original polished alumina surface

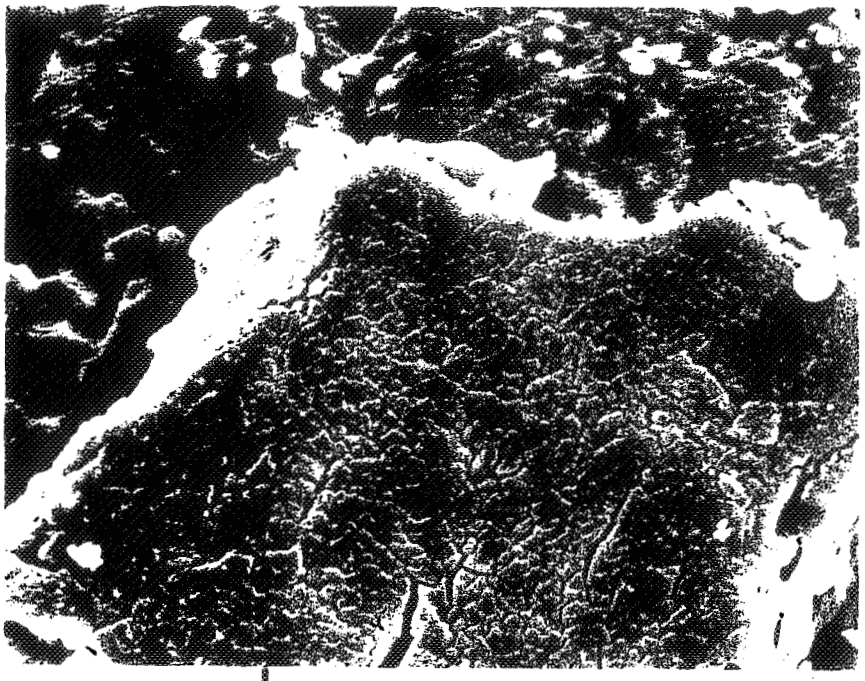

EDAX OF NACL PARTICLE:
TRACE OF SULFUR PRESENT.

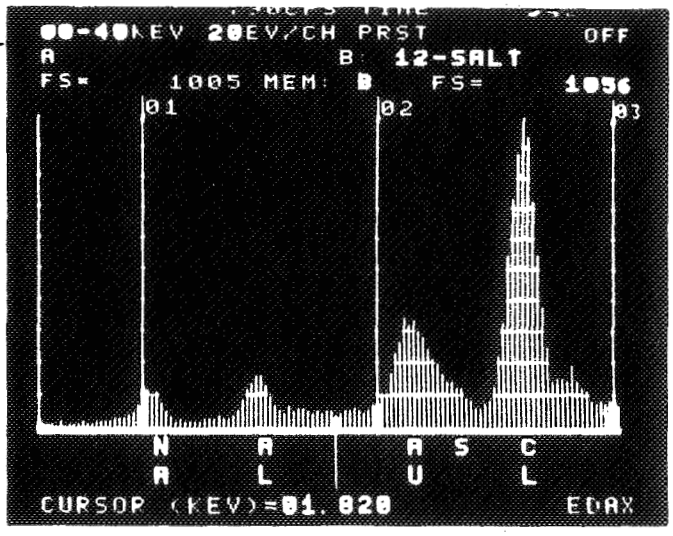

NACL PARTICLE EXPOSED TO AIR PLUS 0.2% SO_2 AT 500^0 C. FOR TWO HOURS.

FIGURE 8

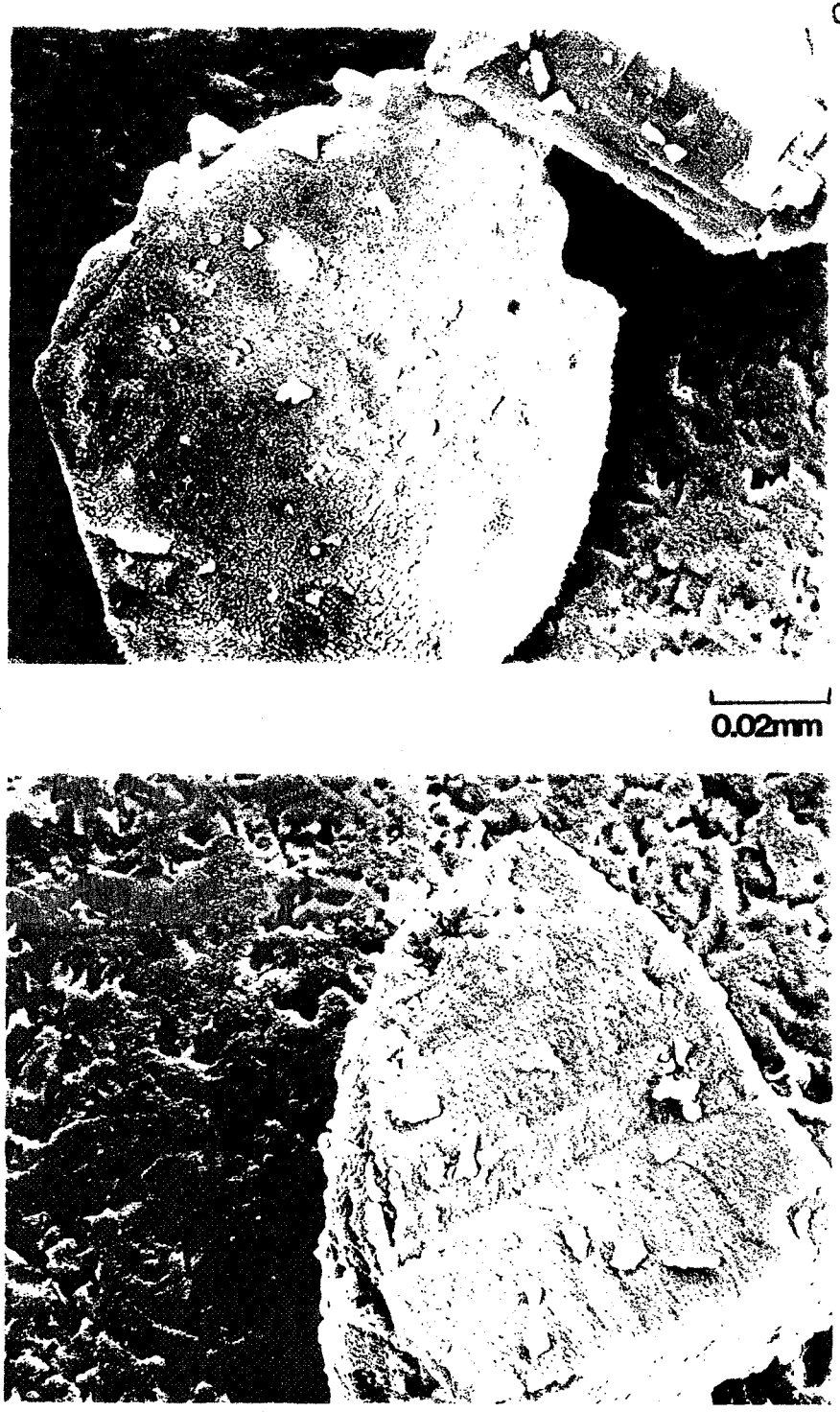

NACL PARTICLES EXPOSED TO AIR AND 0.99 % SO_2 AT 500^{0} C. FOR FOUR HOURS.

FIGURE 9

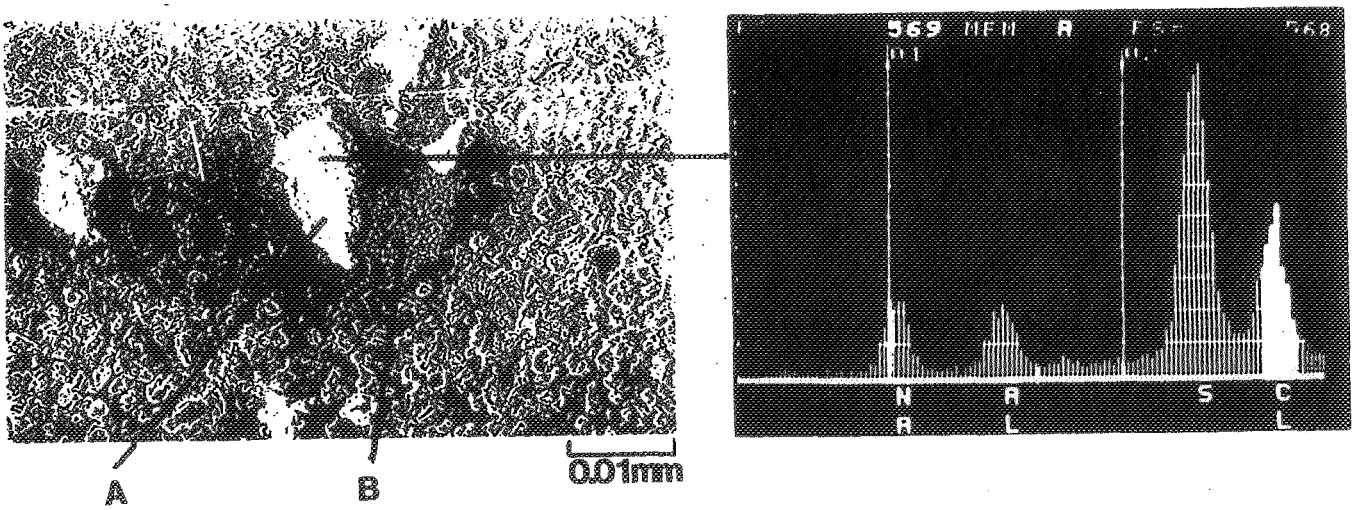

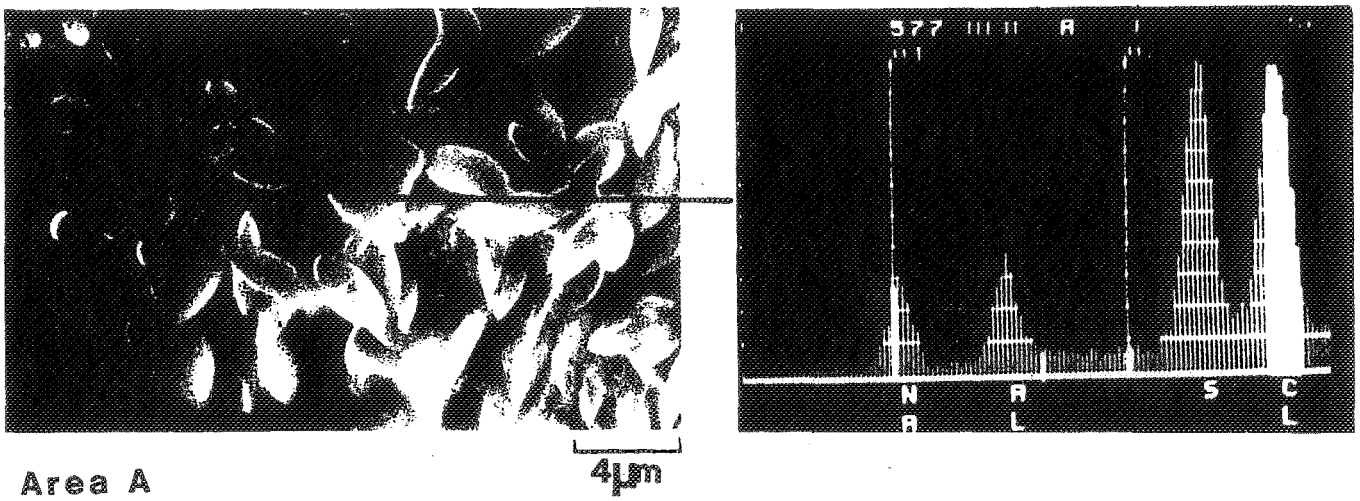

Area A

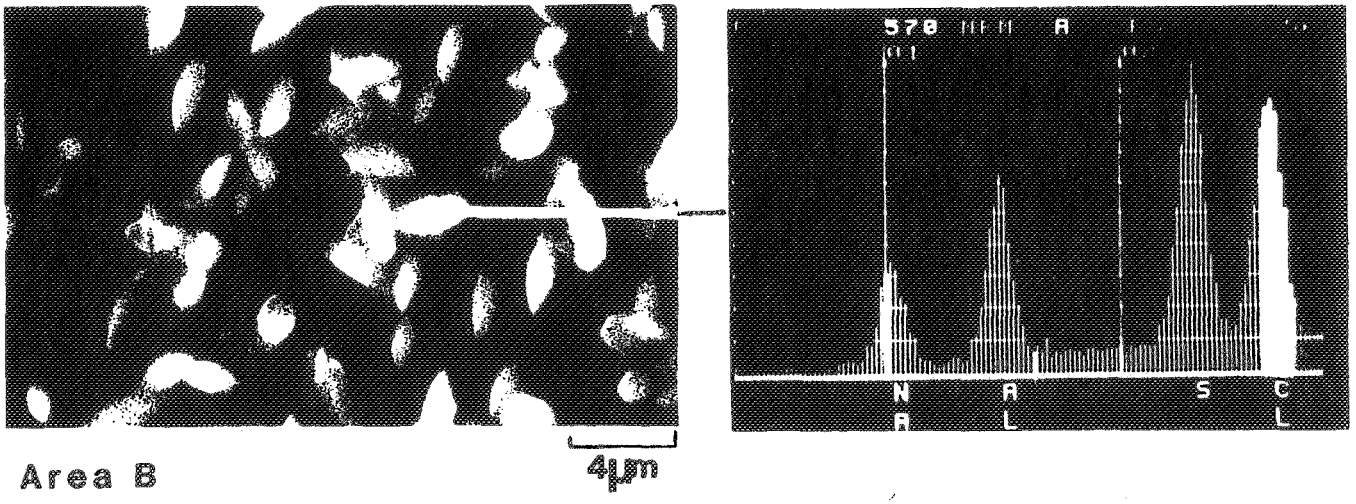

Area B

FIGURE 10 Surface morphology after 480 min exposure to air + 1% SO_2 at 500°C.

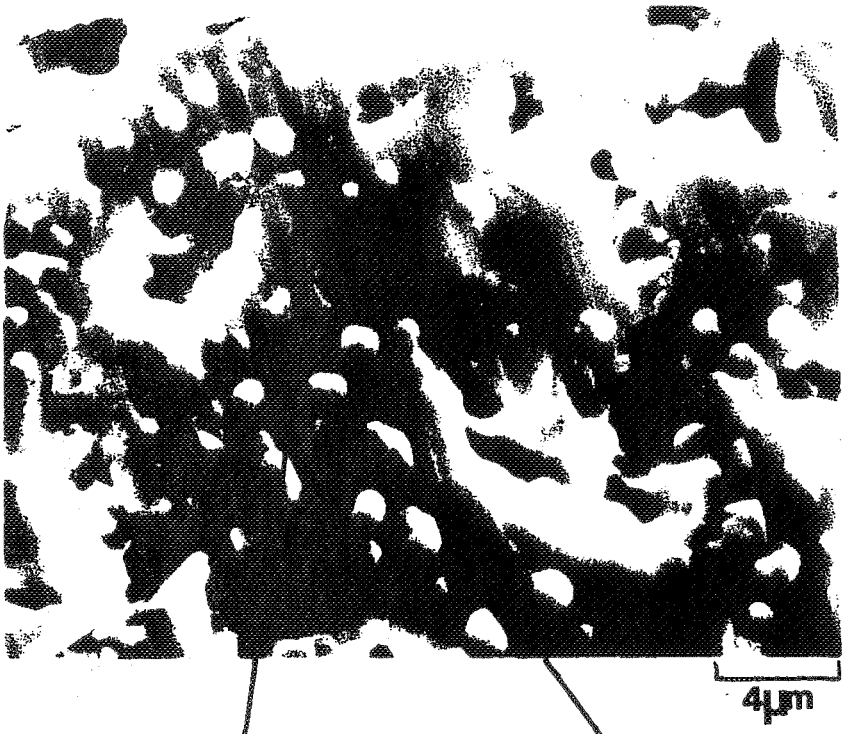

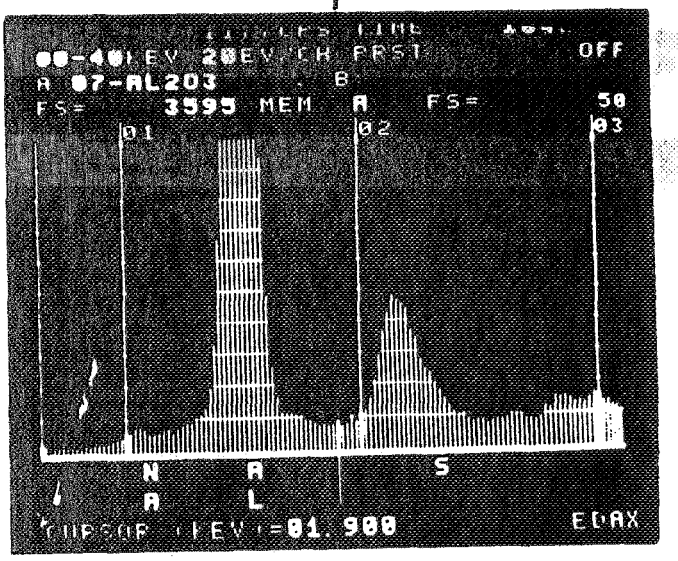

EDAX OF AL_2O_3 SUBSTRATE.

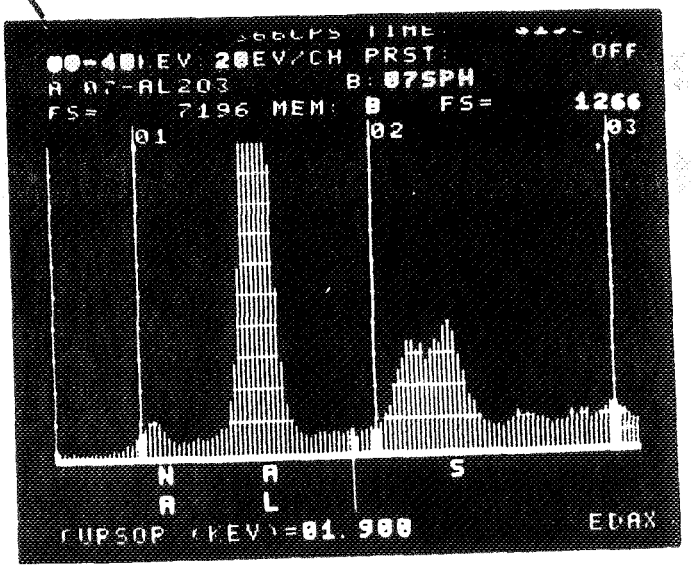

EDAX OF SULFUR-RICH GLOBULES.

AL_2O_3 SUBSTRATE EXPOSED TO AIR AND 0.2% SO_2 AT 600^0 C. FOR 10 MINUTES.

FIGURE 11

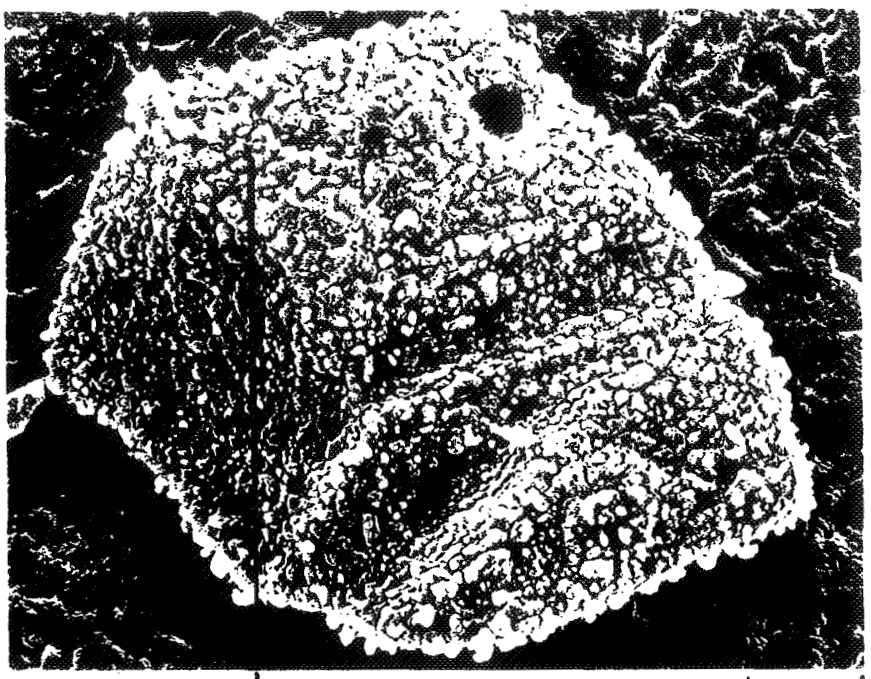

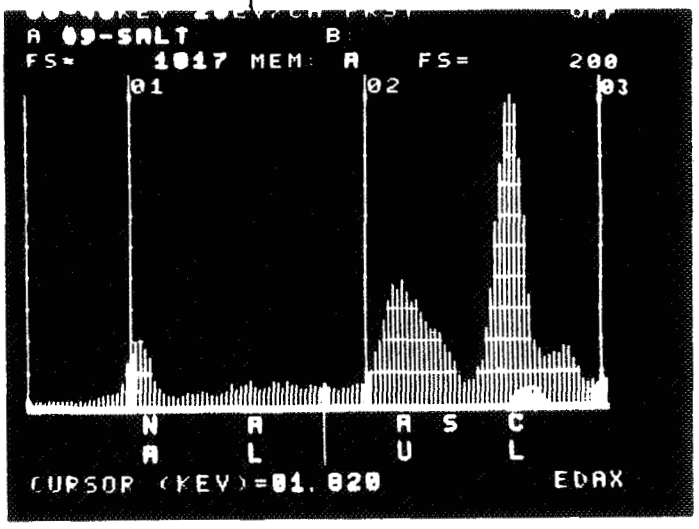

EDAX OF NACL PARTICLE;
SULFUR PEAK PRESENT.

NACL PARTICLE EXPOSED TO AIR AND 0.2% SO_2 AT 600^0 C. FOR 30 MINUTES.

FIGURE 12

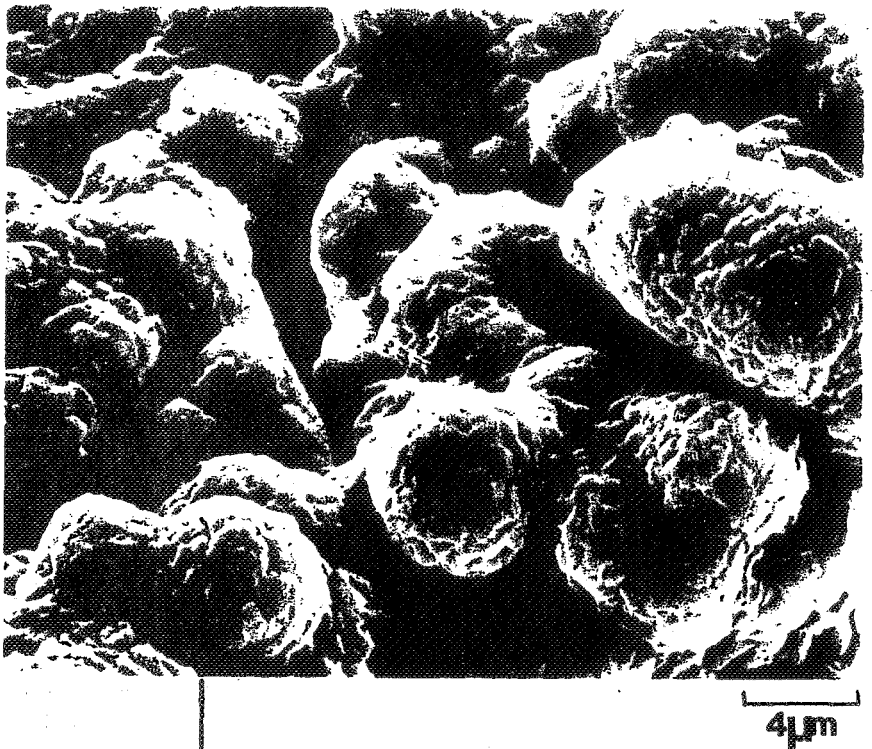

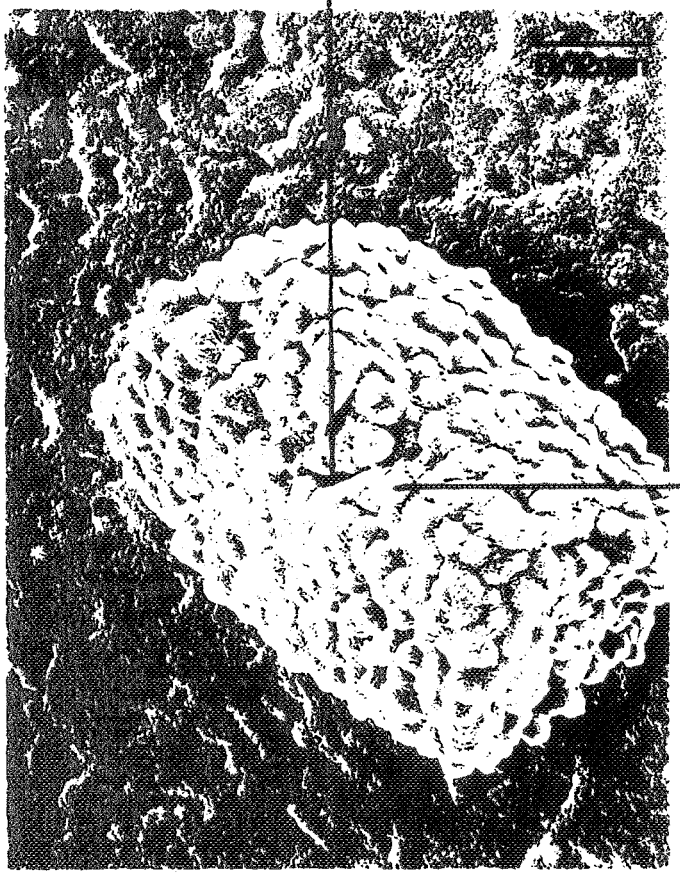

EDAX OF NACL PARTICLE:
HIGH SULFUR CONTENT NOTED.

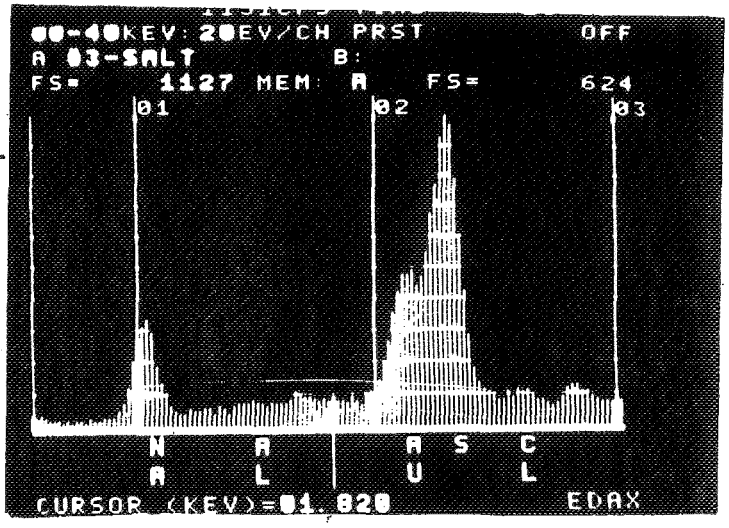

NACL PARTICLE EXPOSED TO AIR AND 0.2% SO_2 AT 600^0 C. FOR TWO HOURS.

FIGURE 13

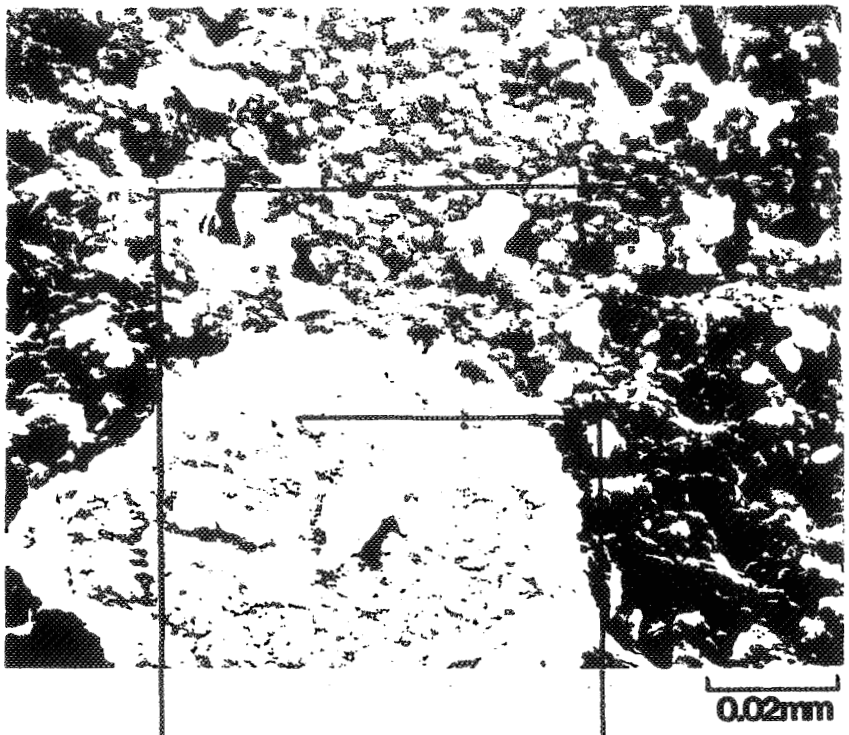

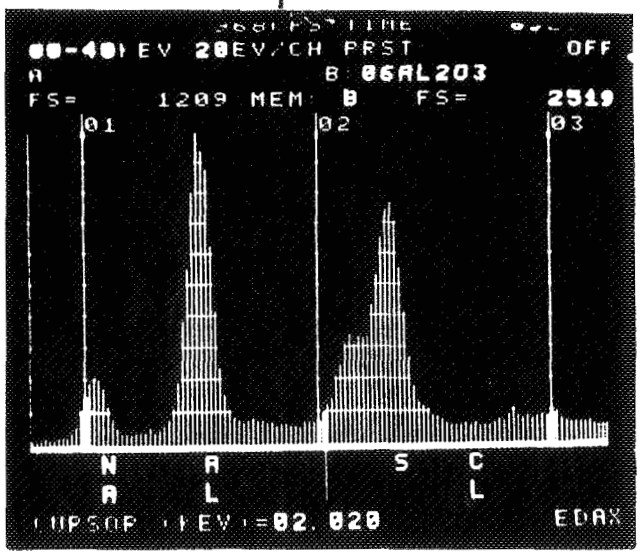

EDAX OF AL_2O_3 SUBSTRATE;
NO CHLORINE PEAK.

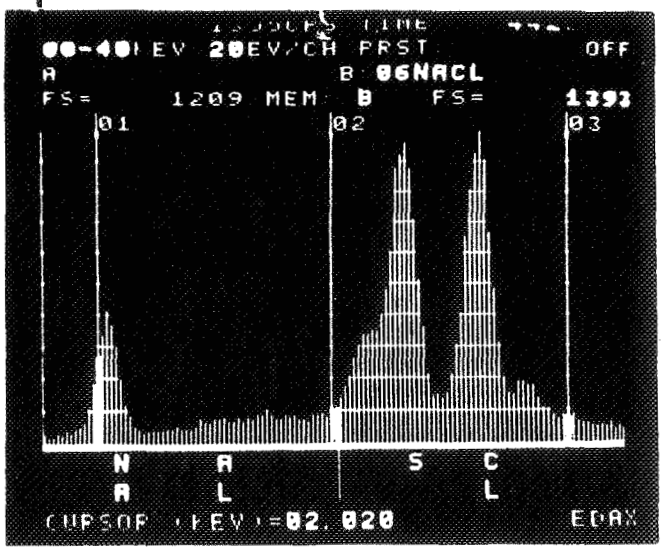

EDAX OF NACL PARTICLE;
SULFUR AND CHLORINE PRESENT.

FIGURE 14

NACL PARTICLE AND AL_2O_3 SUBSTRATE EXPOSED TO AIR AND 0.2% SO_2 AT 600^0 C. FOR FOUR HOURS.

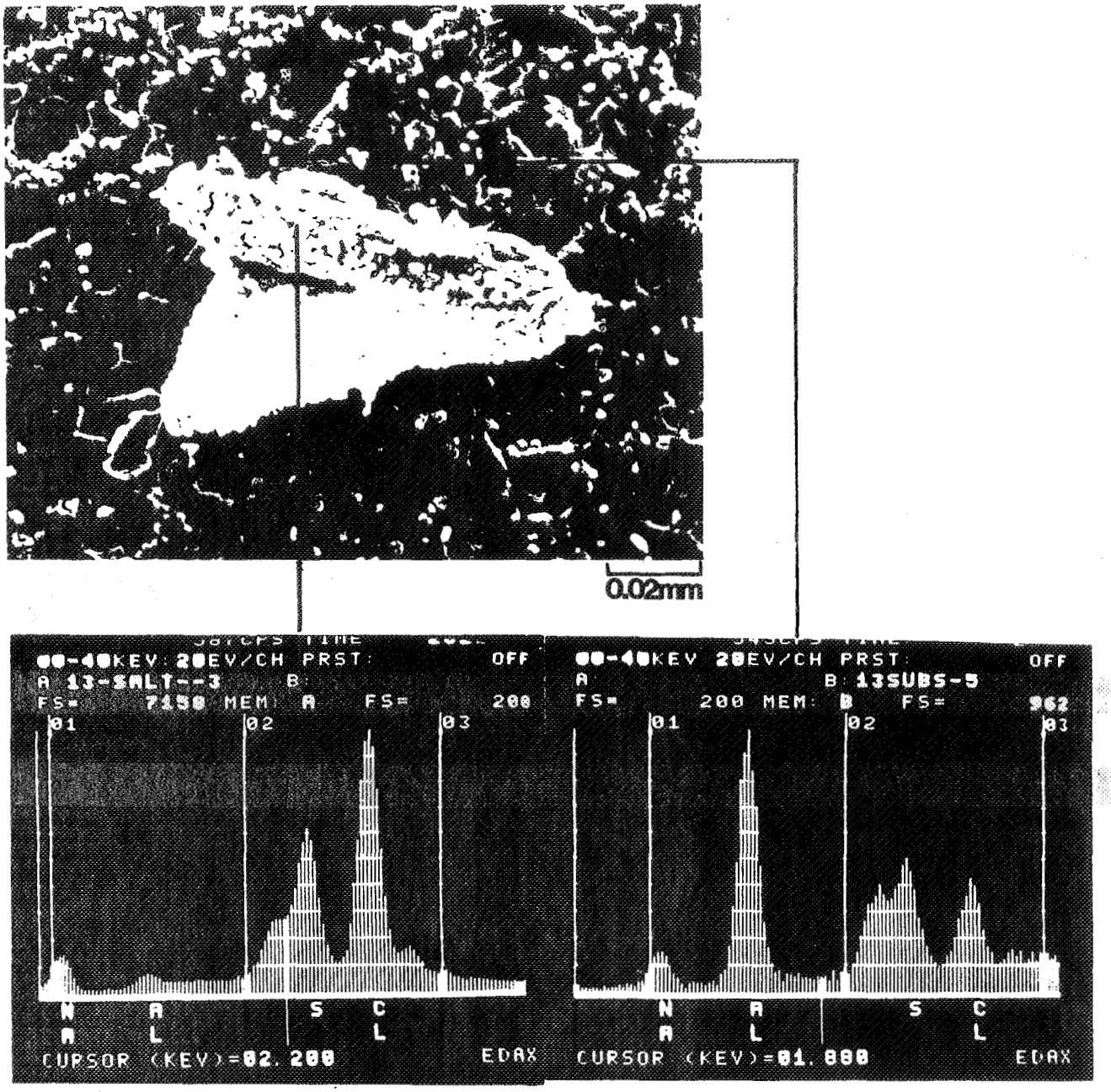

NACL PARTICLE EXPOSED TO AIR PLUS 0.99% SO_2 AT 600^0 C. FOR 10 MINUTES.

F I G U R E 1 5

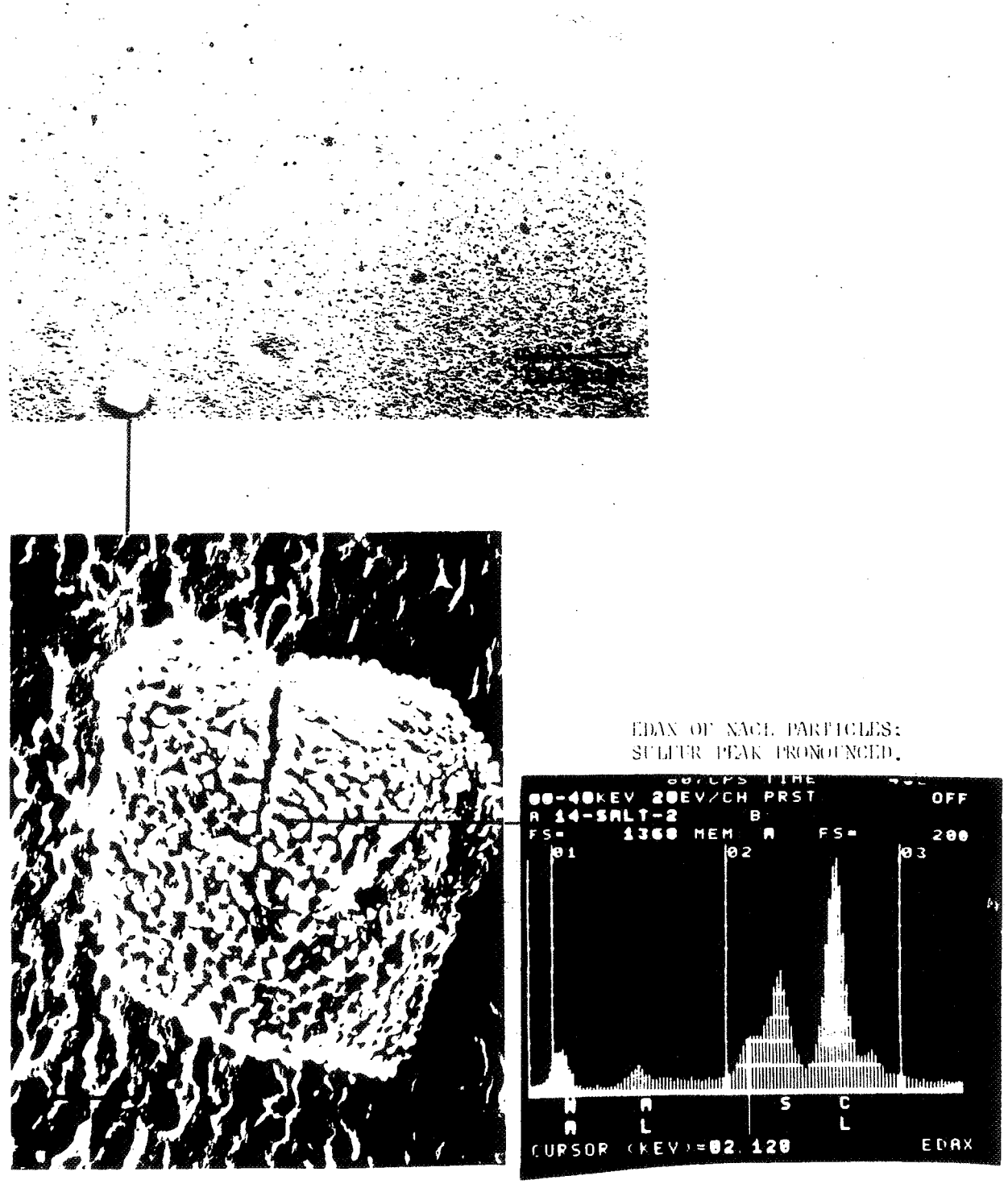

FIGURE 16 NaCl particl exposed to air + 1%SO_2 at 600^{0}C for 30 min.

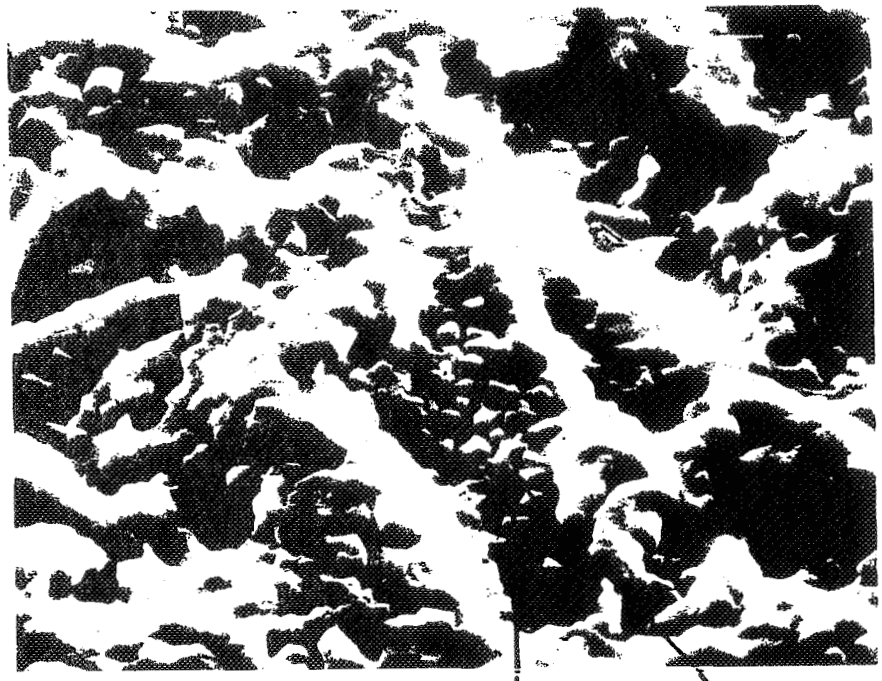

4μm

1μm

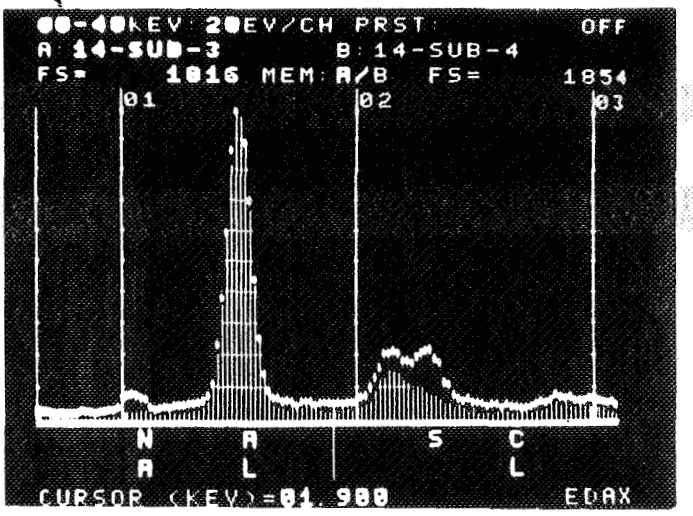

EDAX OF AL_2O_3 SUBSTRATE;
SULFUR CONTENT PRESENT.

AL_2O_3 SUBSTRATE EXPOSED TO AIR AND 0.99% SO_2 AT 600^0 C. FOR 30 MINUTES.

FIGURE 17

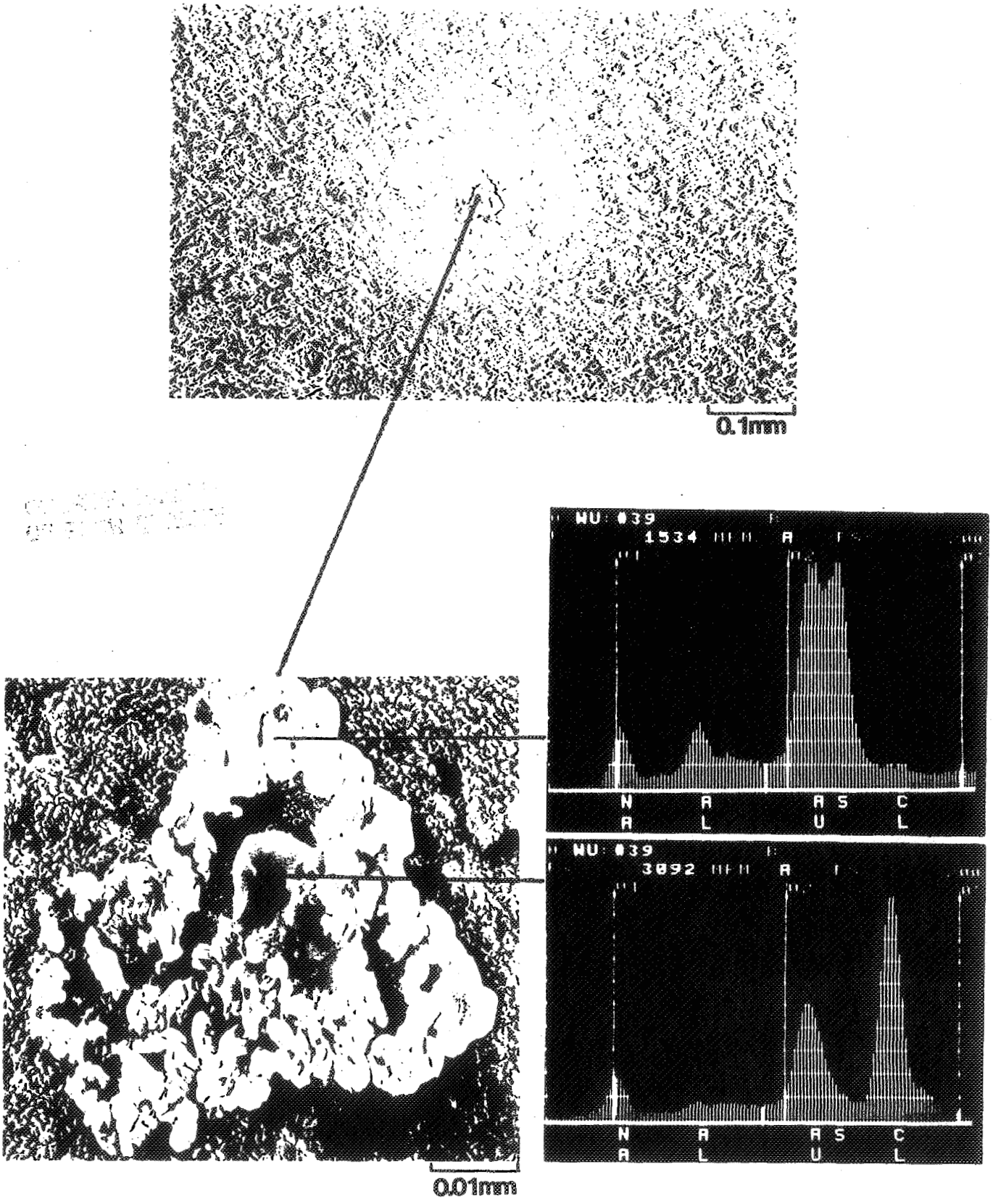

FIGURE 18 Remnant NaCl particle after exposure to air + 1% SO_2 at 600°C for 60 min.

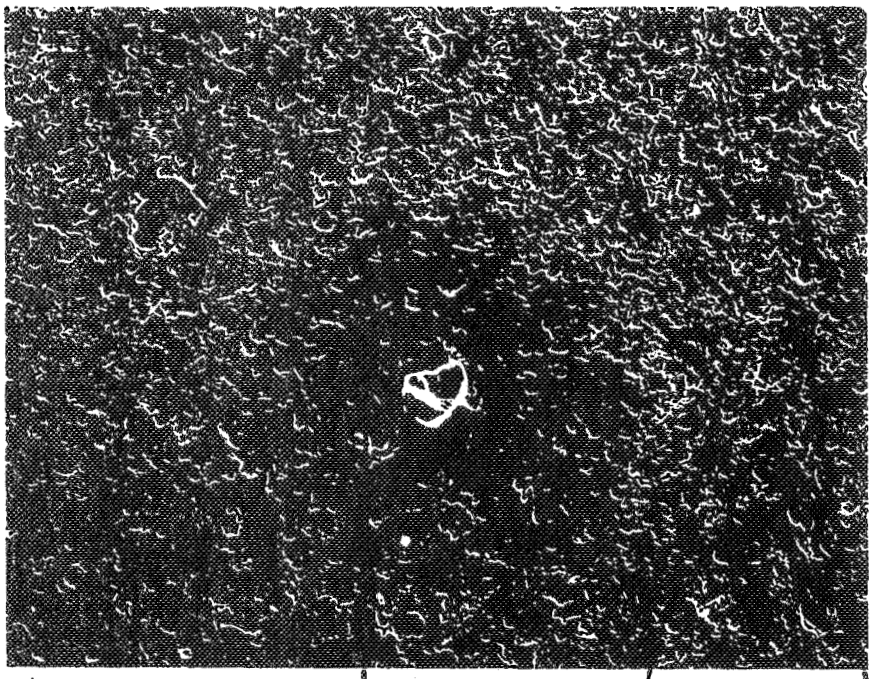

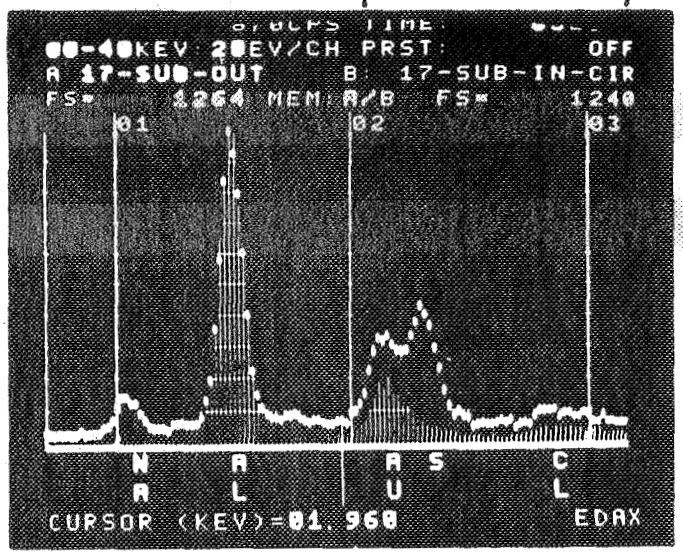

EDAX OF AL_2O_3 SUBSTRATE; COMPARES ELEMENTAL COMPONENTS OF THE INNER AND OUTER RINGS.

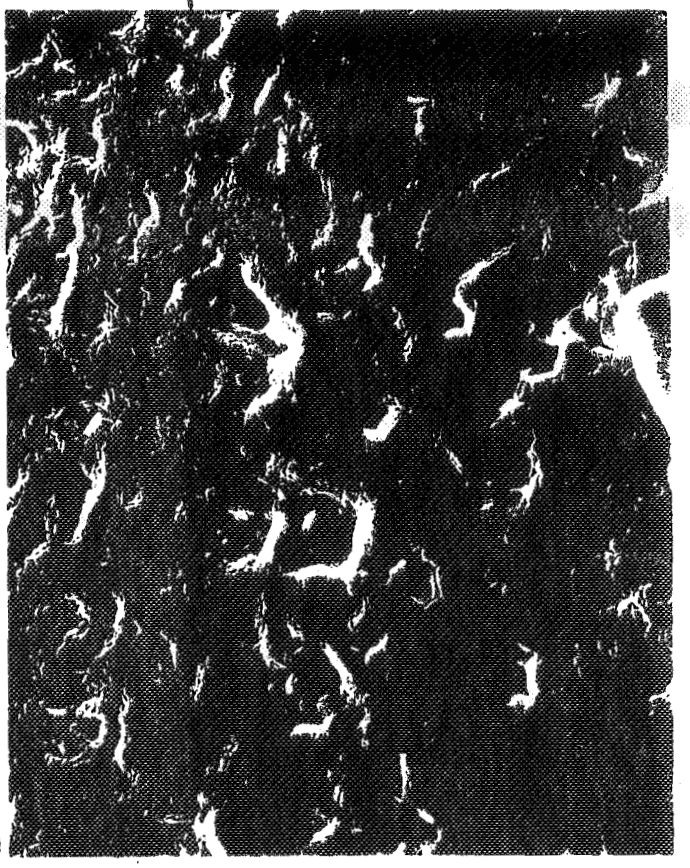

AL_2O_3 SUBSTRATE EXPOSED TO AIR AND 0.99% SO_2 AT 650 ^{0} C. FOR 10 MINUTES.

FIGURE 19

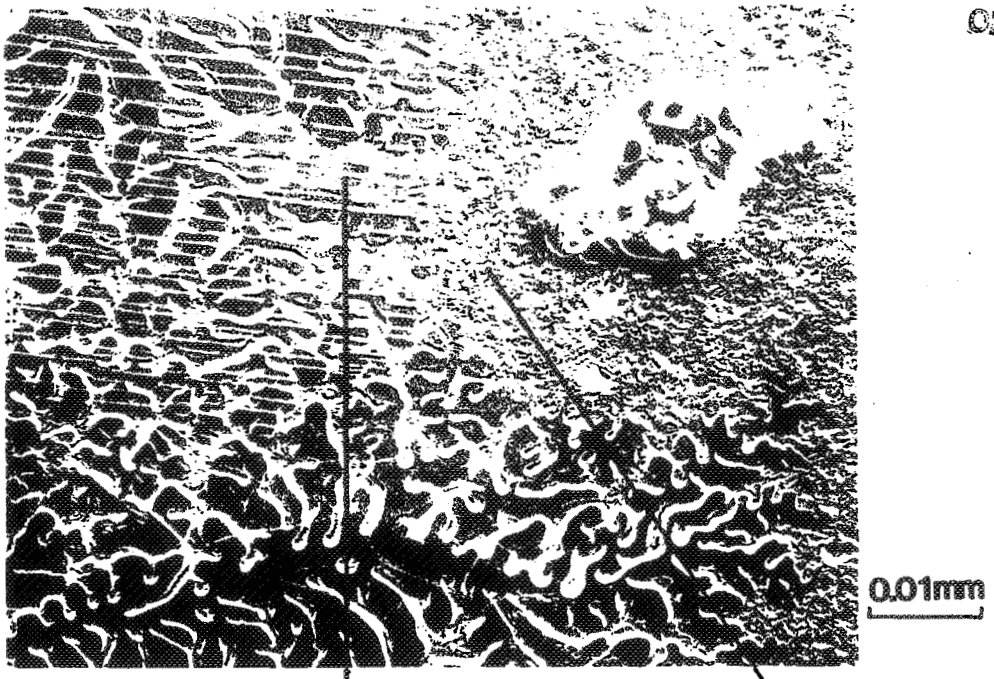

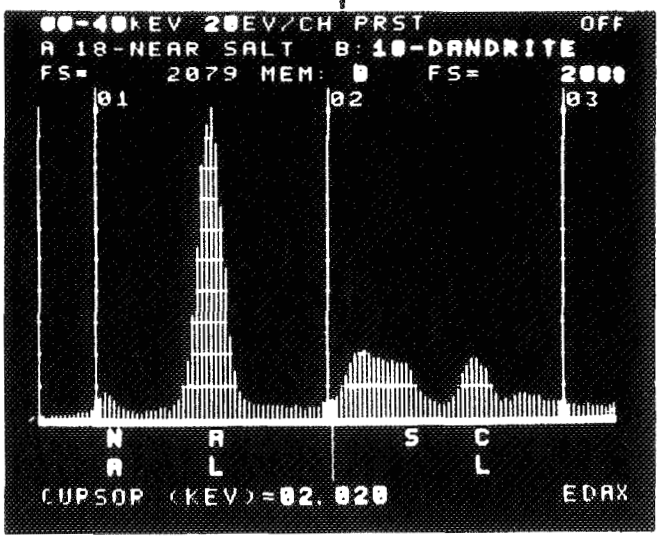

EDAX OF AL_2O_3 SUBSTRATE
IN THE DENDRITE AREA;
HIGH AL PEAKS.

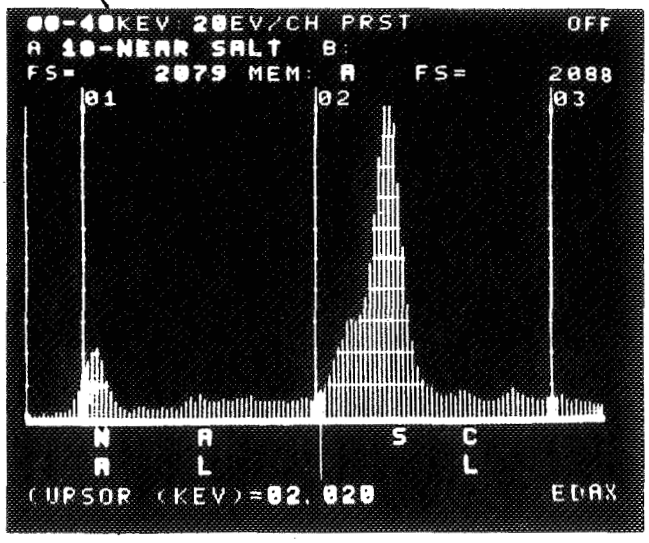

EDAX OF AL_2O_3 SUBSTRATE
NEAR THE NACL PARTICLE;
HIGH SULFUR CONTENT NOTED.

AL_2O_3 SUBSTRATE IN THE VICINITY OF THE NACL PARTICLE AFTER EXPOSURE TO AIR AND 0.99% SO_2 AT 650^0 C. FOR 30 MINUTES.

FIGURE 20

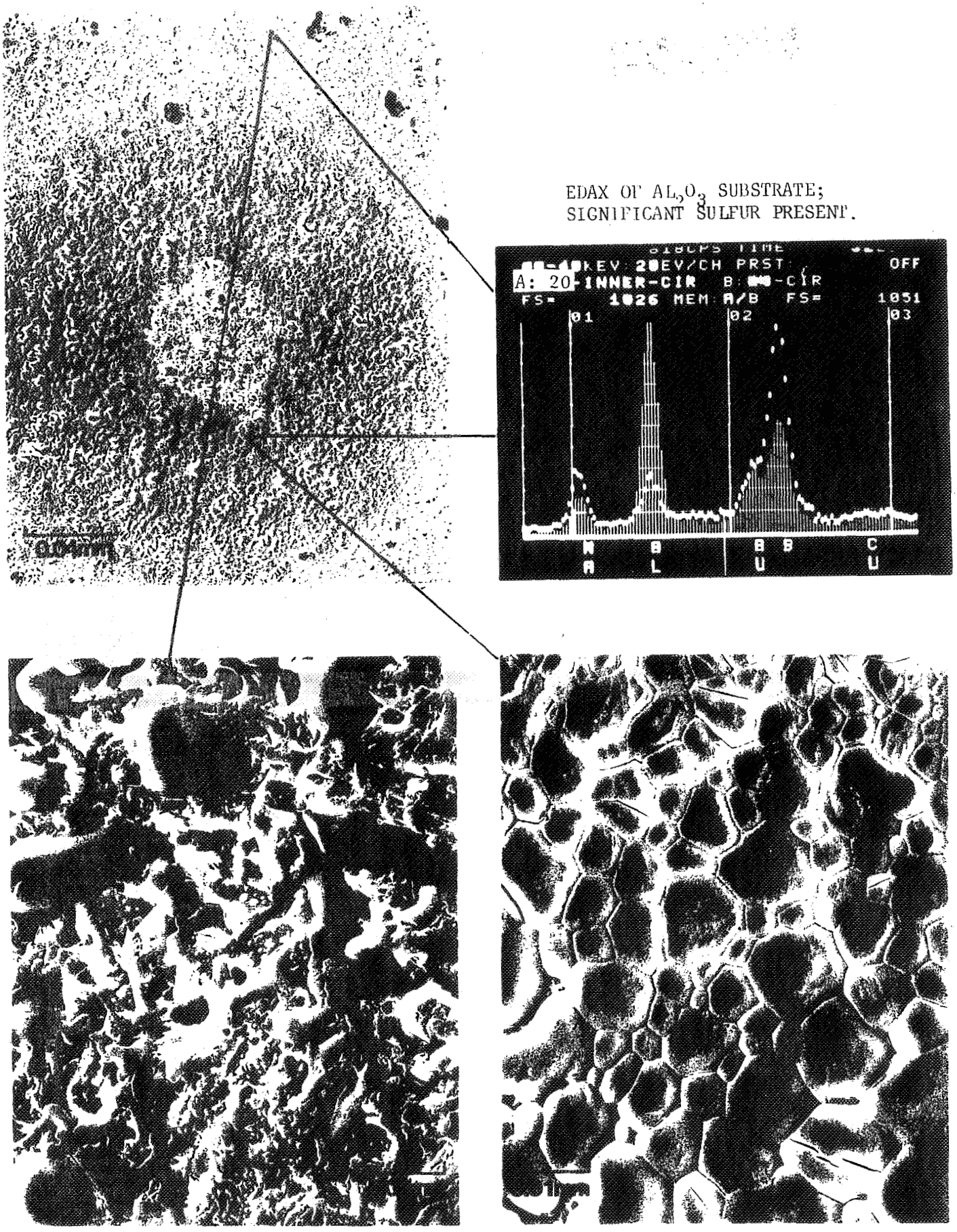

AL_2O_3 SUBSTRATE EXPOSED TO AIR AND 0.99% SO_2 AT 650^0 C. FOR FOUR HOURS.

FIGURE 21

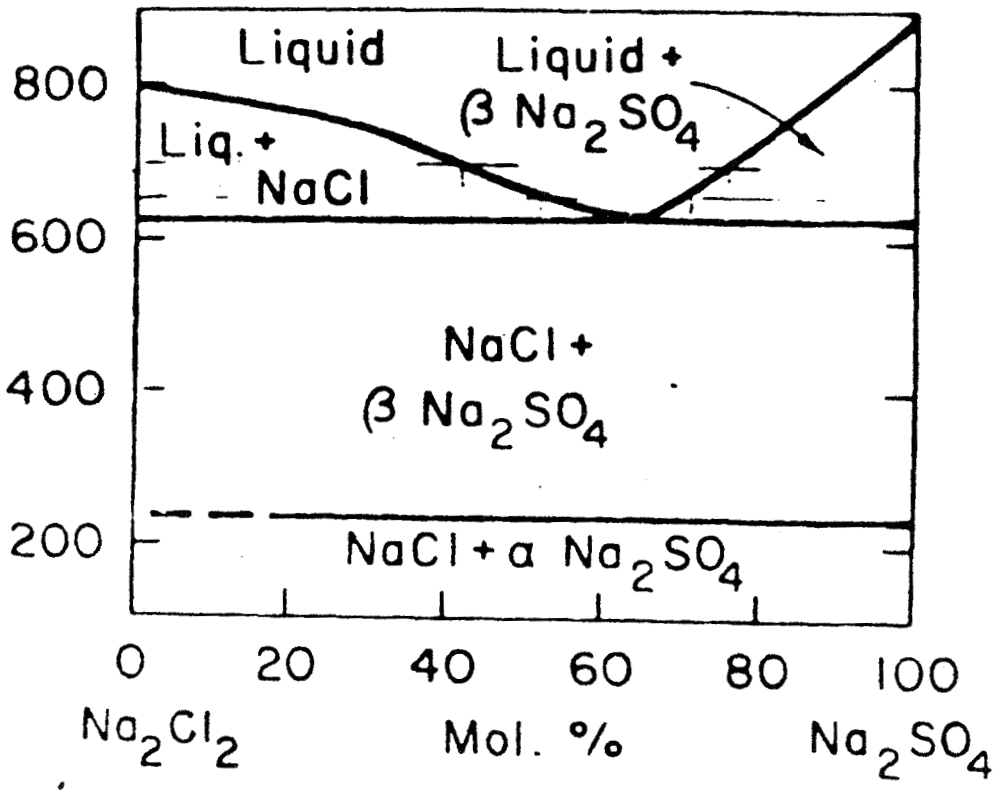

FIGURE 22

Phase diagram of $NaCl$-Na_2SO_4 system.

a.)

10µm

.)

EDAX OF NACL PARTICLE;
SIGNIFICANT SULFUR PEAK.

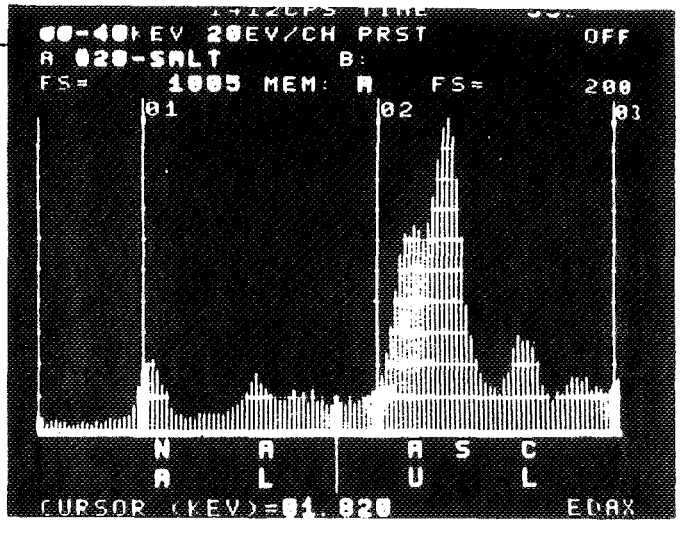

NACL PARTICLE EXPOSED TO AIR, 0.2% SO_2 AND 1.0% H_2O AT 500^0 C. FOR FOUR HOURS.

FIGURE 23

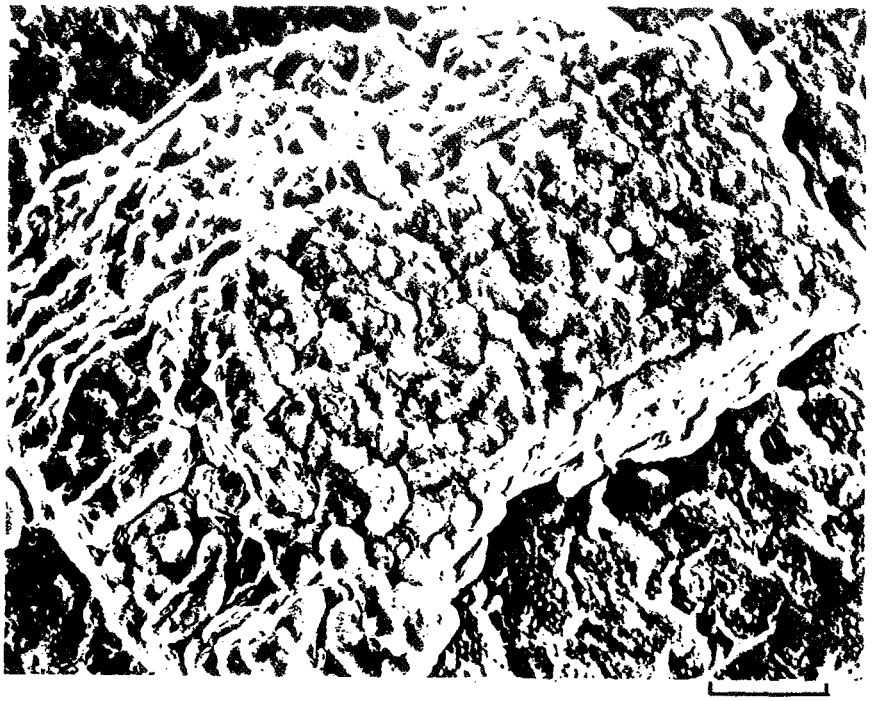

30 min

20μm

240 min

20μm

FIGURE 24 **Morphology of salt particle after exposure to air + 0.1% SO_2 + 1% H_2O at 500°C for 30 min and 240 min.**

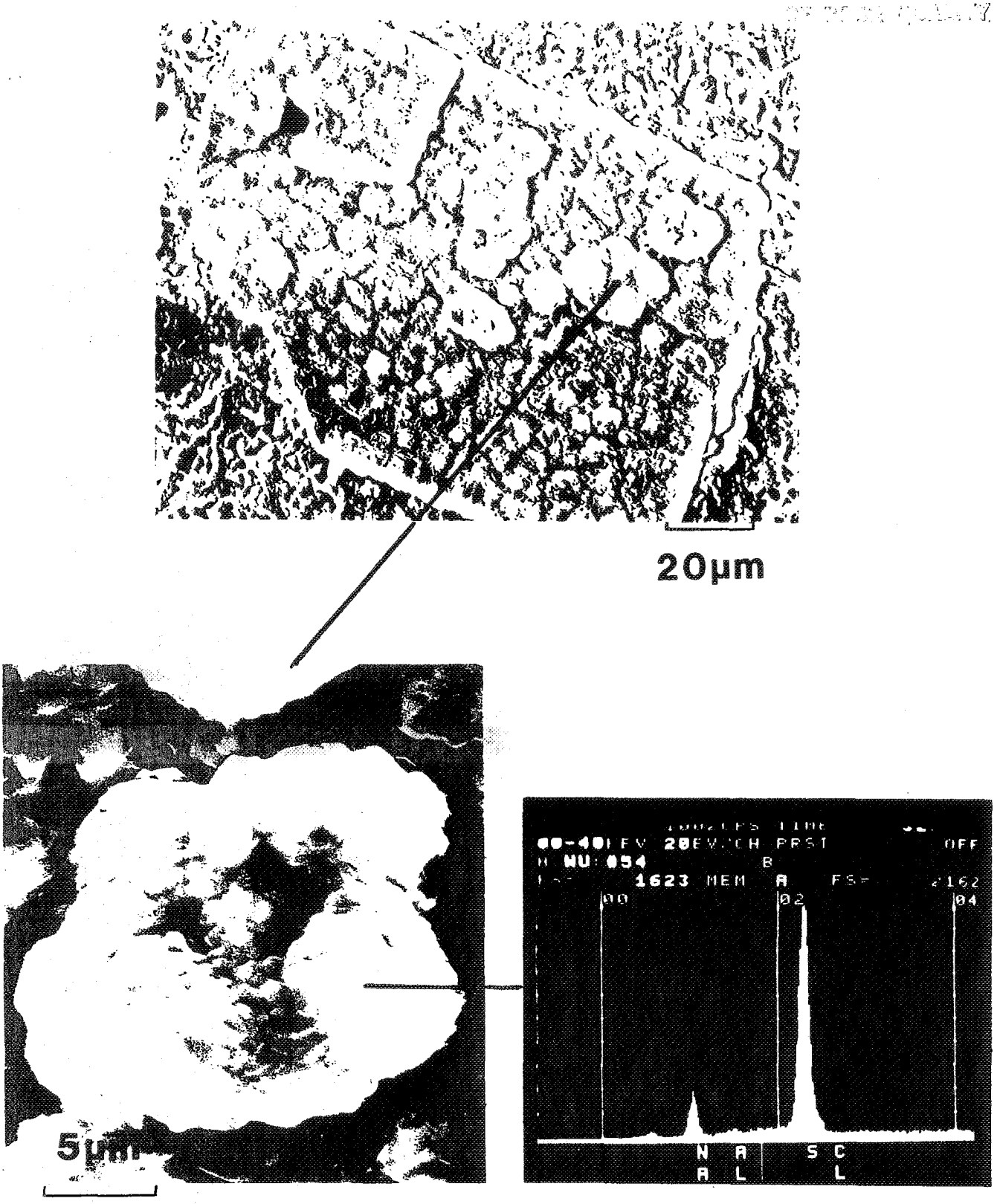

FIGURE 25 Rapid growth of Na_2SO_4 clusters in air + 0.5% SO_2 + 0.5% H_2O at 500°C.

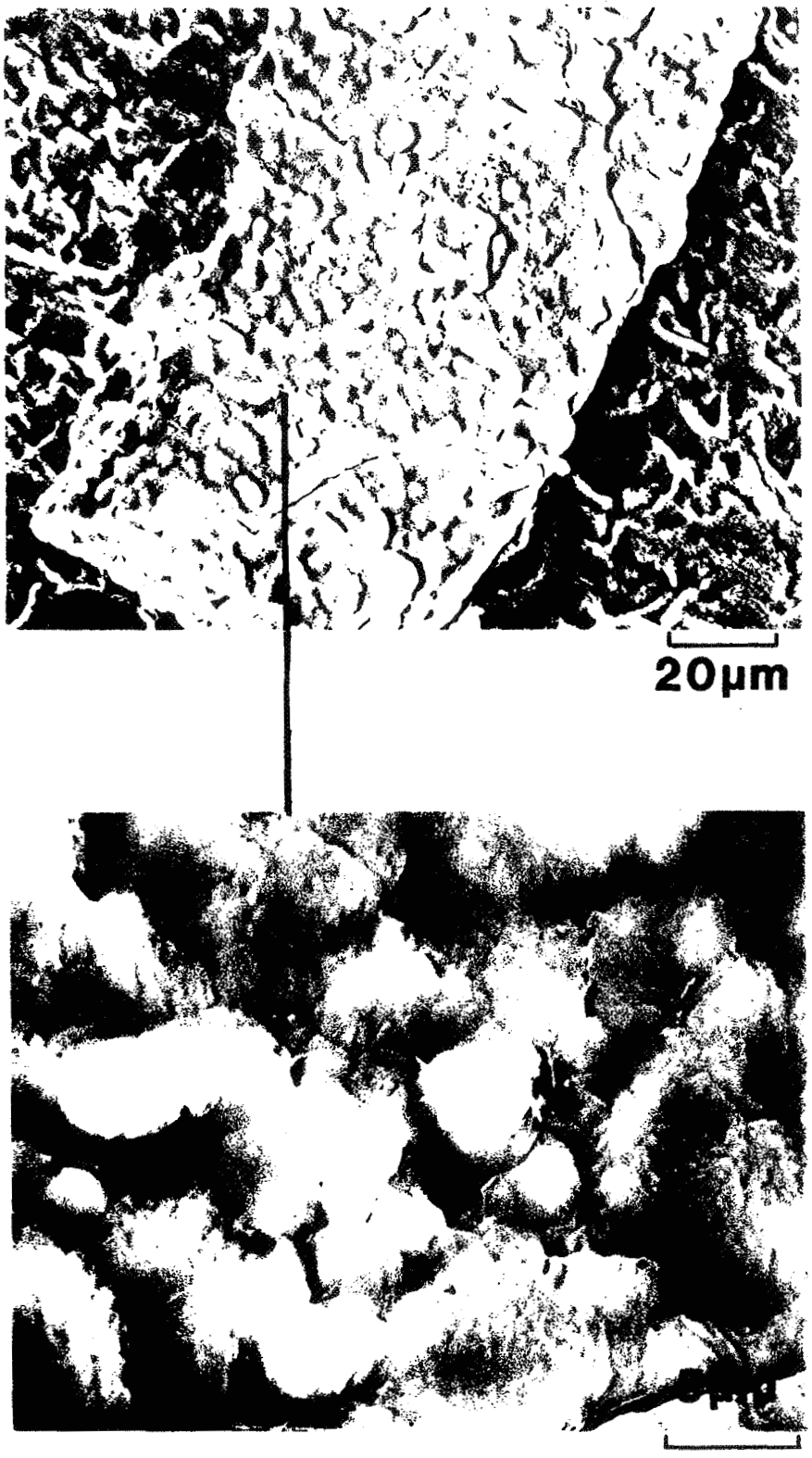

FIGURE 26 Clusters of Na_2SO_4 after 30 min in air + 0.1% SO_2 + 1% H_2O at 600°C.

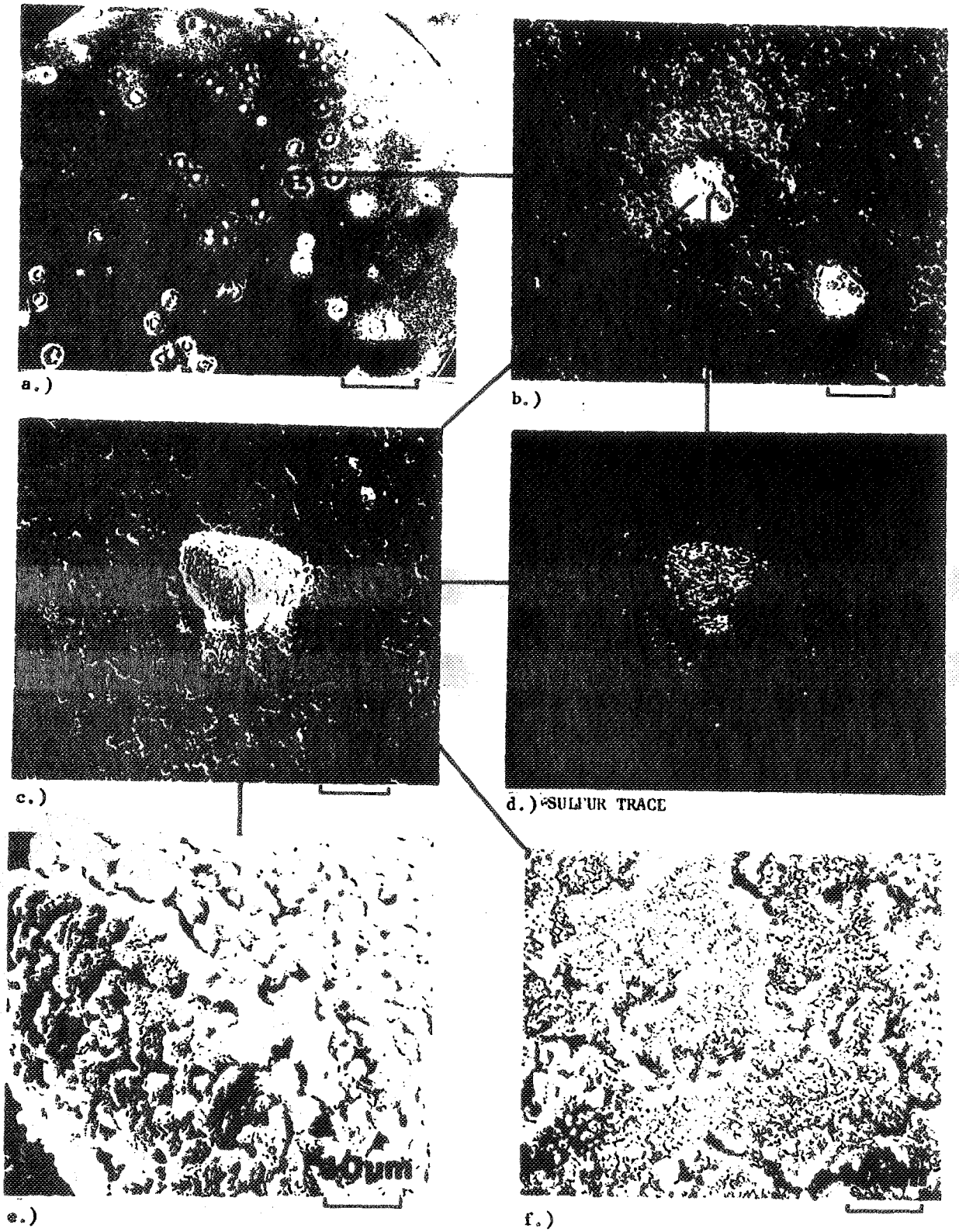

NaCl PARTICLES EXPOSED TO AIR, 0.1% SO_2 AND 1.0% H_2O AT 600°C. FOR 30 MINUTES.

FIGURE 27

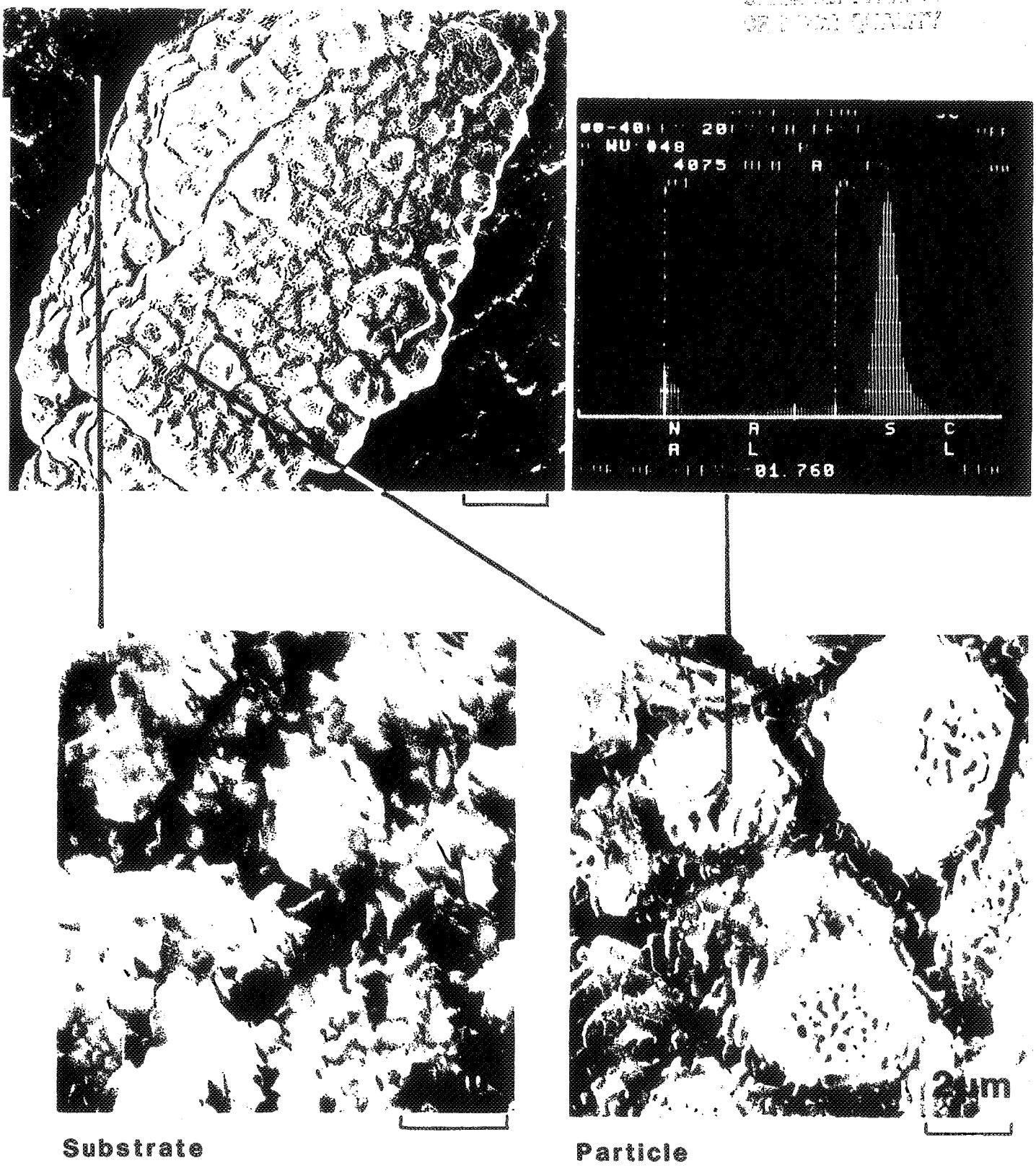

FIGURE 28 Na_2SO_4 clusters formed in air + 0.1% SO_2 + 1% H_2O at 600° C.

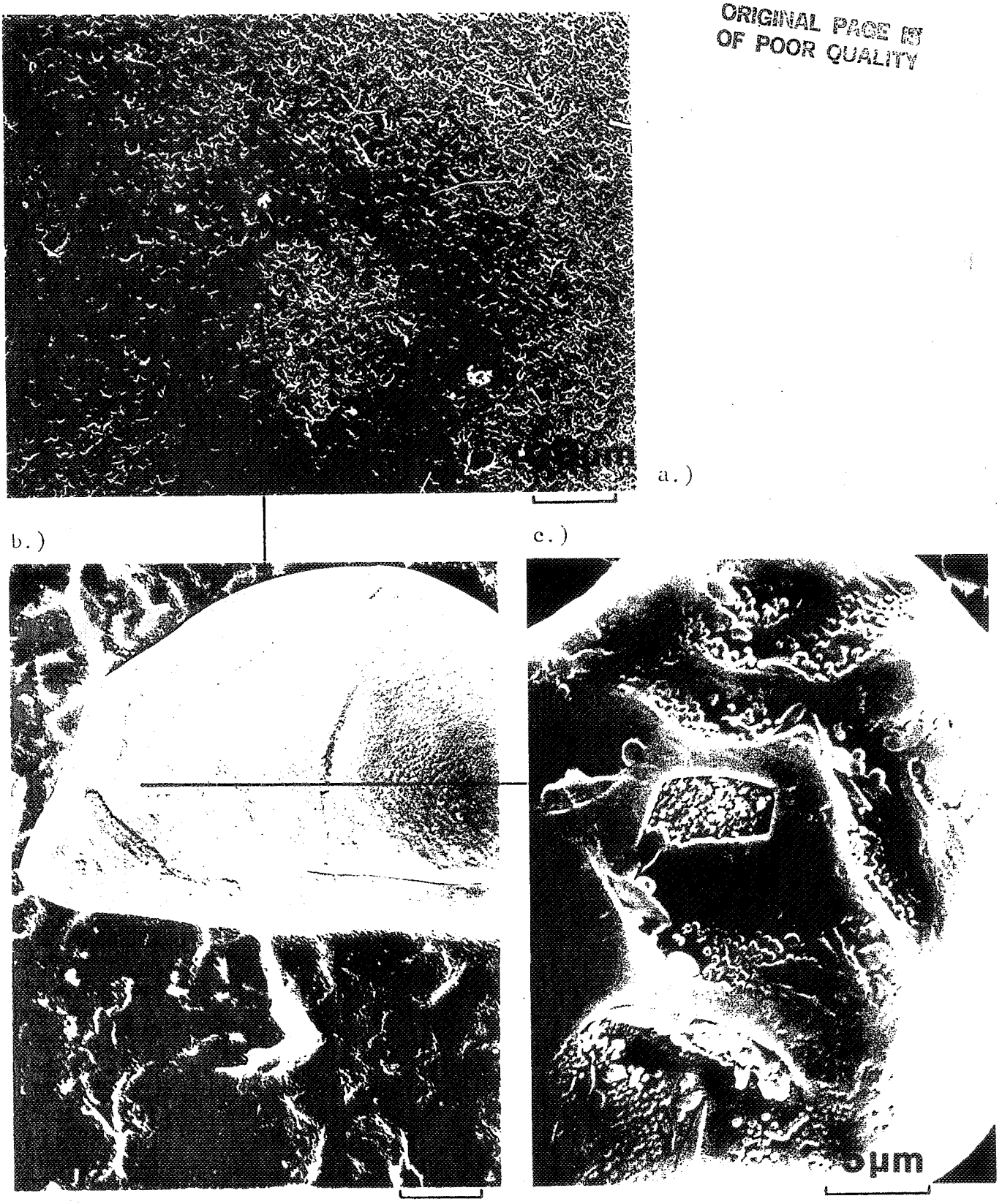

NACL PARTICLES EXPOSED TO AIR, 0.2% SO_2 AND 1.0% H_2O AT 700^0 C. FOR 10 MINUTES.

FIGURE 29

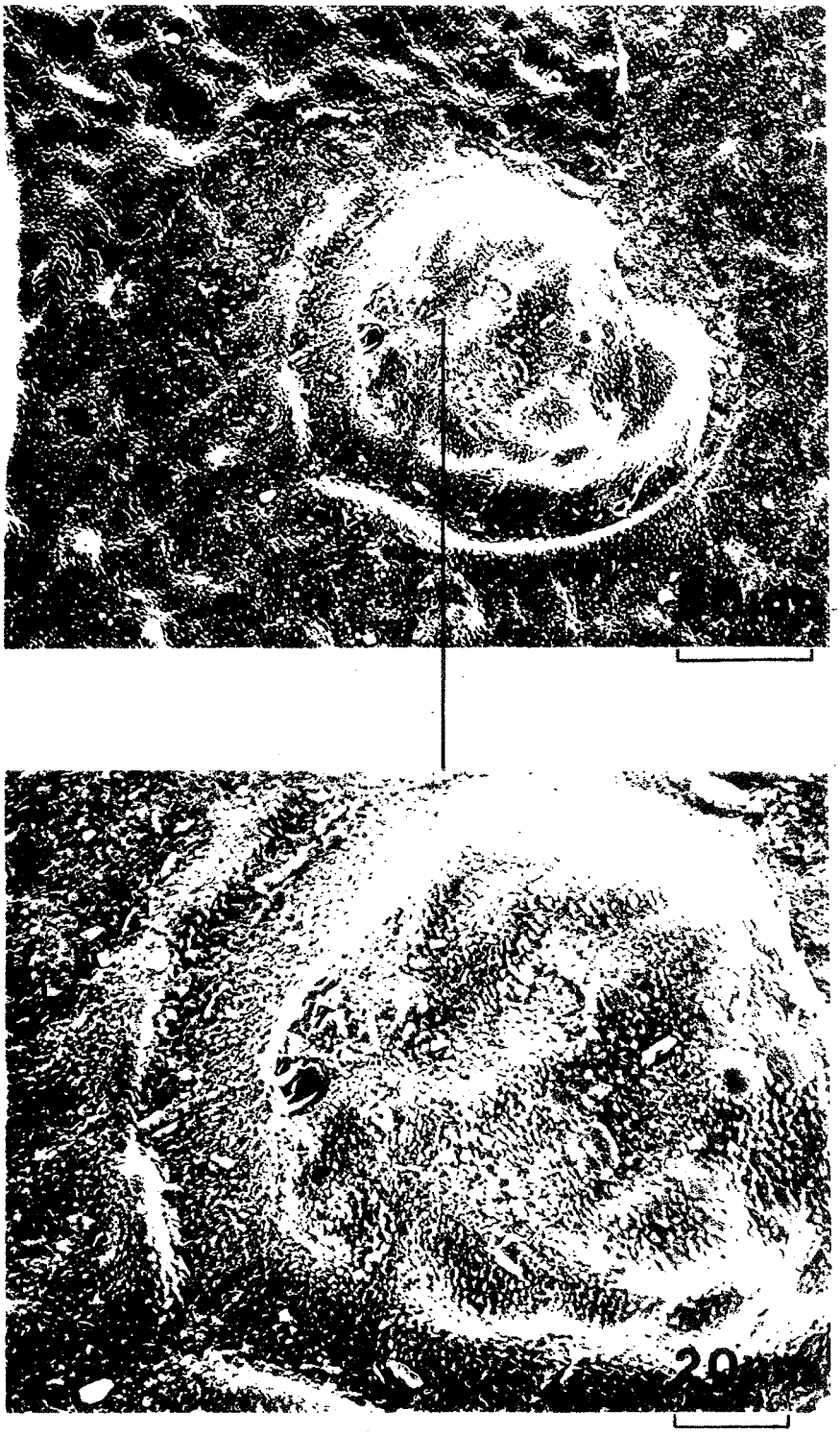

NACL PARTICLE EXPOSED TO AIR, 0.2% SO_2 AND 1.0% H_2O AT 700^0 C. FOR ONE HOUR.

FIGURE 30

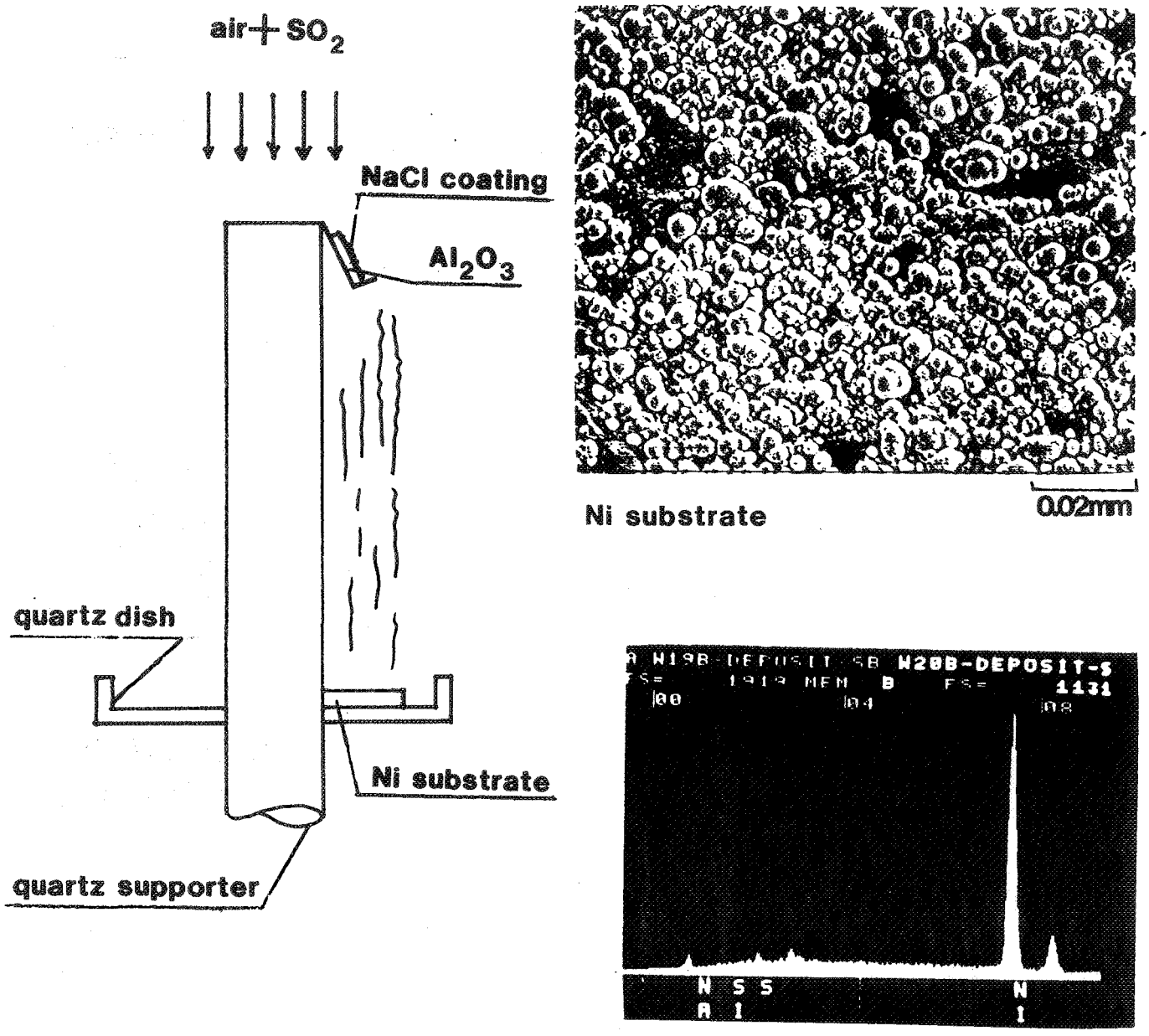

FIGURE 31 **Aluminum free deposit on substrate placed in cold zone of furnace.**

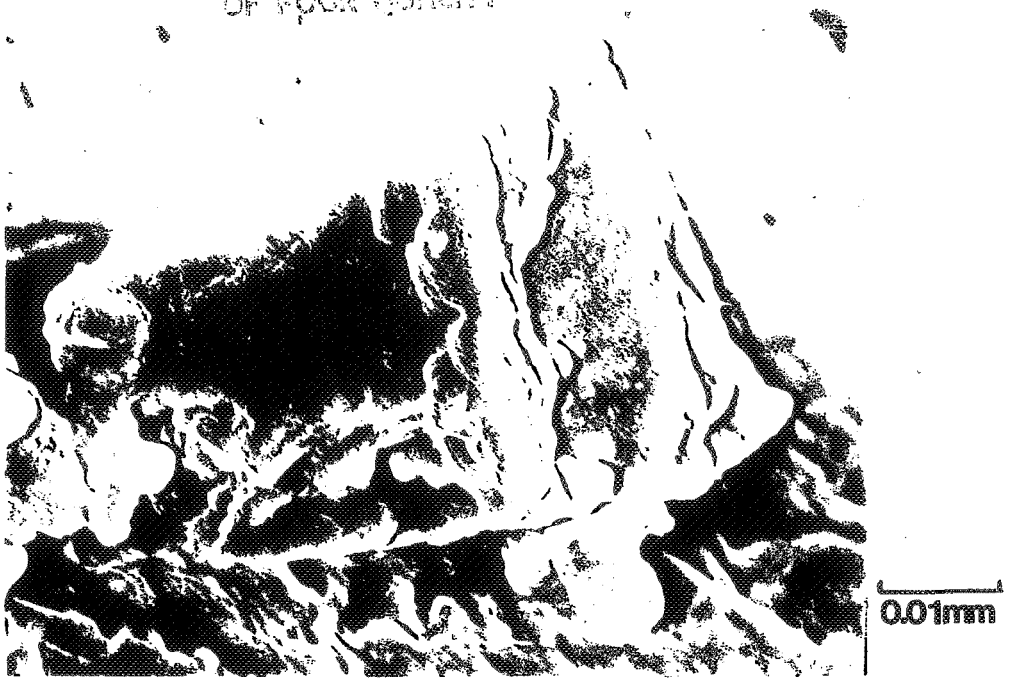

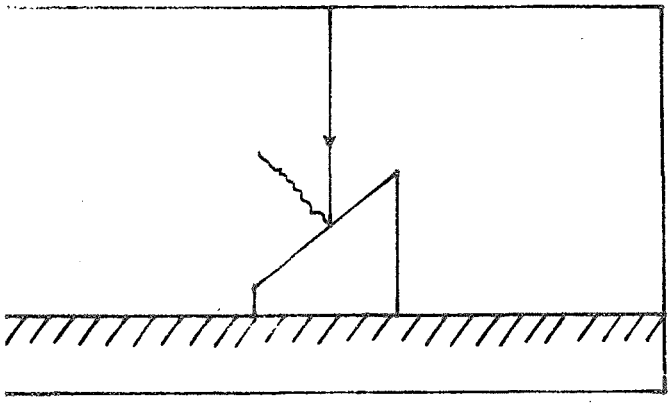

normal position

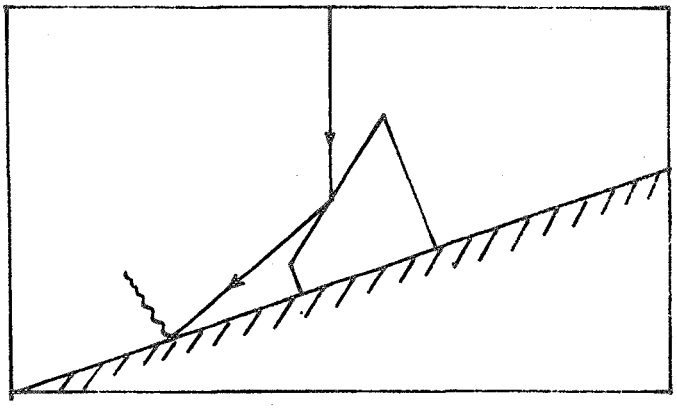

inclined position

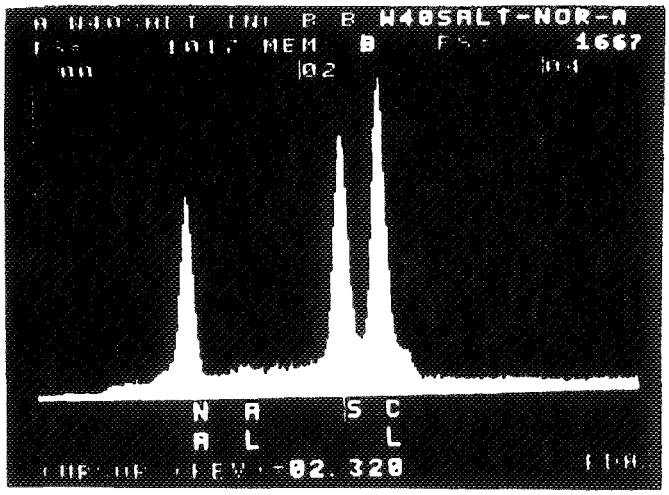

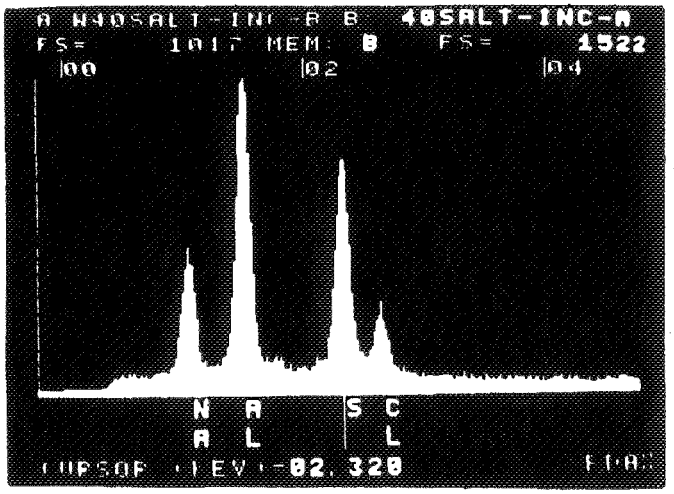

FIGURE 32 **Effect of target orientation on generation of Al peak from substrate.**

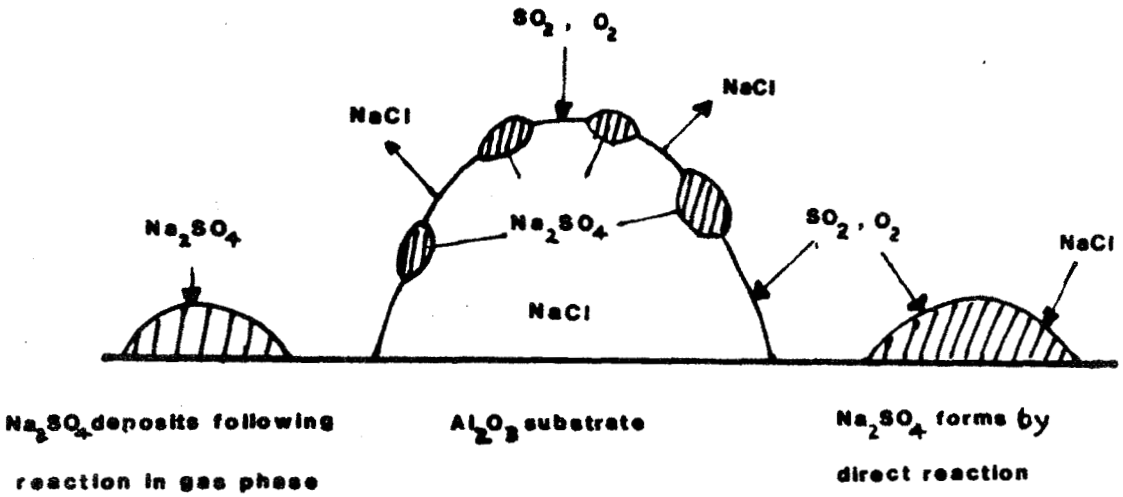

FIGURE 33

Reaction Mechanisms Below 625°C

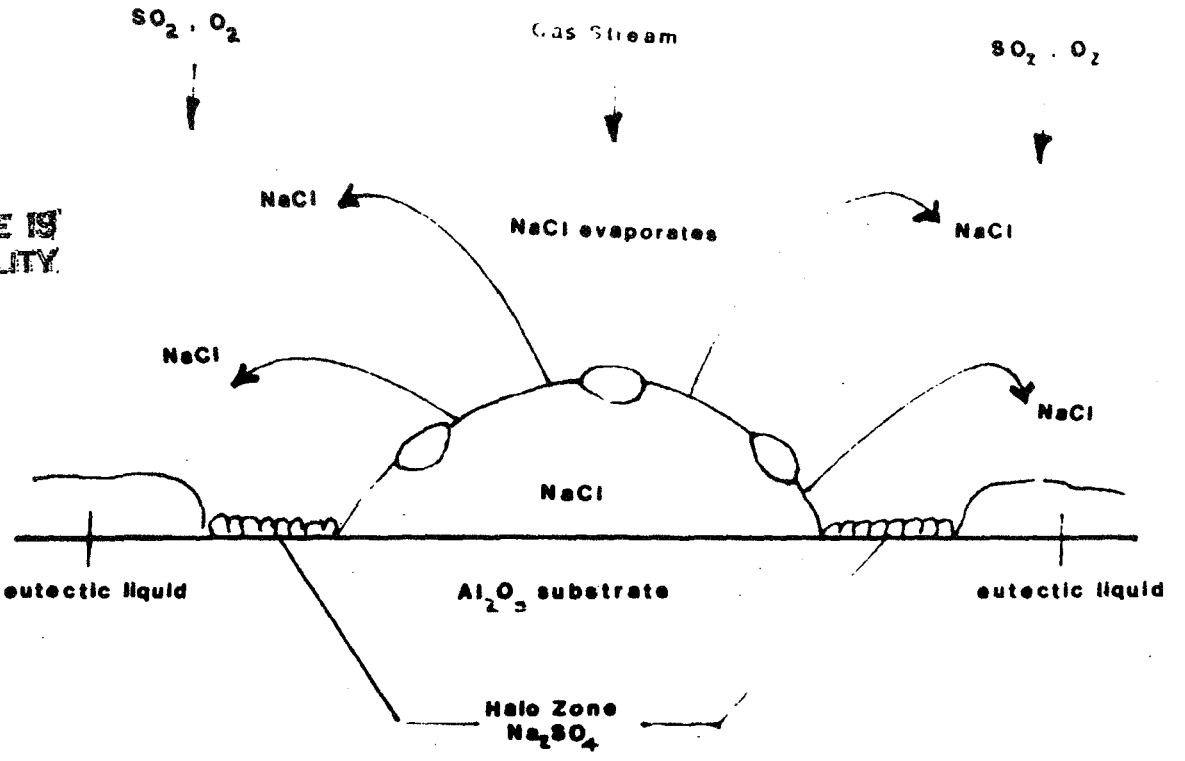

Early stages in presence of NaCl

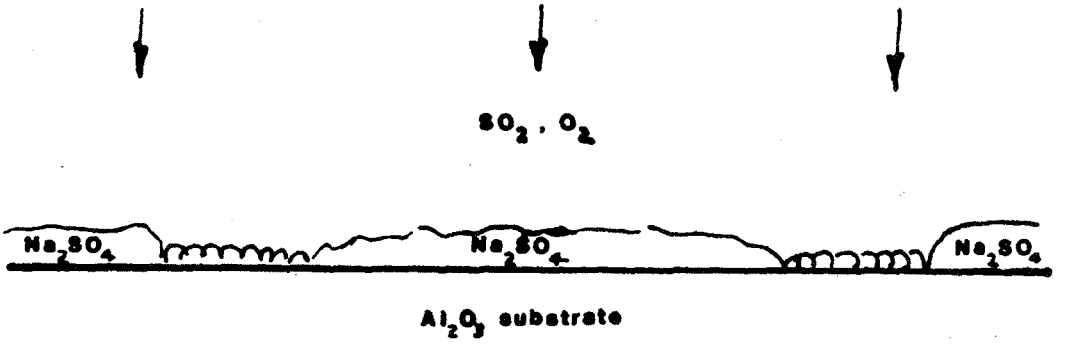

NaCl in eutectic liquid reacts to form Na_2SO_4. Solidification by reaction occurs

Late stages after evaporation of original NaCl

FIGURE 34

Reaction Mechanisms Above 625°C

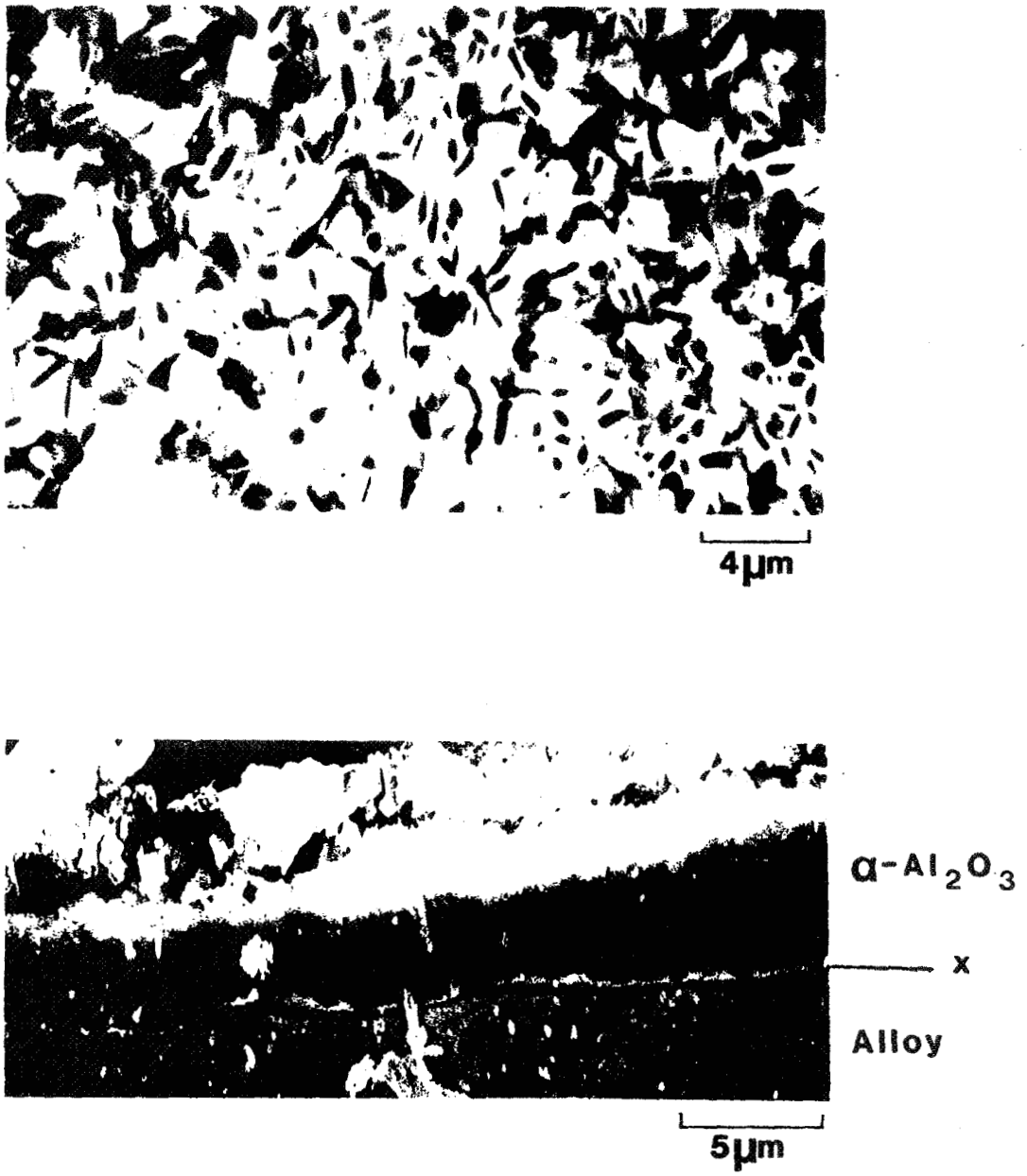

FIGURE 35(a) **Surface and section of α-Al_2O_3 layer on preoxidised HOS-875.**

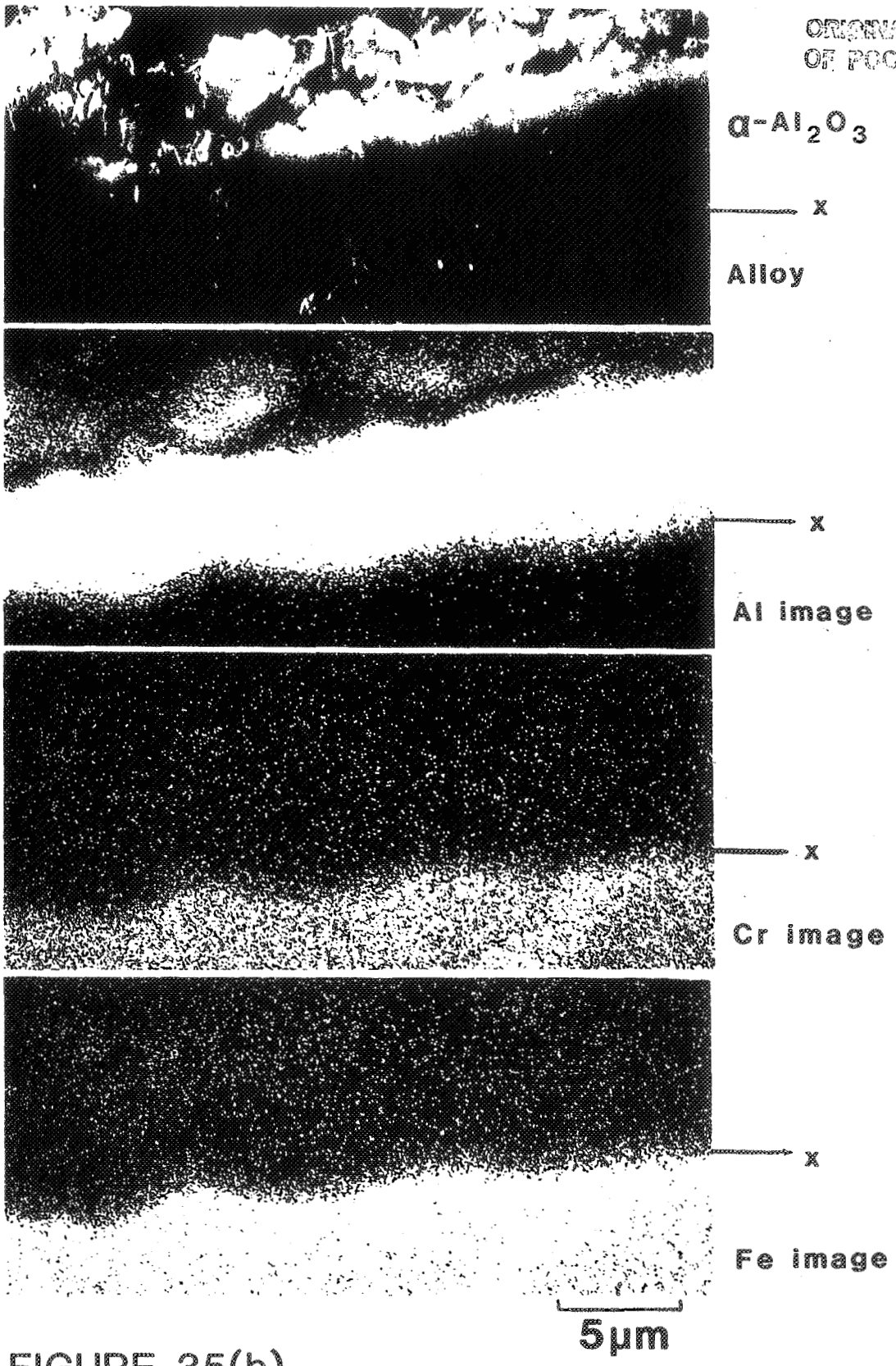

FIGURE 35(b)

Cross section of α-Al_2O_3 formed on HOS-875 after 12 hours in air at 1300°C.

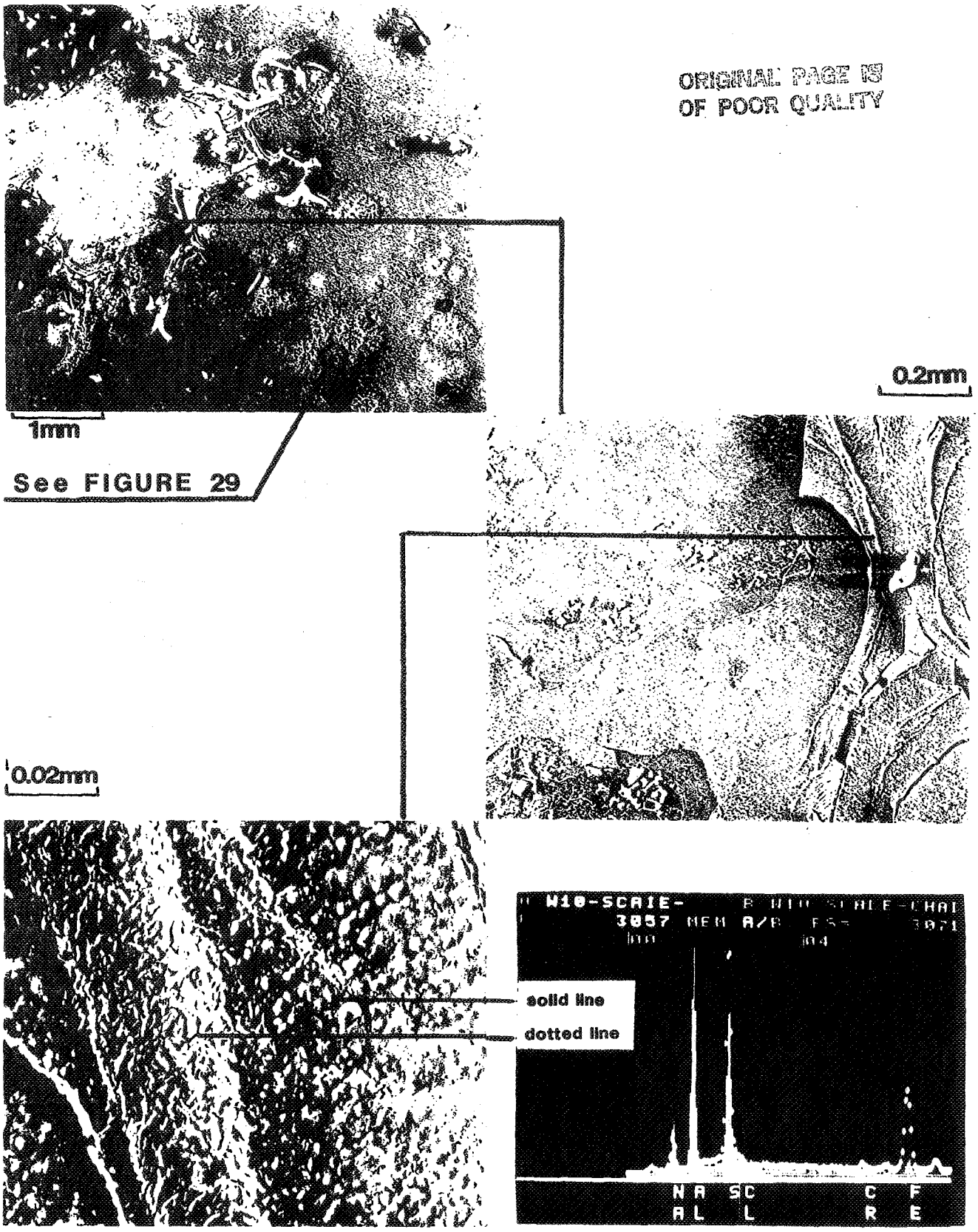

FIGURE 36 700°C Air with 1% SO_2

Preoxidised HOS-875 exposed as above for 20 minutes after salt deposition.

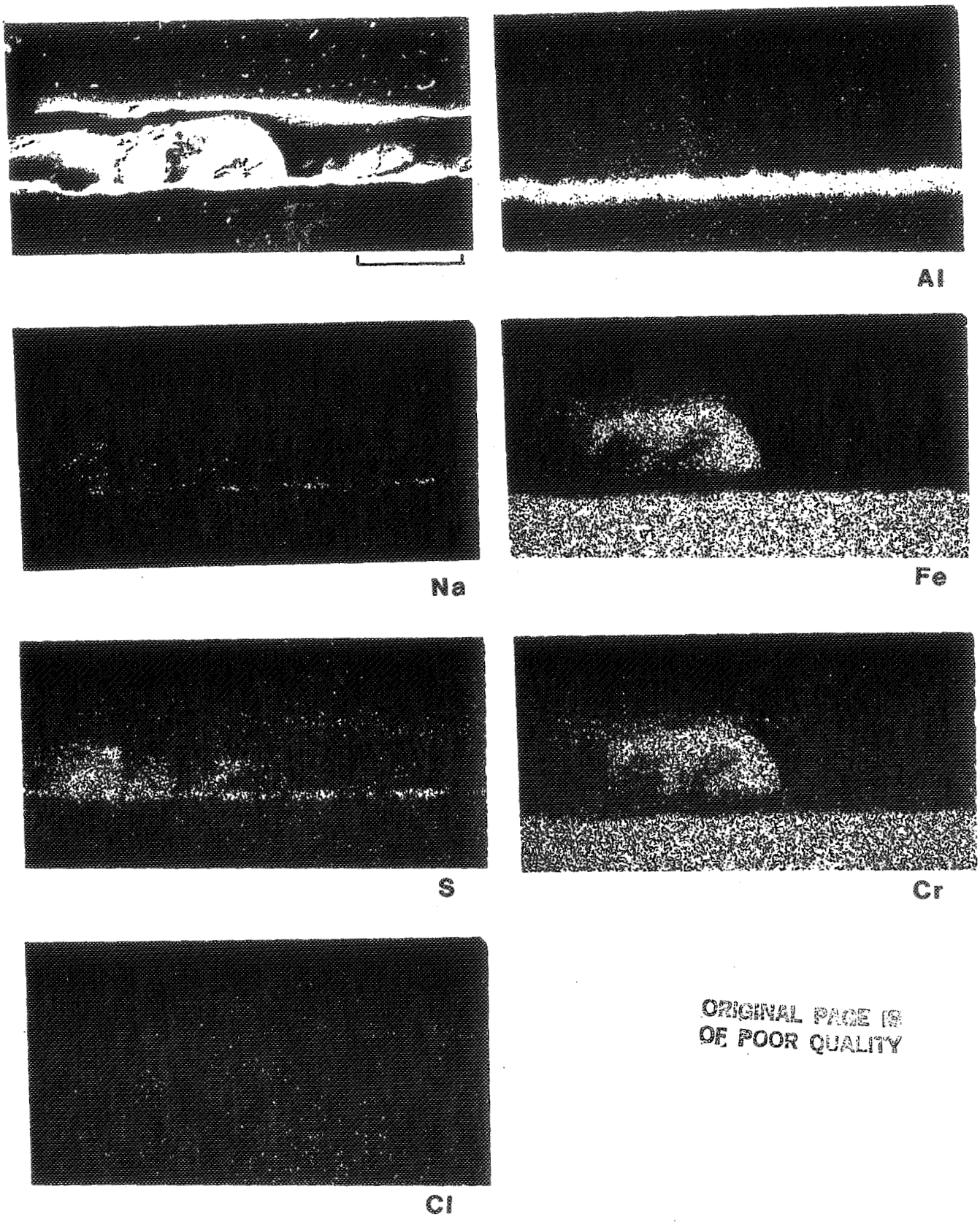

FIGURE 37 700°C Air with 1% SO_2

Preoxidised HOS-875 exposed as above for 30 minutes showing composition details in section.

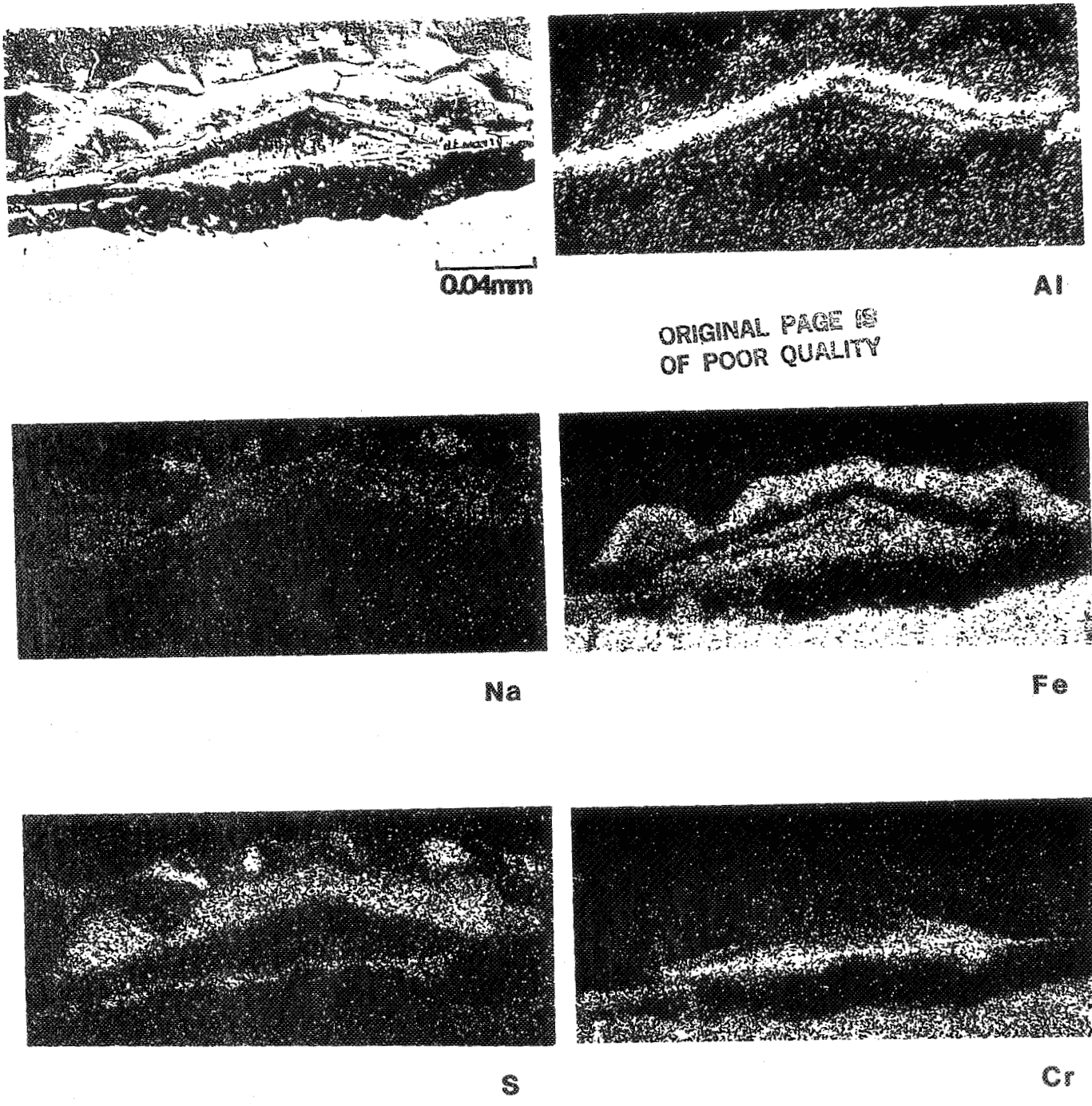

FIGURE 38 700°C Air with 1% SO_2

Preoxidised HOS-875 exposed as above for 60 minutes

showing composition details in section.

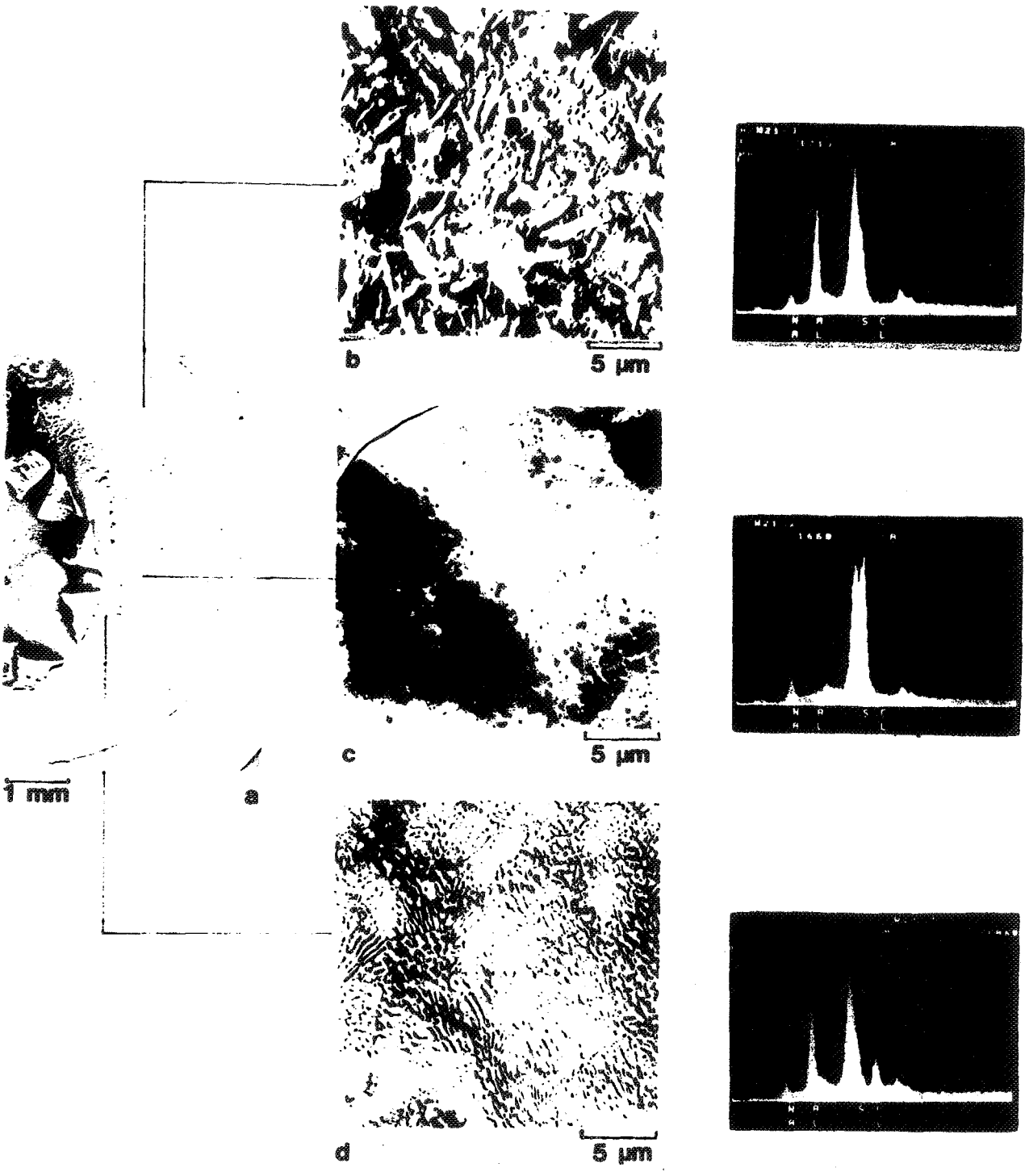

FIGURE 39 Morphology of deposits on Al_2O_3 after 1 hr. at 653°C in air+1%SO_2.

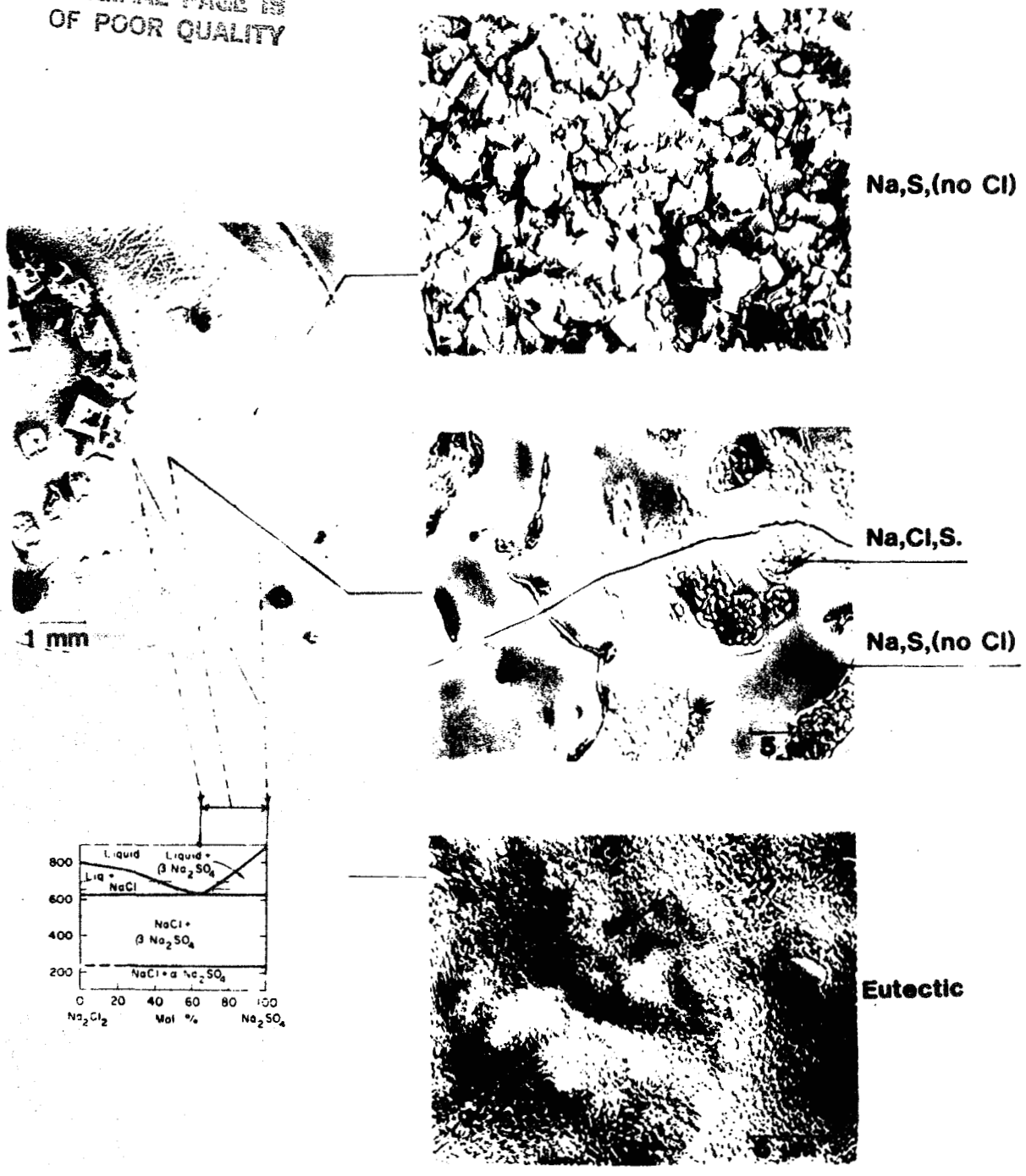

FIGURE 40 Morphology of deposits on Al_2O_3 after 1 hr. at 700°C in air+1%SO_2.

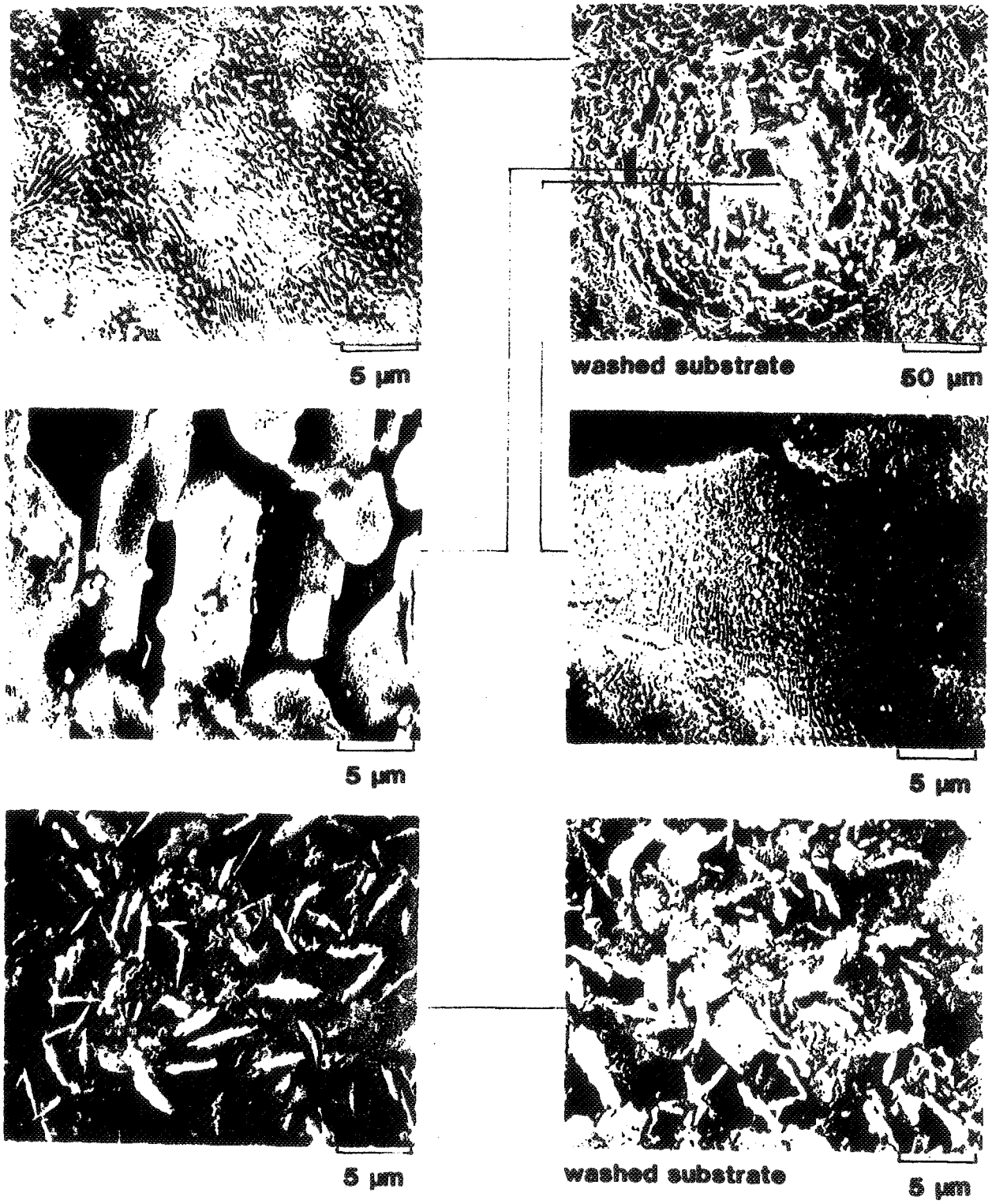

FIGURE 41 Al_2O_3 surface after removal of water soluble salts shows evidence of attack by the liquid eutectic at temperature, but no attack below the solid deposits.

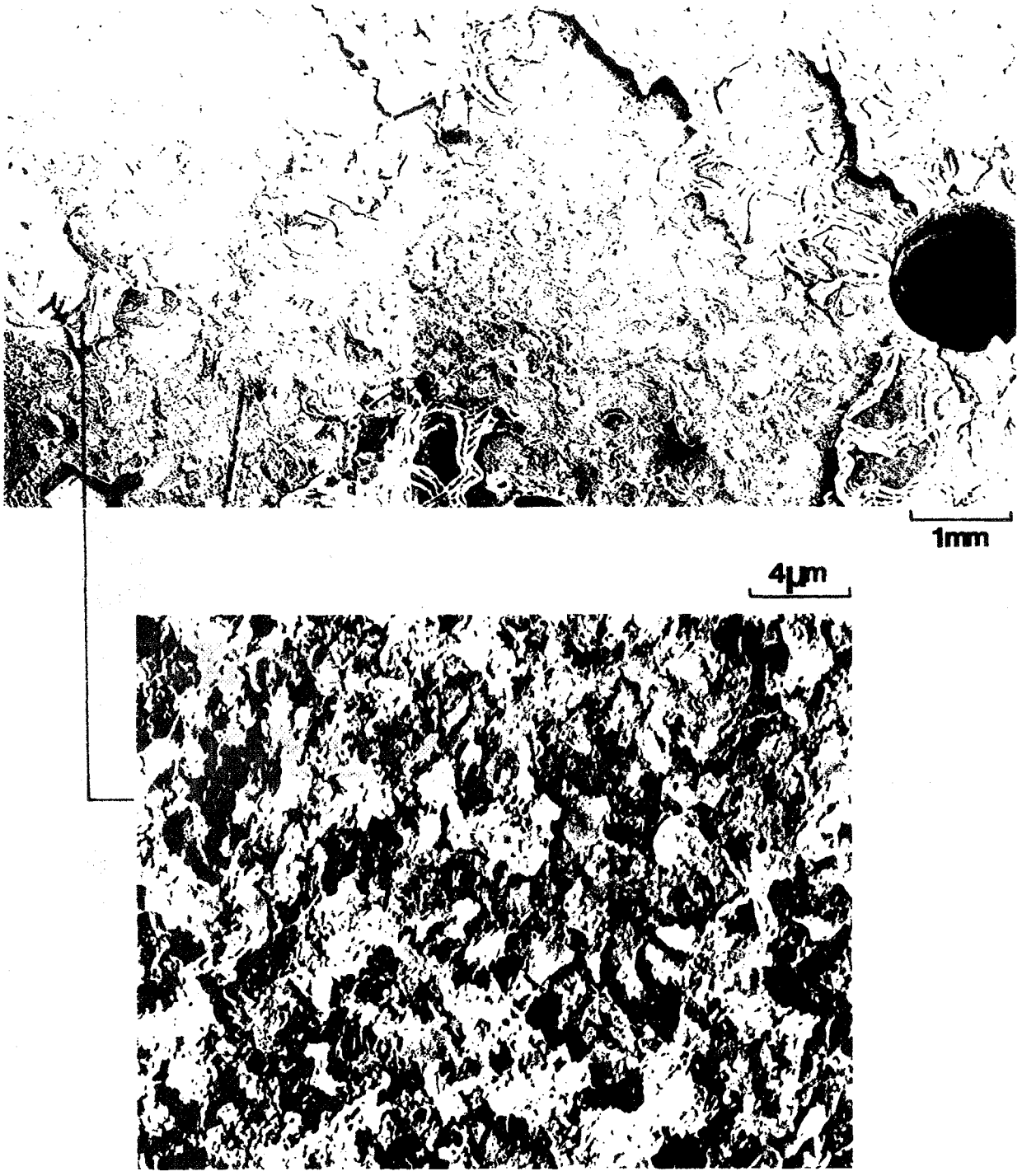

FIGURE 42 **Washed surface : NaCl coated preoxidized HOS-875 exposed to air + 1% SO_2 for 1 hr at 650°C.**

Very porous substrate surface.

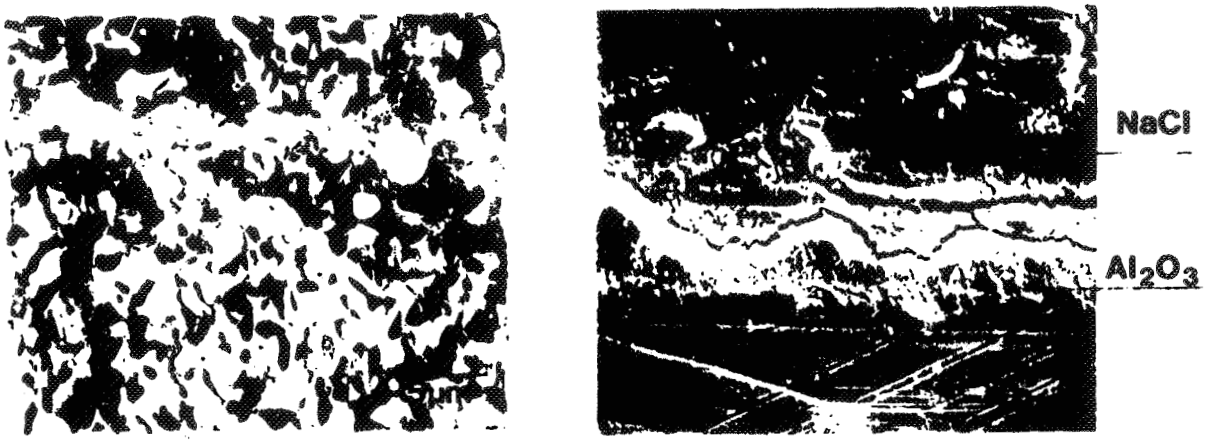

NaCl coated, 2 hrs in air at 653°C

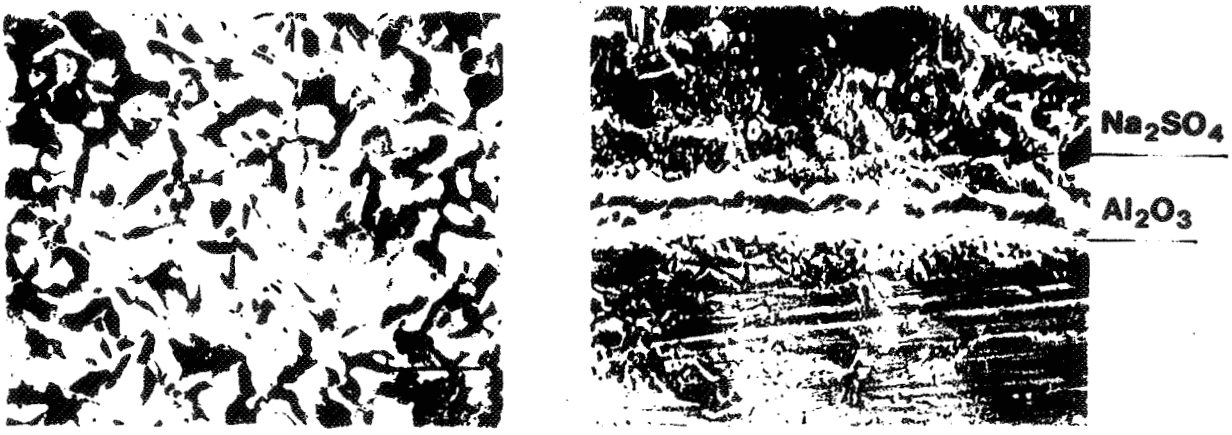

Na_2SO_4 coated, 2 hrs in air + 1%SO_2 at 651°C

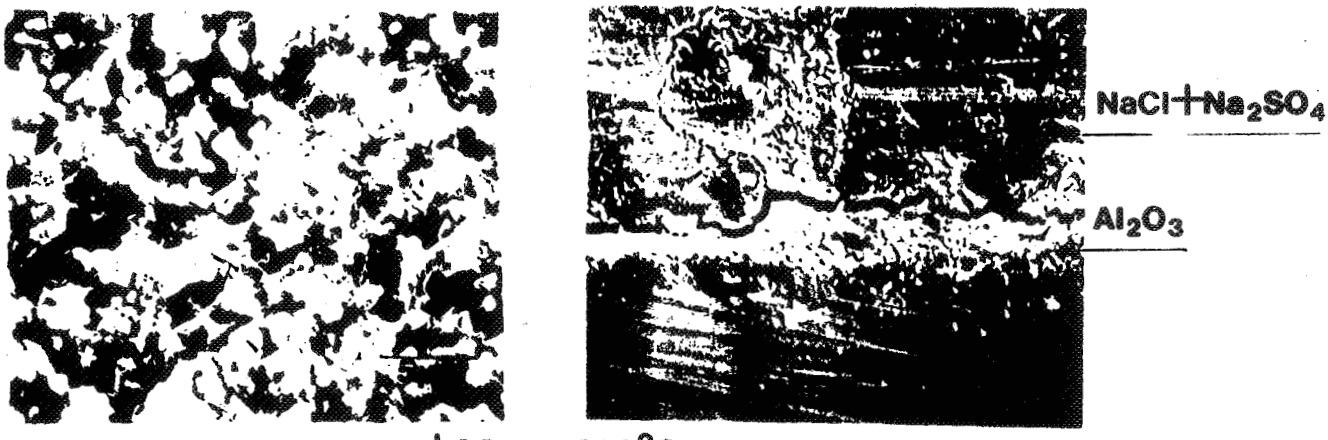

NaCl coated, 2 hrs in air + SO_2 at 600°C

FIGURE 43 Preoxidised HOS-875 substrate coated with NaCl , Na_2SO_4 and heated as indicated to avoid liquid formation, little or no attack of the Al_2O_3.

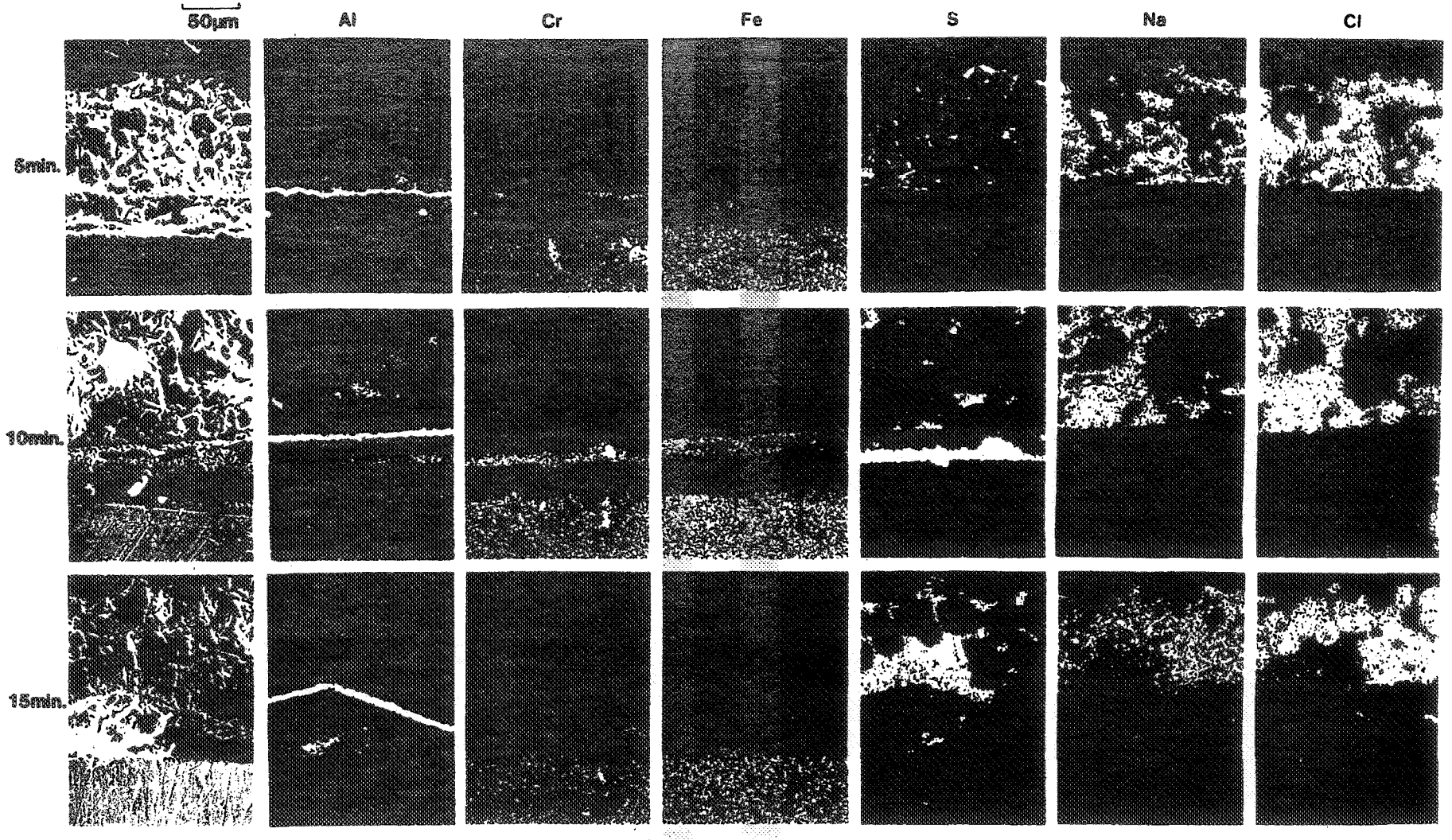

FIGURE 44(a) Development features at scale-metal interface during initiation of hot corrosion attack.

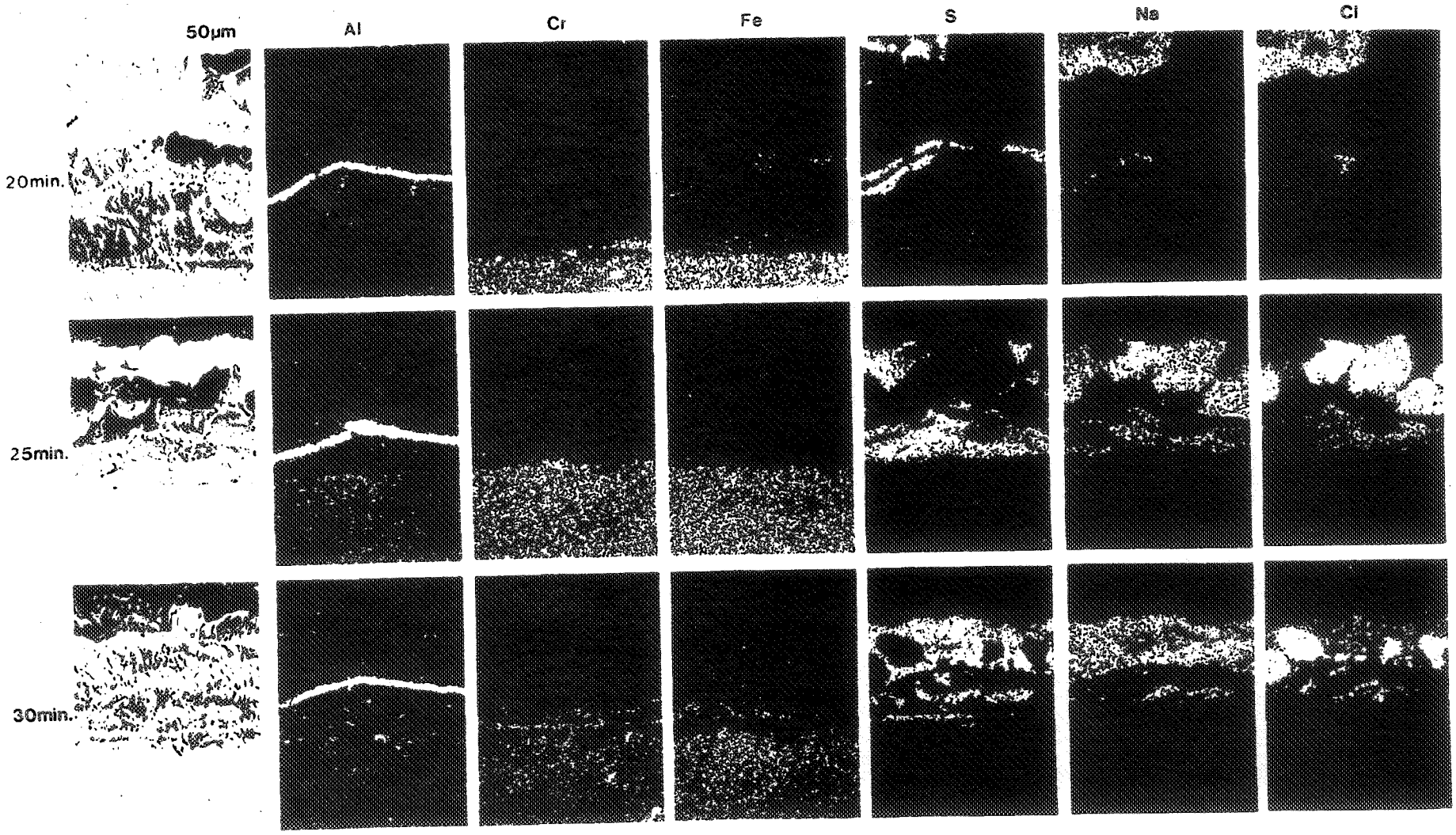

FIGURE 44(b) Development features at scale-metal interface during initiation of hot corrosion attack.

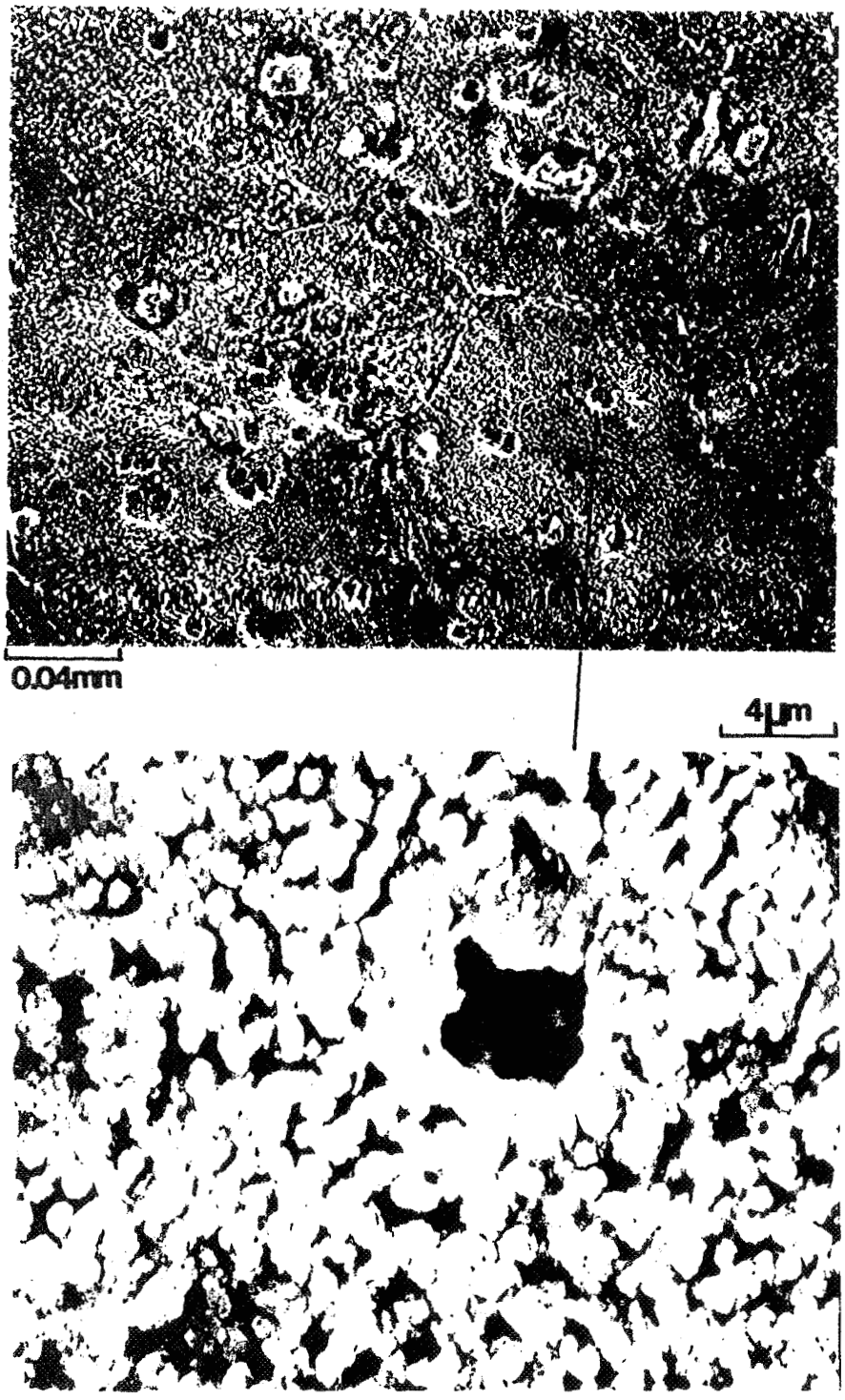

FIGURE 45 **Scale formed on preoxidized HOS-875 after 5 min under NaCl -Na_2SO_4 melt. Note rounded alumina grains and pinholes.**

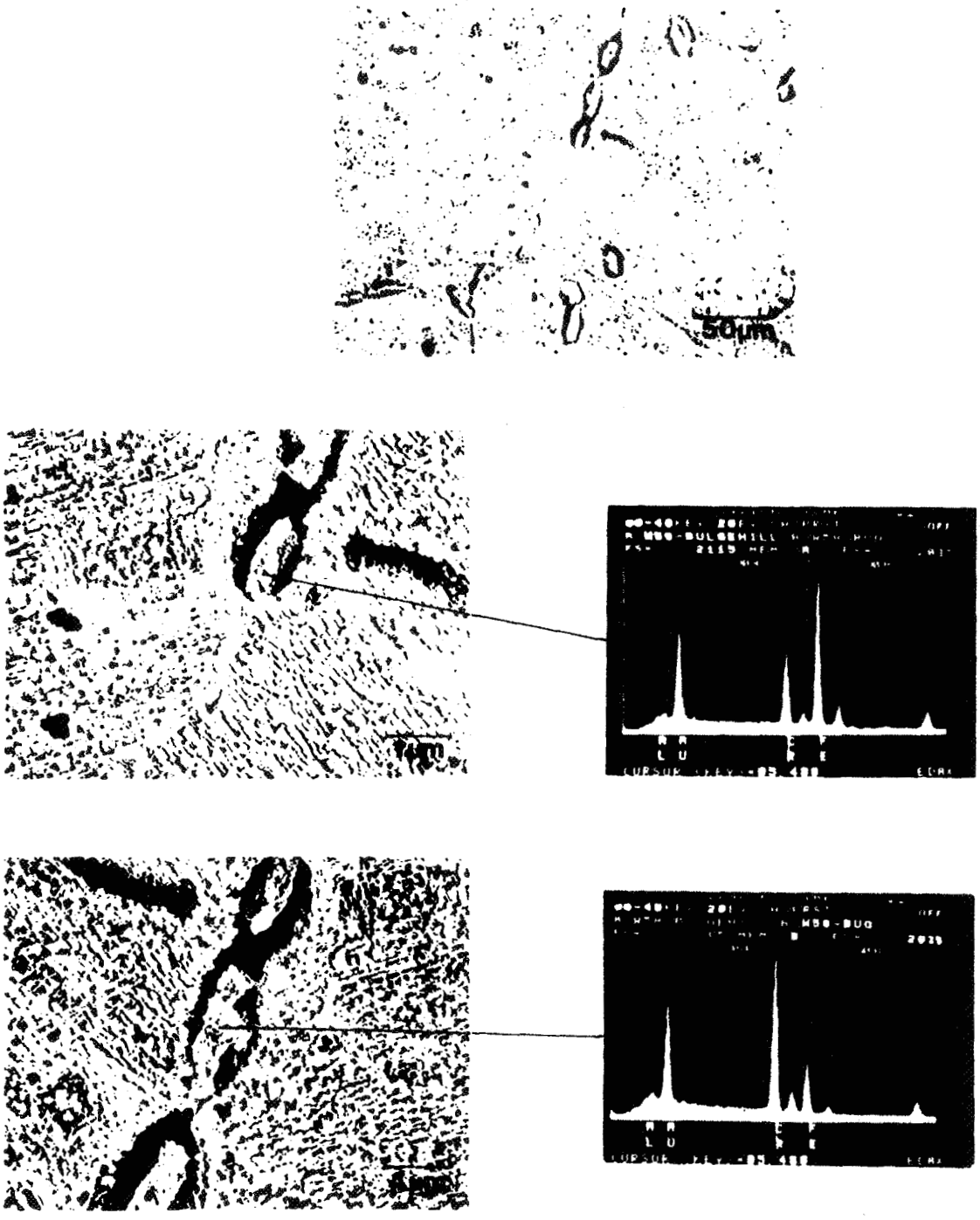

FIGURE 46 Preoxidised HOS-875 after 10 minutes under $NaCl-Na_2SO_4$ melt.

Sulfides growing outwards and scale lifting is apparant.

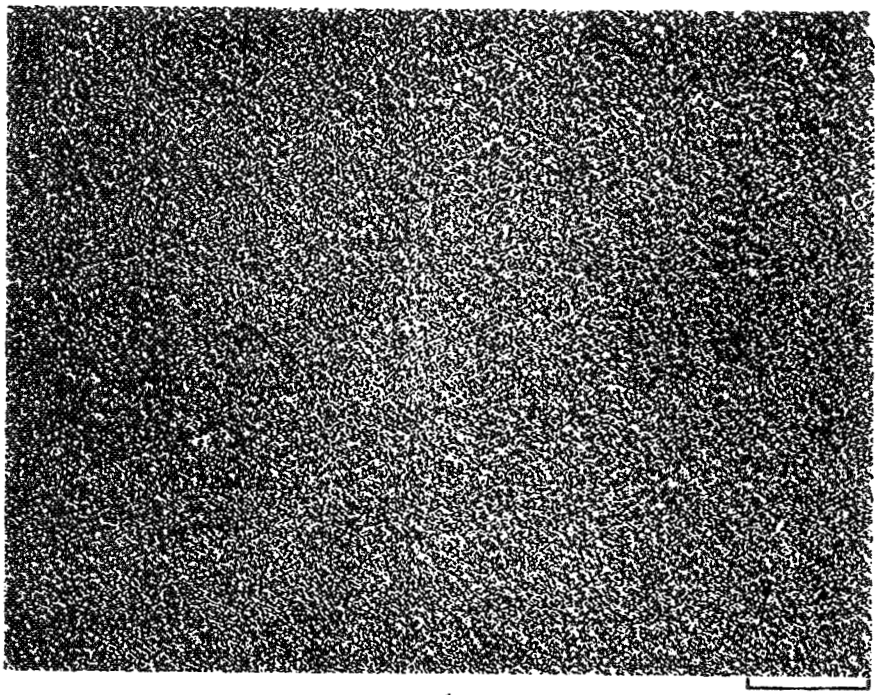

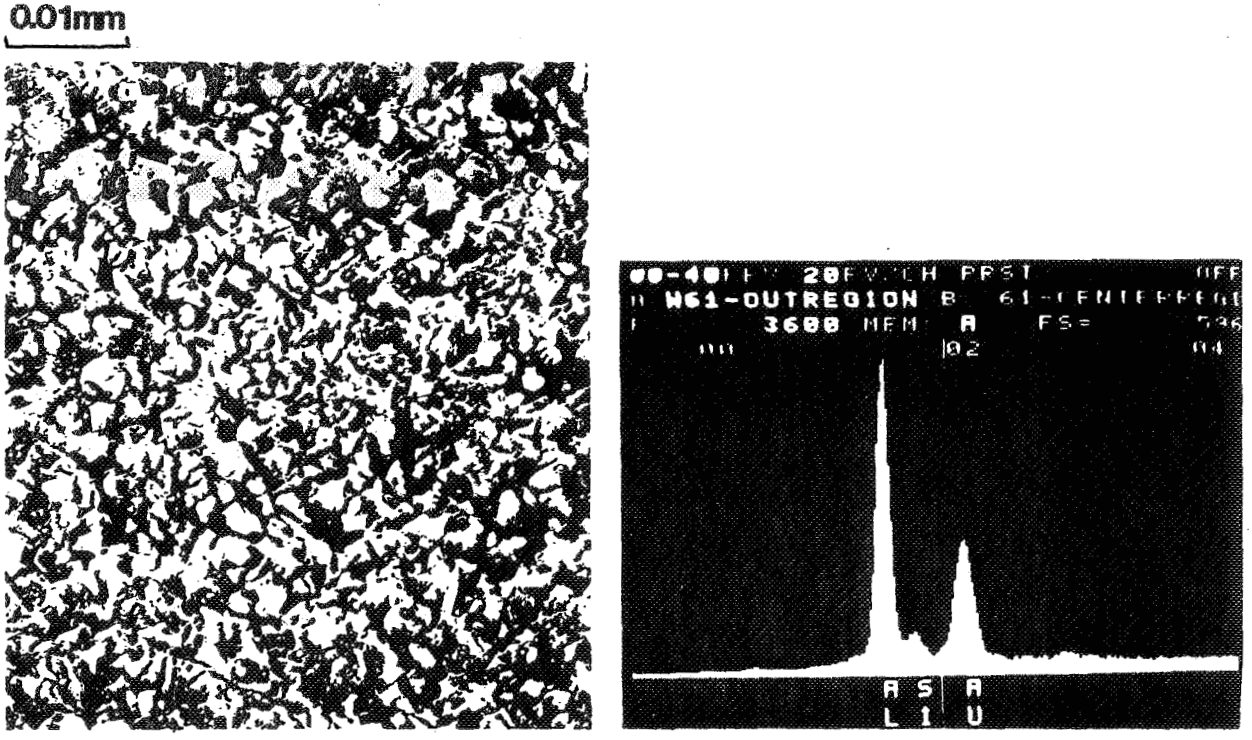

FIGURE 47 **Surface of preoxidized HOS-875 after heating to 700°C and furnance cool to 20°C.**

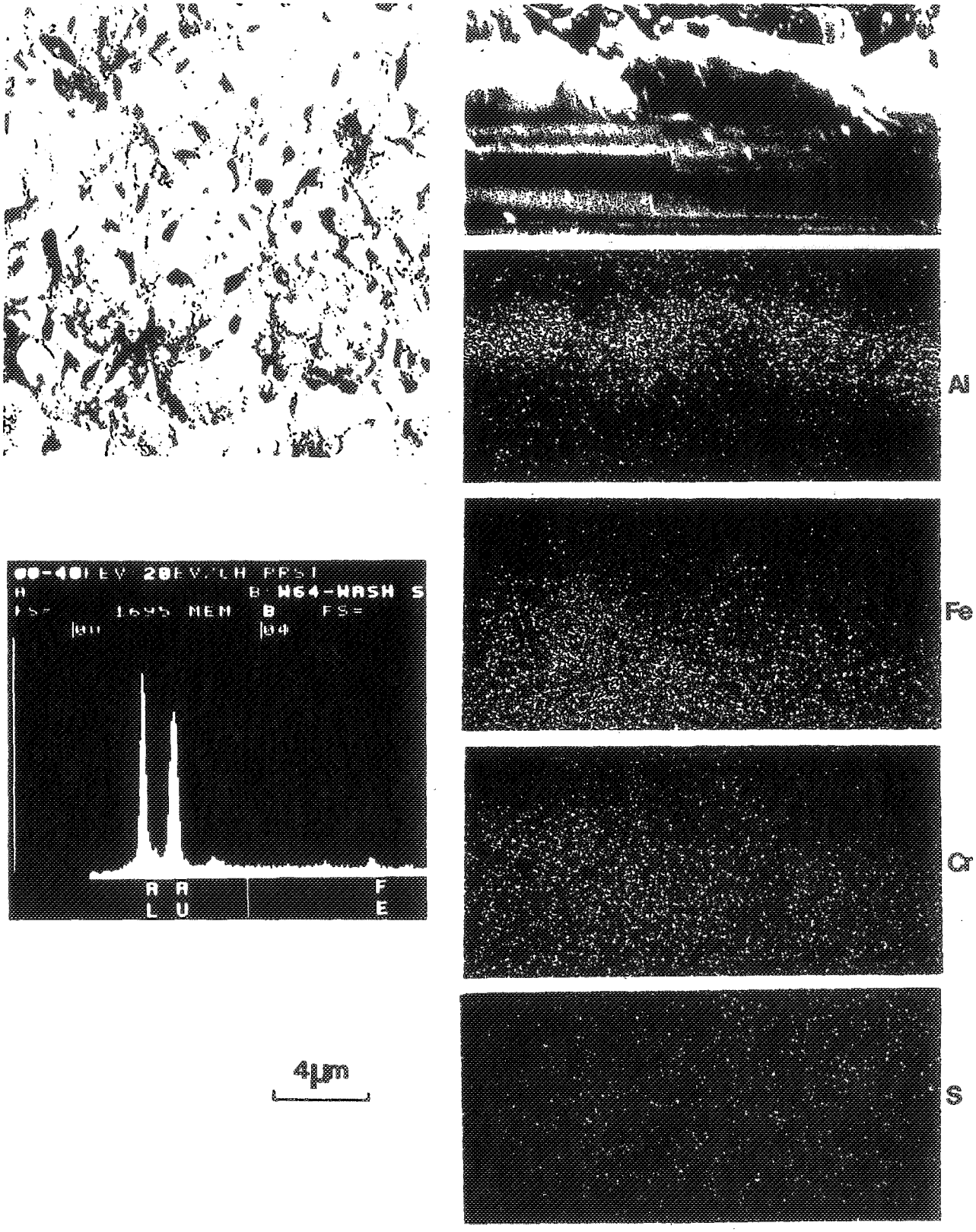

FIGURE 48 Preoxidized HOS-875 without salt coating exposed to air + 1% SO_2 at 700°C for 1 hr. Note : lack of sulfide formation between alumina layer and metal.